Journal of Medicinal Chemistry

Article

Discovery and Optimization of 2-Amino-4-methylquinazoline Derivatives as Highly Potent Phosphatidylinositol 3-kinase Inhibitors for Cancer Treatment

Songwen Lin, Chunyang Wang, Ming Ji, Deyu Wu, Yuanhao Lv, Kehui Zhang, Yi Dong, Jing Jin, Jiajing Chen, Jingbo Zhang, Li Sheng, Yan Li, Xiaoguang Chen, and Heng Xu

J. Med. Chem., **Just Accepted Manuscript** • DOI: 10.1021/acs.jmedchem.8b00416 • Publication Date (Web): 21 Jun 2018

ACS Publications

is published by the American Chemical Society. 1155 Sixteenth Street N.W., Washington, DC 20036

Discovery and Optimization of 2-Amino-4-methylquinazoline Derivatives as Highly Potent Phosphatidylinositol 3-kinase Inhibitors for Cancer Treatment

Songwen Lin,[†,‡,▽] Chunyang Wang,[†,▽] Ming Ji,[†] Deyu Wu,[†,‡,] Yuanhao Lv,[†] Kehui Zhang,[†,‡] Yi Dong,[†,‡] Jing Jin,[†] Jiajing Chen,[†,‡] Jingbo Zhang,[†,‡] Li Sheng,[#] Yan Li,[#] Xiaoguang Chen,[†] Heng Xu*[†,‡]*

[†]State Key Laboratory of Bioactive Substance and Function of Natural Medicines, Institute of Materia Medica, Chinese Academy of Medical Sciences and Peking Union Medical College, Beijing 100050, China.

[‡]Beijing Key Laboratory of Active Substances Discovery and Drugability Evaluation, Institute of Materia Medica, Chinese Academy of Medical Sciences and Peking Union Medical College, Beijing 100050, China.

[#]Beijing Key Laboratory of Non-Clinical Drug Metabolism and PK/PD study, Chinese Academy of Medical Sciences and Peking Union Medical College, Beijing 100050, China

KEYWORDS (Word Style "BG_Keywords"). Phosphoinositide 3-kinase, hybridization, scaffold-hopping, brain penetration, *in vivo* anti-tumor efficacy

ABSTRACT

Increased phosphatidylinositol 3-kinase (PI3K) signaling is among the most common alterations in cancer, spurring intensive efforts to develop new cancer therapeutics that target this pathway. In this work, we discovered a series of novel 2-amino-4-methylquinazoline derivatives through a hybridization and subsequent scaffold hopping approach that were highly potent class I PI3K inhibitors. Lead optimization resulted in several promising compounds (e.g. **19**, **20**, **37**, and **43**) with nanomolar PI3K potencies, prominent anti-proliferative activities, favorable PK profiles and robust *in vivo* antitumor efficacies. More interestingly, compared with **19** and **20**, **37** and **43** demonstrated improved brain penetration and *in vivo* efficacy in an orthotopic glioblastoma xenograft model. Furthermore, preliminary safety assessments including hERG channel inhibition, AMES, CYP450 inhibition and single-dose toxicity were performed to characterize their toxicological properties.

INTRODUCTION

Phosphoinositide 3-kinases (PI3Ks) are a family of signaling enzymes that play crucial roles in cell growth and proliferation, survival, metabolism, and migration.[1-3] PI3Ks are subdivided into three classes (I-III) according to their subunit composition and substrate specificity for phosphoinositides.[4, 5] Class I PI3Ks are the best characterized and consist of four subtypes (alpha, beta, gamma and delta). PI3Ks phosphorylate phosphatidylinositol 4,5-diphosphate (PIP2) at the 3′ position on its inositol ring, converting PIP2 to the second messenger phosphatidylinositol 3,4,5-triphosphate (PIP3) at the plasma membrane, an activity that is downstream of receptor tyrosine kinases (RTKs) or G-protein coupled receptors (GPCRs). PIP3 levels are negatively

regulated by phosphatase and tensin homologue (PTEN).[6] Subsequently, PIP3 recruits AKT (also known as protein kinase B) to the membrane through its pleckstrin homology (PH) domain.[7] AKT activation involves the phosphorylation of two residues: threonine 308 (Thr308) in the activation loop and serine 473 (Ser473) in the C-terminal hydrophobic motif.[1, 8, 9] Once activated, signaling through AKT can be propagated to a diverse array of substrates, including the mammalian target of rapamycin (mTOR), a key regulator of protein translation. mTOR is an atypical serine/threonine protein kinase that interacts with several proteins, forming two distinct complexes named mTOR complex 1 (mTORC1) and 2 (mTORC2), which regulate different cellular processes including metabolism, growth, proliferation and survival. [10, 11]

It is well documented that PI3K pathway dysregulation is involved in human cancers.[1, 3, 12] The oncogenic potential of the PI3K pathway is largely associated with its molecular aberrations.[13] Through molecular profiling of 19784 consecutive diverse solid tumor samples submitted by clinicians from more than 60 countries, Millis et al. recently demonstrated that PI3K pathway aberrations are among the most common in cancer; overall 38% of patients had an alteration in one or more PI3K pathway components, including PTEN loss (30%) and mutations in PIK3CA (13%), PTEN (6%), and AKT1 (1%).[14] The PI3K pathway has been extensively studied over the past two decades for new cancer therapeutics, and quite a few PI3K inhibitors have entered into clinical trials.[15-19] Based on their target specificity, these PI3K inhibitors can be characterized into three classes (Figure 1), including dual PI3K/mTOR inhibitors (e.g. PF-04691502, GSK2126458, GDC-0084 and PQR309),[20-23] pan-class I PI3K inhibitors (e.g. BKM-120 and copanlisib),[24, 25] and isoform selective PI3K inhibitors (e.g. alpha-selective BYL-719, beta-selective GSK2636771 and delta-selective idelalisib).[26-28] Among them, the PI3K delta-selective inhibitor idelalisib was the first PI3K inhibitor approved by the FDA for the treatment of three

types of blood cancers (chronic lymphocytic leukemia, follicular lymphoma, and small lymphocytic lymphoma) in 2014,[29] while copanlisib was the second.[30] Of particular note, copanlisib, a pan-PI3K inhibitor with alpha and delta isoform potencies slightly higher than beta and gamma isoforms, obtained an accelerated FDA approval in 2017 for relapsed FL based on its phase II clinical trial that included only 104 patients. While these two drugs validated PI3K as a target for blood cancers, the clinical progress regarding solid tumor treatment was not significant until recent Phase III trials demonstrated that BKM-120 prolonged progression-free survival (PFS) from 4 to 6 months in metastatic breast cancer patients with activating PI3K mutations.[31] Significant efforts are currently in clinical development by pharmaceutical companies and academic institutes to realize the full potential of PI3K inhibitors for solid tumor treatment, including exploring effective combinations, predictive biomarkers, target patient populations as well as underlying resistance mechanisms. [19, 32] In addition to the range of solid tumor types that would benefit from PI3K inhibitors, including breast cancer, head and neck squamous cell carcinoma (HNSCC) and non-small cell lung carcinoma (NSCLC), these inhibitors might offer an effective treatment option for brain tumors, such as primary brain tumors or brain metastases, as these tumors also show a high frequency of PI3K pathway alterations.[22, 23, 33,] For example, PI3K signaling is implicated in more than 80% of glioblastoma multiforme (GBM) cases.[33] This is of great value, particularly considering the limited progress that has been made in treating brain tumors with kinase inhibitors. However, the molecular design of such PI3K inhibitors requires additional consideration of the brain-blood barrier, which limits penetration of the inhibitor into the brain. Few PI3K inhibitors (e.g. GDC-0084 and PQR309, Figure 1) have been reported to be brain penetrant or demonstrated to be effective in orthotopic brain models,[22, 23] suggesting there is rationale for them to be indicated to treat brain tumors or brain metastases.

Therefore, the discovery of structurally distinct PI3K inhibitors, in particular those capable of penetrating into the brain, would facilitate drug discovery for cancer therapeutics.

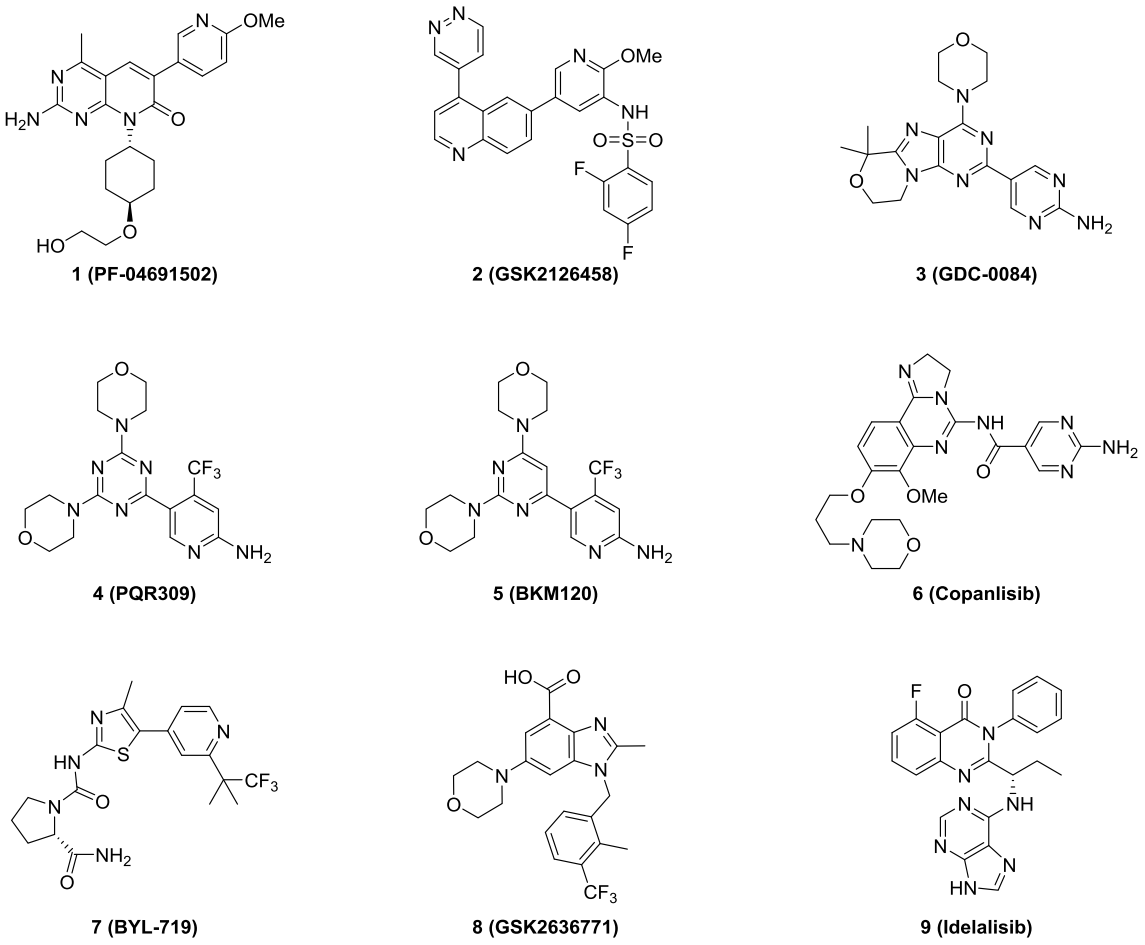

Figure 1. Selected examples of PI3K inhibitors: the dual PI3K/mTOR inhibitors **1**-**4**, *pan*-PI3K inhibitors **5**-**6**, a PI3K alpha-selective inhibitor **7**, a PI3K beta-selective inhibitor **8**, a PI3K delta-selective inhibitor **9**.

RESULTS AND DISCUSSION

Our initial design was inspired from two known PI3K inhibitors PF-04691502 and GSK2126458. Using insight from their co-crystal structures with PI3Kγ, we noticed that both compounds established hydrogen bonding interactions with Val882 and a conserved water molecule bridge with Tyr867 and Asp841, while they had one additional hydrophobic interaction within the ribose pocket and one charged interaction between the deprotonated sulfonamide and Lys833, respectively.[20, 21] Based on this analysis, we intended to exploit the hybrid drug design approach to access all four aforementioned interactions with the goal of identifying novel chemical scaffolds with better drug-like properties.

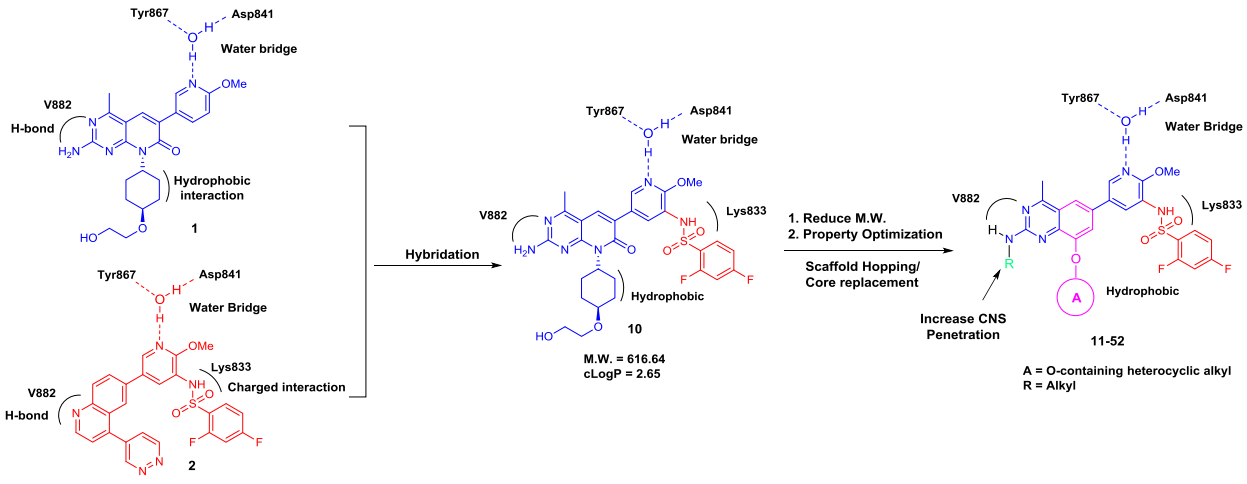

Figure 2. Design strategy of quinazoline-based PI3K inhibitors.

Compound **10** was synthesized to validate the hybrid design. In a PI3K enzymatic assay, compound **10** potently inhibited PI3Kα with an IC_{50} of 0.87 nM, displaying approximately 4-fold increased potency compared with PF-04691502. However, the translation of inhibited enzymatic activity into cellular potency was suboptimal. Compound **10** was approximately 2-fold less potent than PF-04691502 against human NCI-H460 cells. We attributed this drop in cellular

potency to its unfavorable physicochemical properties. In particular, its molecular weight (M.W. = 616.64) and polar surface area (PSA = 168.3) were far from the desired range.[34, 35] This prompted us to reduce its M.W. and PSA through a scaffold hopping approach. As seen from the docking study, the cyclic amide functionality in the pyrido[2,3-d]pyrimidin-7(8H)-one core of compound **10** was not directly involved in the binding to the kinase, and thus, provided a reasonable place to make structural changes (Figure 3A). The quinazoline scaffold, which is capable of allowing similar orientations for both aminopyrimidine and methoxyl pyridine moieties, was then chosen to replace the pyrido[2,3-d]pyrimidin-7(8H)-one core (Figure 3B). Additionally, the synthetic feasibility of attaching various functionalities to the 8-position of the quinazoline to access hydrophobic interactions within the ribose pocket of the protein made this scaffold more attractive for exploration.

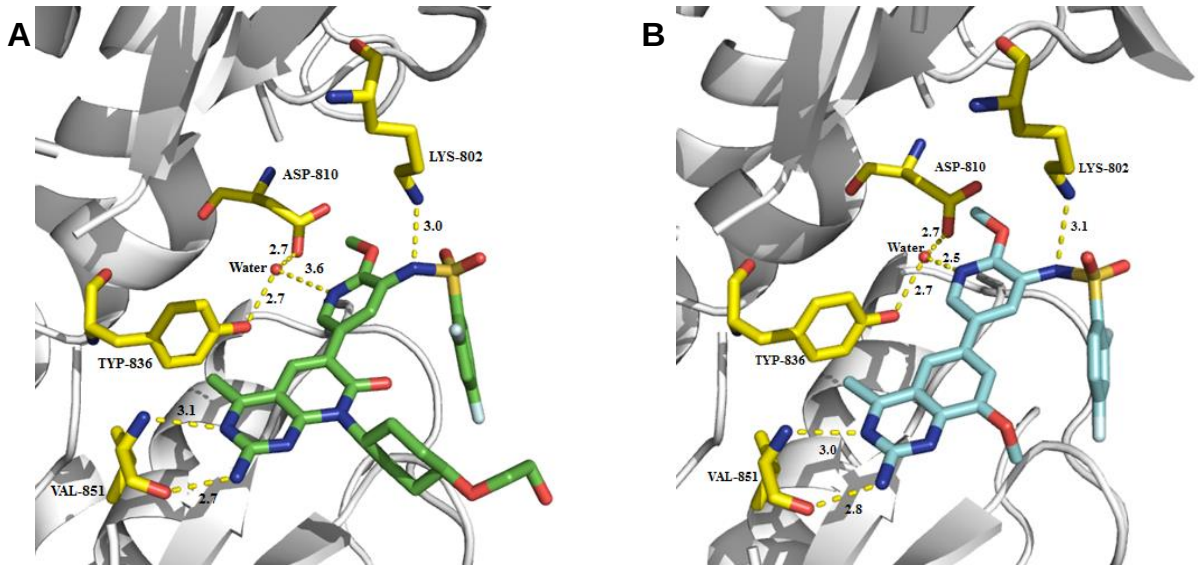

Figure 3. Predicted binding mode for **10** (A) and **11** (B) with PI3Kα (PDB ID: 4JPS). Hydrogen bonds are shown as yellow dashed lines to Val851 in PI3Kα (Val882 in PI3Kγ) in the hinge region, Lys802 in PI3Kα (Lys 833 in PI3Kγ), and the conserved water molecule bridge between Tyr 836 and Asp810 in PI3Kα (Tyr867 and Asp841 in PI3Kγ). Images generated by PyMol.

Table 1. SAR studies of the ether functionalities

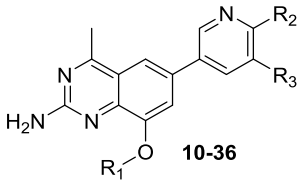

Compd.	R_1	R_2	R_3	cLogP[a]	PSA[a]	PI3Kα (nM)[b]	NCI-H460 (μM)[c]
1	--	--	--	1.2	122.1	3.3±0.92	0.20±0.03
10	--	--	--	2.7	168.3	0.87±0.19	0.36±0.09
11		CH_3O	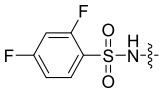	4.6	127.7	1.2±0.06	0.28±0.06
12		CH_3O	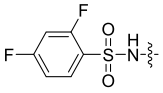	5.5	127.7	0.70±0.13	0.14±0.02
13		CH_3O	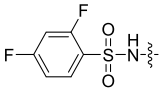	5.6	127.7	1.4±0.49	0.20±0.09
14	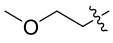	CH_3O	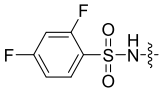	4.5	137.0	1.6±0.01	0.20±0.04
15		CH_3O	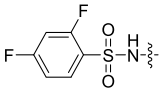	5.6	127.7	0.95±0.21	0.063±0.015
16		CH_3O	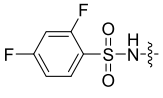	6.1	127.7	1.1±0.07	0.094±0.069
17		CH_3O	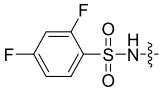	6.6	127.7	0.95±0.49	0.096±0.064
18	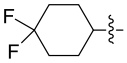	CH_3O	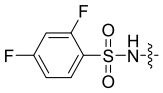	6.1	127.7	1.6±1.0	0.083±0.007
19	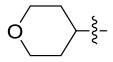	CH_3O	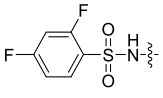	4.3	137.0	0.80±0.01	0.029±0.013
20		CH_3O	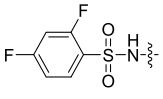	4.4	137.0	1.0±0.24	0.093±0.028

21		CH_3O	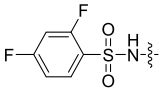	4.4	137.0	0.83±0.16	0.094±0.048
22	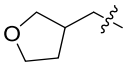	CH_3O	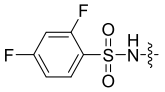	4.5	137.0	1.2±0.28	0.063±0.030
23	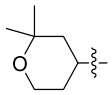	CH_3O	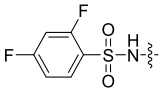	5.3	137.0	1.0±0.04	0.041±0.029
24	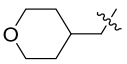	CH_3O	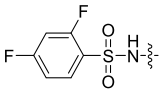	4.9	137.0	0.73±0.16	0.021±0.016
25	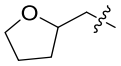	CH_3O	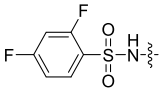	5.0	137.0	1.1±0.34	0.24±0.10
26	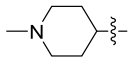	CH_3O	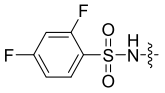	4.5	131.0	4.8±0.99	0.66±0.33
27	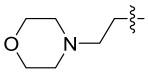	CH_3O	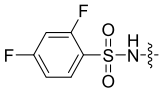	4.8	140.2	3.3±1.1	1.1±0.24
28	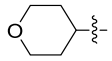	CH_3O	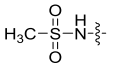	2.3	137.0	2.6±0.21	0.86±0.19
29	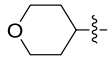	CH_3O	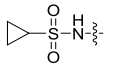	2.8	137.0	2.5±0.28	0.93±0.24
30	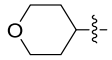	CH_3O	F	2.8	90.8	16±7.8	1.1±0.15
31	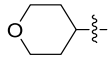	CH_3O	H	2.8	90.7	31±1.4	0.98±0.03
32	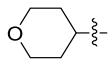	CH_3O	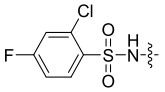	4.5	137.0	1.1±0.55	0.017±0.003
33	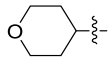	CH_3O	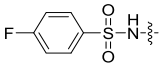	4.1	137.0	1.2±0.14	0.096±0.014
34	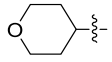	CH_3O	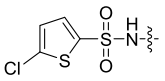	4.4	137.0	1.1±0.47	0.025±0.017
35	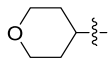	CH_3	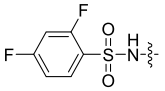	3.4	127.7	1.4±0.35	2.1±0.41
36	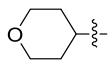	Cl	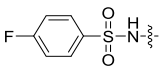	3.5	127.7	1.7±0.92	1.2±0.51

[a]Calculated from ChemBioDraw Ultra 14.0. [b]Mean of at least two separate experiments. [c]Mean of at least three separate experiments.

First, simple methyl ether **11** was synthesized and its IC_{50} values against PI3Kα and NCI-H460 cells were 1.2 nM and 0.28 μM respectively, showing comparable enzymatic and cellular potencies to PF-04691502 (Table 1). Isopropyl ether **12** displayed approximately two-fold increased potency for PI3Kα and NCI-H460 cells relative to **11**. We attribute this increased potency to better hydrophobic interactions brought by the two methyl group of the isopropyl moiety. The cyclopropyl methyl ether **13** and 1-methoxyethyl ether **14** exhibited cellular potencies similar to PF-04691502. When cycloalkyl groups were incorporated through the ether linkage, the generated compounds **15**–**18** had IC_{50} values against PI3Kα within a range of 0.95–1.6 nM. More impressively, they inhibited NCI-H460 cell growth with IC_{50} values below 100 nM. It has been noted that the cellular activities of these cycloalkyl compounds incrementally increase as their cLogPs decrease. While these cycloalkyl compounds give excellent cellular potency, all their cLogP values were greater than 5.5. Such high cLogPs often give rise to poor oral absorption and low metabolic stability.[36] With this in mind, we further explored heterocycloalkyl analogues to decrease the cLogP. Among O-containing heterocycloalkyls, tetrahydropyrane **19** and tetrahydrofuran **20** were very potent against both PI3Kα ($IC_{50} \leq 1$ nM) and NCI-H460 cells ($IC_{50} < 0.1$ μM). Notably, the chiral tetrahydrofuran **20** displayed equal in vitro potencies with its enantiomer **21**. When the tetrahydrofuran moiety was one carbon away from the oxygen atom, the racemic compound **22** had an incremental improvement in cellular potency over **20** and **21**. In particular, tetrahydropyrane **19** showed a remarkable IC_{50} value of 0.029 μM against NCI-H460 cells, over 3-fold more potent than the cyclohexyl compound **17**. Its close analogues of 2,2-dimethyl tetrahydropyrane **23** and 4-methyl tetrahydropyrane **24** also showed excellent cellular potencies ($IC_{50} < 0.05$ μM). More importantly, relative to the cycloalkyl compounds (e.g. **15**–**18**), cLogP values of these O-containing heterocycloalkyl

compounds (e.g. **19**–**22**, **24**) fell into a range that could potentially be translated into better oral absorption and metabolic stability. In addition to O-containing heterocyclic alkyls, methylpiperidine **26** and morpholine **27** were also examined. However, the introduction of the polar nitrogen resulted in a noticeable decrease in enzymatic potency, indicating that the piperidine and morpholine moieties formed unfavorable interactions with the lipophilic side chains of the residues in its ribose binding pocket. The exploration of various ether analogues revealed that the tetrahydropyrane moiety yielded excellent enzymatic and cellular potencies as well as reasonable cLogPs, and thus were retained for further structure-activity relationship (SAR) studies. Sulfonamide functionality was then targeted for the next round of modifications. Consistent with earlier findings, alkyl sulfonamide (e.g. **28**) and cycloalkyl sulfonamide (e.g. **29**) were less potent than phenyl sulfonamides (e.g. **19**), which was largely attributed to the resonance effect of phenyl sulfonamides that rendered the more acidic sulfonamide NH proton to have a stronger charged interaction with Lys802 in PI3Kα (Lys833 in PI3Kγ).[21] As expected, removal of the sulfonamide moiety (e.g. **30** and **31**) significantly decreased both PI3Kα and cellular potencies. Small substitution changes to the phenyl ring could also make an impact on cellular activity. For example, compared with 2,4-difluoro-phenyl sulfonamide **19**, 2-chloro-4-floro-phenyl sulfonamide **32** was slightly more potent (NCI-H460 IC_{50}: 0.017 vs 0.029 μM), whereas 4-fluoro-phenyl sulfonamide **33** was slightly less potent (NCI-H460 IC_{50}: 0.096 vs 0.029 μM). In addition to phenyl sulfonamide, 5-chlorothiophene-2-sulfonamide **3**4 was also demonstrated to be a favorable moiety for in vitro potencies. Notably, when the methoxyl group adjacent to the pyridine nitrogen was replaced by methyl (e.g. **35**) or chloride (e.g. **36**), the cellular potencies dropped over 10-fold.

Table 2. SAR Studies of substitutions on the pyrimidylamine.

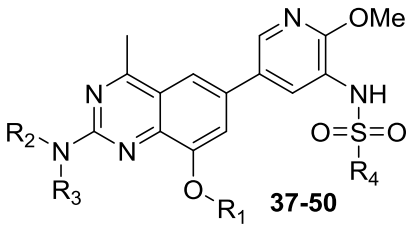

37-50

Compd.	R_2R_3N-	R_1	R_4	cLogP[a]	PSA[a]	PI3Kα (nM)[b]	NCI-H460 (μM)[c]
37	CH_3NH-	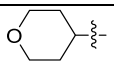	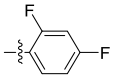	5.1	123.0	1.4±0.35	0.059±0.023
38	C_2H_5NH-	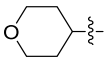	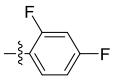	5.6	123.0	1.5±0.21	0.24±0.12
39	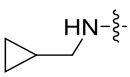	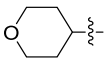	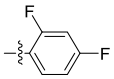	6.1	123.0	5.4±2.3	0.41±0.02
40	$(CH_3)_2N$-	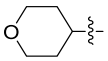	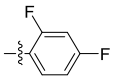	5.2	114.2	125±16	4.3±0.64
41	AcNH-	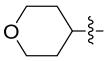	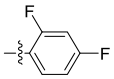	3.8	140.0	1.4±0.35	0.053±0.027
42	AcNH-	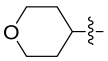	CH_3	1.8	140.0	11±0.71	3.2±1. 8
43	CH_3NH-		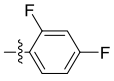	5.2	123.0	0.96±0.20	0.10±0.01
44	CH_3NH-		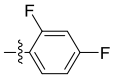	5.2	123.0	1.4±0.61	0.10±0.003
45	CH_3NH-	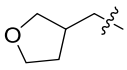	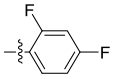	5.3	123.0	2.0±0.42	0.31±0.06
46	CH_3NH-	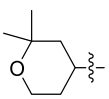	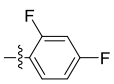	6.1	123.0	1.8±0.71	0.25±0.01
47	CH_3NH-	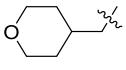	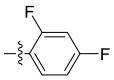	5.7	123.0	1.8±0.64	0.40±0.03

48	CH_3NH-		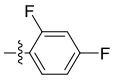	6.4	113.7	4.1±1.3	1.4±0.26
49	CH_3NH-		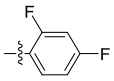	6.9	113.7	6.6±2.8	2.0±0.31
50	CH_3NH-	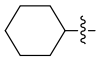	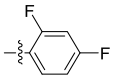	7.5	113.7	9.8±7.4	1.7±0.22

[a]Calculated from ChemBioDraw Ultra 14.0. [b]Mean of at least two separate experiments. [c]Mean of at least three separate experiments.

Finally, our SAR exploration focused on derivatizations on the pyrimidine amine (Table 2). When a methyl, ethyl or cyclopropylmethyl group was attached, methyl amine **37** had the highest enzymatic and cellular potencies, whereas the cyclopropylmethyl amine **39** had the lowest. We found that the in vitro potencies of above alkylated compounds were inversely correlated with the size of the alkyl group. Of particular note, the cellular potency of methylated tetrahydropyrane **37** was comparable to its corresponding amine **19**. For tertiary amine **40**, its PI3K potency dropped >100-fold compared with **19**, indicating that the NH proton was critical for protein binding. Besides the methyl group, acetyl **41** was also favorable for in vitro potency, consistent with the earlier findings from another PI3K series.[37] Similar to tetrahydropyrane **37**, tetrahydrofuran **43** and **44** retained their potencies after methylation. Methylation reactions were also performed with other O-containing heterocyclic compounds. Compared with their corresponding pyrimidine amines **21**–**24**, methylated compounds **44**–**47** generally displayed decreased PI3K potencies (>1.5-fold) and cellular activities (>4-fold), respectively. A more pronounced decrease in potency was observed for methylated compounds **48**–**50** that featured a cycloalkyl moiety versus their corresponding amines (>4-fold decrease in PI3Kα potency; >10-fold decrease in cellular potency). Compared to the cycloalkyls, the O-atom in a tetrahydropyran

or tetrahydrofuran moiety (e.g., compounds **37** and **43**) could be aligned with Gln859 in PI3Kα to form one hydrogen bond (Figure S1), which may explain the more pronounced potency decrease for compounds **48**-**50** that do not have such an interaction.

Table 3. Enzymatic and cellular potencies of compounds **19**, **20**, **37** and **43**

	Enzyme/Cell line	**19**	**20**	**37**	**43**
Enzyme Inhibition IC_{50} (nM)[a]	PI3K alpha	0.80±0.01	1.0±0.24	1.4±0.35	0.96±0.20
	PI3K beta	0.53±0.09	0.40±0.08	1.2±0.27	1.1±0.39
	PI3K gamma	1.3±0.05	1.2±0.25	1.7±0.16	0.93±0.41
	PI3K delta	0.18±0.004	0.23±0.04	0.35±0.06	0.37±0.02
	AKT1	>10000	>10000	>10000	>10000
	mTOR	7.9±0.77	9.9±0.48	43±14	56±8.4
Cell proliferation IC_{50} (μM)[b]	NCI-H460	0.029±0.013	0.093±0.028	0.059±0.023	0.10±0.01
	A549	0.053±0.020	0.084±0.014	0.11±0.02	0.12±0.01
	MDA-MB-231	0.18±0.02	0.30±0.05	0.26±0.07	0.48±0.24
	HGC-27	0.025±0.001	0.056±0.007	0.016±0.002	0.027±0.001
	DU145	1.7±0.25	2.1±0.51	5.2±0.77	6.5±0.24
	PC3	0.15±0.02	0.28±0.16	0.38±0.03	0.24±0.03
	U87MG	0.12±0.05	0.26±0.20	0.25±0.02	0.40±0.15
	SH-SY-5Y	0.28±0.06	0.95±0.40	0.51±0.08	1.3±0.51
	U251	0.32±0.12	0.14±0.05	0.70±0.10	0.46±0.36
	T98G	0.42±0.09	0.28±0.08	0.39±0.20	0.41±0.10

[a]Mean of at least two separate experiments. [b]Mean of at least three separate experiments.

A

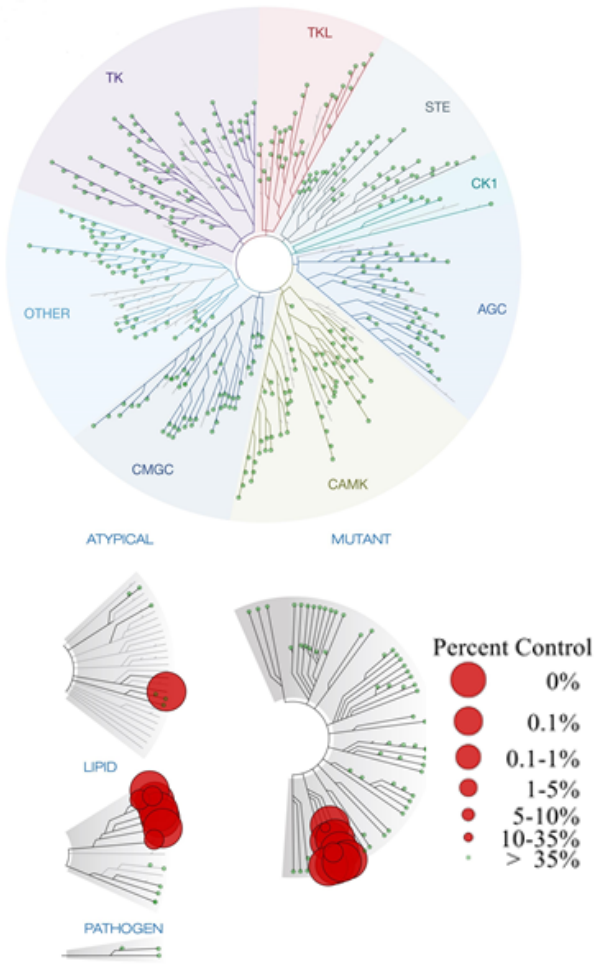

B

Compound **19**
468 target tested
18 interactions mapped
S(1) score = 0.015

Target		% Control
Class I PI3K	PI3KCA	0
	PIK3CA(C420R)	0
	PIK3CA(E542K)	0
	PIK3CA(E545A)	0
	PIK3CA(E545K)	0
	PIK3CA(H1047L)	0
	PIK3CA(H1047Y)	1.4
	PIK3CA(I800L)	0
	PIK3CA(M1043I)	12
	PIK3CA(Q546K)	0
	PIK3CB	1.6
	PIK3CD	2.4
	PIK3CG	0
Class II PI3K	PIK3C2B	0
	PIK3C2G	0
Class III PI3K	VPS34	0
PIK4CB	PIK4CB	2
mTOR	mTOR	0

Figure 4. Kinase selectivity profiling of compound **19** at a concentration of 1 μM (Kinomescan™, DiscoveRx). A) TREEspot™ interaction maps for **19** among 468 kinase targets. B) 9 non-mutant kinases were hit with <35% control binding remaining. Results for primary screen binding interactions are reported as % control, where lower numbers indicate stronger hits in the matrix. S-score is a quantitative measure of compound selectivity and it is calculated by dividing the number of kinases that compounds bind to by the total number of distinct kinases tested, excluding mutant variants.

Based on their superior enzymatic and cellular potencies as well as their favorable physicochemical properties, compounds **19**, **20**, **37** and **43** were selected for further profiling. As illustrated in Table 3, these compounds potently inhibited all four class I PI3K isoforms with sub- to low-nanomolar IC_{50}s. While the PI3K delta isoform was most potently inhibited, these compounds did not show much isoform selectivity. Compounds **19**, **20**, **37** and **43** also had potent inhibitory activities against mTOR. In contrast with compounds **19** and **20**, their methylated counterparts **37** and **43** displayed more than 20-fold increased selectivity for mTOR over class I PI3Ks, which can be explained by the unfavorable interaction between the methyl on the pyrimidine amino group and the side chain of TRP-80 that is unique to mTOR.[20] Moreover, these compounds did not inhibit AKT1 (IC_{50} >10 μM), a key downstream effector of PI3K. To further understand their kinase selectivity, compound **19** was chosen as a representative for this quinazoline chemotype to examine its kinome-wide selectivity profile using DiscoverX's Kinomescan technology. As depicted in Figure 4, **19** possessed a high selectivity, as indicated by the selectivity S score (1) of 0.015 against 468 kinases and mutants tested at a 1 μM concentration. **19** did not show any binding activity to this broad panel of kinases except for the PI3Ks and mTOR, illustrating excellent kinase selectivity for this quinanoline chemotype. Compounds **19**, **20**, **37** and **43** were also tested against a panel of human cancer cell lines (Table 3). Among them, the most sensitive (with IC_{50}s in double-digit nanomolar concentration ranges) was HGC-27 gastric cancer cells, which harbor both a PIK3CA mutation and PTEN loss, while the least sensitive was DU145 prostate cancer cells with wild-type PTEN. Notably, they also potently inhibited the proliferation of brain tumor cells such as U87MG, U251, SH-SY-5Y and T98G with sub-micromolar IC_{50}s.

Compounds **19**, **20**, **37** and **43** were further progressed into in vivo pharmacokinetic studies (Table 4). When intravenously administered at a dose of 3 mg/kg in mice, compounds **19**, **20**, **37** and **43** had moderate clearances with CL values of 7.58, 54.9, 14.3 and 34.5 mL/min/kg, respectively. Compounds **19** and **37** featuring a tetrahydropyrane moiety displayed a slower clearance rate than compounds **20** and **43** that bear a tetrahydrofuran moiety. When orally administered at a dose of 30 mg/kg, compounds **19**, **20**, **37** and **43** were quickly absorbed with Tmax values of <30 min. These compounds gave reasonable oral exposures with area under the curve (AUC) values of >9000 h*ng/mL. Among them, the oral exposure of compound **19** was the highest (normalized $AUC_{(0-\infty)}$ = 1205 h*ng/mL). The oral bioavailability of compounds **19**, **20**, **37** and **43** were determined to be 33.2%, 96.2%, 44.4% and 78.4% respectively, supporting a further evaluation of their in vivo efficacy.

Table 4. Murine pharmacokinetic profiles of compounds **19**, **20**, **37** and **43**

Cmpd	Route	Dose mg/kg	T_{max} h	C_{max} ng/mL	$AUC_{(0-t)}$ h*ng/mL	$AUC_{(0-\infty)}$ h*ng/mL	$T_{1/2}$ h	Vss L/kg	CL mL/min/kg	F%
19	iv[a,c]	3	0.03	10283	7192	7238	1.48	0.853	7.58	/
	po[b,d]	30	0.5	4287	23877	36160	11.1	/	/	33.2
20	iv[a,c]	3	0.03	1583	904	911	0.54	2.57	54.9	/
	po[b,d]	30	0.08	8827	8694	9040	4.68	/	/	96.2
37	iv[a,c]	3	0.05	7723	3484	3501	0.62	0.763	14.3	/
	po[b,d]	30	0.18	12844	15478	16109	4.25	/	/	44.4
43	iv[a,c]	3	0.03	2623	1453	1462	0.53	1.56	34.5	/
	po[b,d]	30	0.25	5390	11396	17097	16.2	/	/	78.4

[a]Three mice per study for IV; [b]three to five mice per study for PO; [c]iv formulation: 10% DMSO/saline; [d]po formulation: 0.1% PEG400/ 0.5% CMC/water

Next, we evaluated the brain penetration properties of these compounds. Compounds **19**, **20**, **37** and **43** were orally administered at a dose of 30 mg/kg, and mouse brain tissues were analyzed to determine their brain pharmacokinetic profiles. As shown in Figure 5, compounds **19**, **20**, **37** and **43** were capable of crossing the brain-blood-barrier with brain Cmax values of 93, 161, 723 and 433 ng/g and brain AUC_{0-t} values of 234, 28.6, 895, 742 ng/g*h, respectively. It should be noted that compared with **19** and **20**, compounds **37** and **43** demonstrated significantly higher maximum brain concentrations and brain exposures. Based on our rational design, compounds **37** and **43** have one less hydrogen-bond donor than their corresponding non-methylated forms **19** and **20**. Lower hydrogen-bond formation potential in a molecule generally favors brain penetration.[38] Compounds **37** and **43**, with significantly higher brain penetration compared with **19** and **20**, provide solid evidence that the number of hydrogen bonding donors in the molecule is inversely correlated with its capability of crossing the brain-blood-barrier.

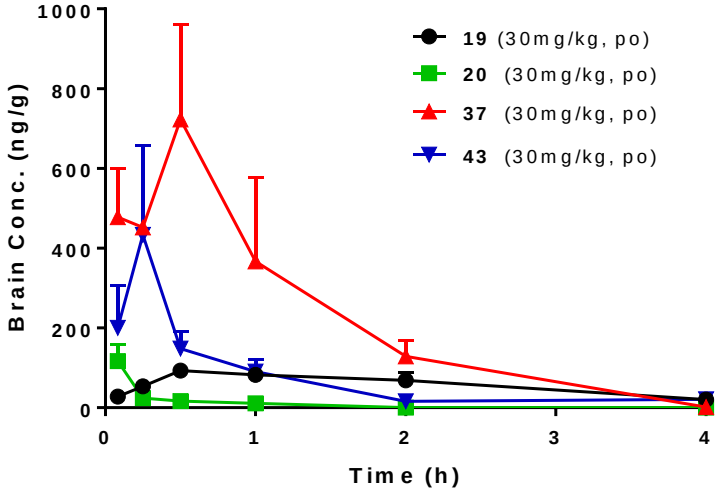

Figure 5. Brain concentration versus time curves for compounds **19**, **20**, **37** and **43**. Results are expressed as the mean brain concentration and standard deviation (SD) (n = 3 for each time point).

Next, compounds **19**, **20**, **37** and **43** were tested for their in vivo antitumor activities in lung and gastric cancer xenograft models (Figures 6 and 7). In an NCI-H460 NSCLC xenograft model, compound **19** orally administered at 5 and 10 mg/kg daily demonstrated robust in vivo antitumor activity, and both dosage groups showed tumor growth inhibition (TGI) of >70%. Compound **19** showed greater efficacy than PF-04691502 (PF-04691502: TGI= 67.4% at 10 mg/kg vs 19: TGI=79.8% at 10 mg/kg). In a separate NCI-H460 xenograft model, compound **20** orally administrated at 5, 10 and 20 mg/kg daily effectively inhibited tumor growth in a dose-dependent manner, with the high-dose group of 20 mg/kg achieving TGI of 75.9%. We also evaluated compound **19** in a SCLC NCI-H209 xenograft model, in which compound **19** orally administered at doses of 2.5 and 5 mg/kg daily for 19 consecutive days produced a dose-dependent effect on TGI. In a MGC-803 gastric cancer xenograft model, compounds **19** and **20** dose-dependently suppressed tumor growth. It was found that both **19** and **20** had significant exposures in the tumor tissue and the exposure correlated with the dose as well as the anti-tumor efficacy (Figure 7C). In a HGC-27 gastric cancer xenograft model, compounds **19**, **37** and **43** achieved significant tumor regression at oral daily doses of 2.5, 2.5 and 10 mg/kg respectively, demonstrating that HGC-27 cells harboring both PIK3CA mutation and PTEN deletion were more sensitive to these compounds (Figure 7D). Their plasma concentrations at 2h after the final dose were also determined to show the correlation between exposure and antitumor efficacy (Figure 7F). It was also noted that in these lung and gastric cancer xenograft models, compounds **19**, **20**, **37** and **43** induced body weight loss and that their antitumor efficacy was correlated with the severity of body weight loss.

Compounds **37** and **43** (with reasonable brain exposures) were further evaluated in a mouse U87MG/Luc orthotopic xenograft model (Figure 8 and Figure S2). In this model, the

U87MG/Luc cell suspension was stereotaxically injected into the mouse brain to grow orthotopic tumors, and then compounds **37** and **43** were orally administered to test whether they could inhibit growth of the orthotopic brain tumor. This model demonstrated that both **37** and **43** exhibited remarkable efficacy in suppressing brain tumor growth, comparable to the positive control trimetazidine (TMZ), which is the only oral anticancer agent approved by the FDA for GBM treatment. Of particular note, at the same dose level (5 mg/kg), compound **37** showed better efficacy than **43**, which was correlated with their absolute brain exposures.

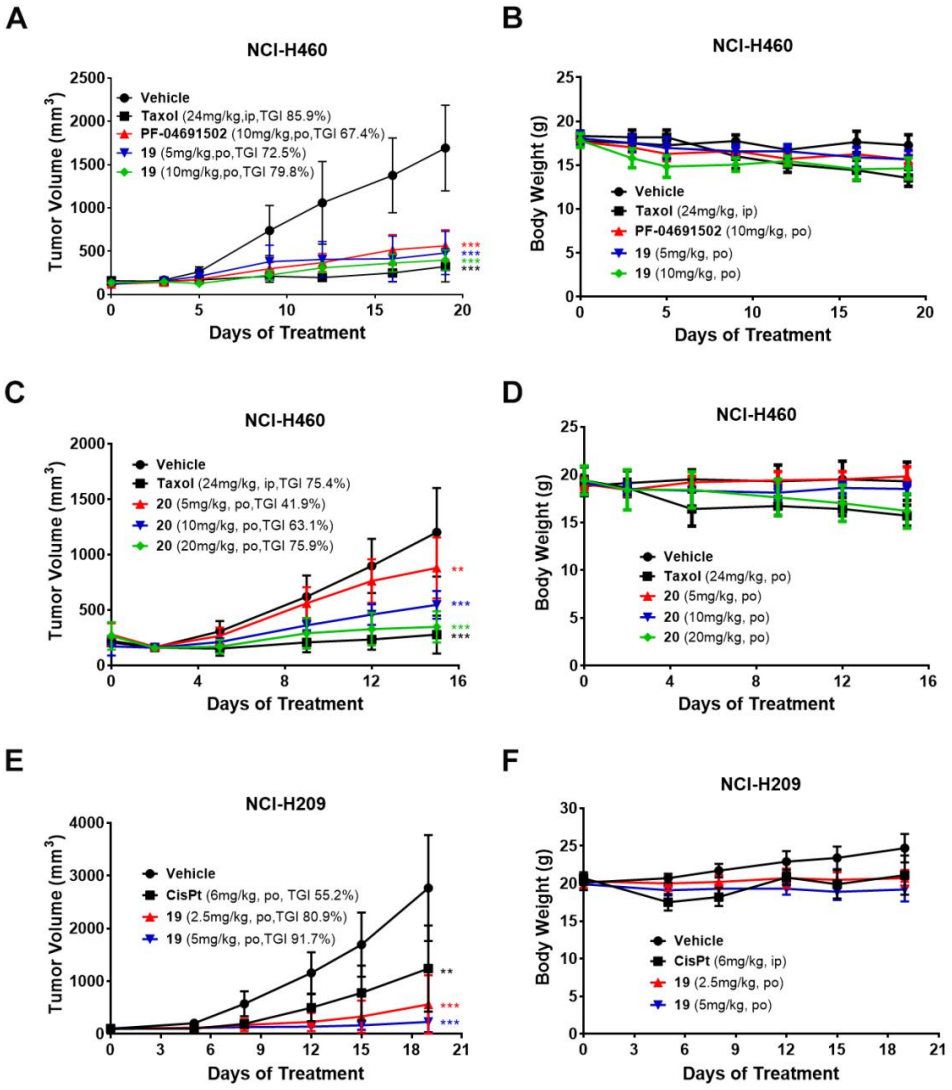

Figure 6. *In vivo* antitumor efficacy of compounds **19** and **20** in lung cancer xenograft models. Non-small cell lung cancer NCI-H460 cells and small cell lung cancer NCI-H209 cells were subcutaneously implanted into nude mice. A) Tumor volume changes following treatment with **19** in the NCI-H460 xenograft model; B) body weight changes after treatment with **19** in the NCI-H460 xenograft model; C) tumor volume changes following treatment with **20** in the NCI-H460 xenograft model; D) body weight changes after treatment with **20** in the NCI-H460 xenograft model; E) tumor volume changes after treatment with **19** in the NCI-H209 xenograft model; F) body weight changes after treatment with **19** in the NCI-H209 xenograft model. Results are expressed as the mean ± SD (n = 5–7 for each group); **p <0.01 and ***p <0.001 vs vehicle.

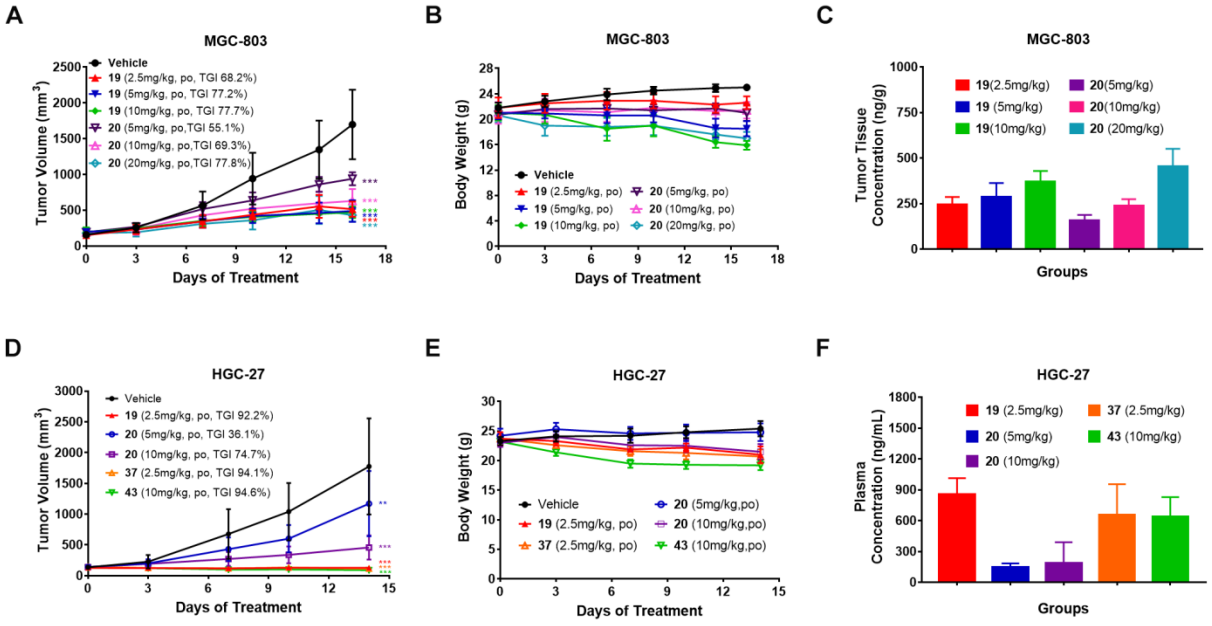

Figure 7. In vivo antitumor efficacy of compounds **19**, **20**, **37** and **43** in gastric cancer xenograft models. Gastric cancer MGC-803 and HGC-27 cells were subcutaneously implanted into nude

mice. A) Tumor volume changes after treatment with **19** and **20** in the MGC-803 xenograft model; B) body weight changes after treatment with **19** and **20** in the MGC-803 xenograft model; C) concentrations of **19** and **20** in tumor tissue at 24h after the final dose in the MGC-803 xenograft model; D) tumor volume changes after treatment with **19**, **20**, **37** and **43** in the HGC-27 xenograft model; E) body weight changes after treatment with **19**, **20**, **37** and **43** in the HGC-27 xenograft model; F) concentrations of **19**, **20**, **37** and **43** in plasma at 2h after the final dose in the HGC-27 xenograft model. Results are expressed as the mean ± SD (n = 6 for each group); **p <0.01 and ***p <0.001 vs vehicle.

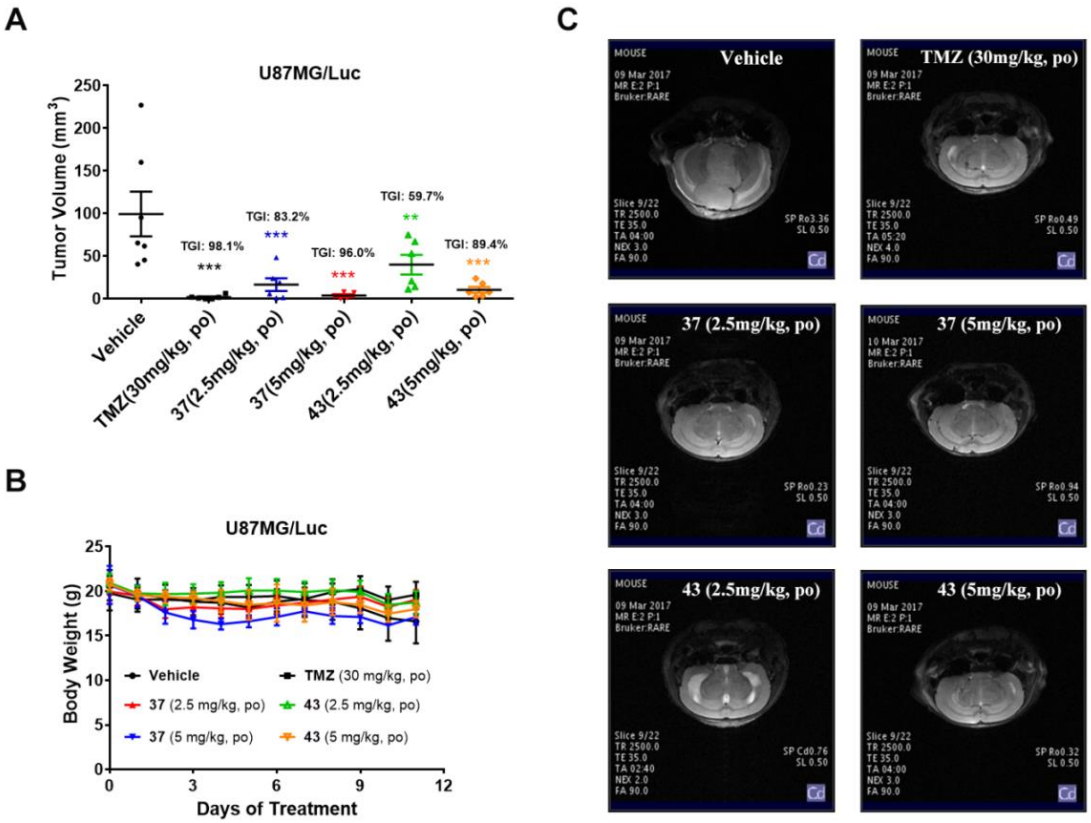

Figure 8. *In vivo* antitumor efficacy of **37** and **43** in the U87MG/Luc glioblastoma orthotopic xenograft model. A) Tumor volume in the mouse brain at the end of treatment; B) body weight

changes; C) representative NMR images of U87MG/Luc tumors in the mouse brain at the end of treatment. Results are expressed as the mean ± SD (n = 5–7 for each group). **p <0.01 and ***p <0.001 vs vehicle. Temozolomide (TMZ) was used as the positive control.

To measure the magnitude and duration of the pharmacodynamic response, phosphorylated (p)AKT levels in tumor tissues from the NCI-H460 xenograft model following a single oral dose of 10 mg/kg were determined over a time course. As shown in Figure 9, compounds **19** and **37** significantly reduced pAKT levels, and the duration of the pharmacodynamic response was greater than 24 h. Their plasma and tumor tissue concentrations at each time point greatly exceeded their PI3K IC_{90}s and NCI-H460 antiproliferative IC_{50}s. Considering protein binding (human 95.78%, mouse 91.77%, for **19**; human 95.46%, mouse 91.58%, for **37**), their theoretical free drug concentrations at each time point are still higher than the PI3K IC_{90}s, rationalizing the PD effect over the time course. Of particular note, the ratios of $AUC_{(0\text{-}24h)}$ in tumor to $AUC_{(0\text{-}24h)}$ in plasma of compounds **19** and **37** were calculated to be 0.71 (Tumor $AUC_{(0\text{-}24h)}$ = 8456 ng/g*h vs plasma $AUC_{(0\text{-}24h)}$ = 11831 ng/mL*h) and 1.02 (Tumor $AUC_{(0\text{-}24h)}$ = 5576 ng/g*h vs plasma $AUC_{(0\text{-}24h)}$ = 5455 ng/mL*h), respectively, illustrating their high tumor uptakes.

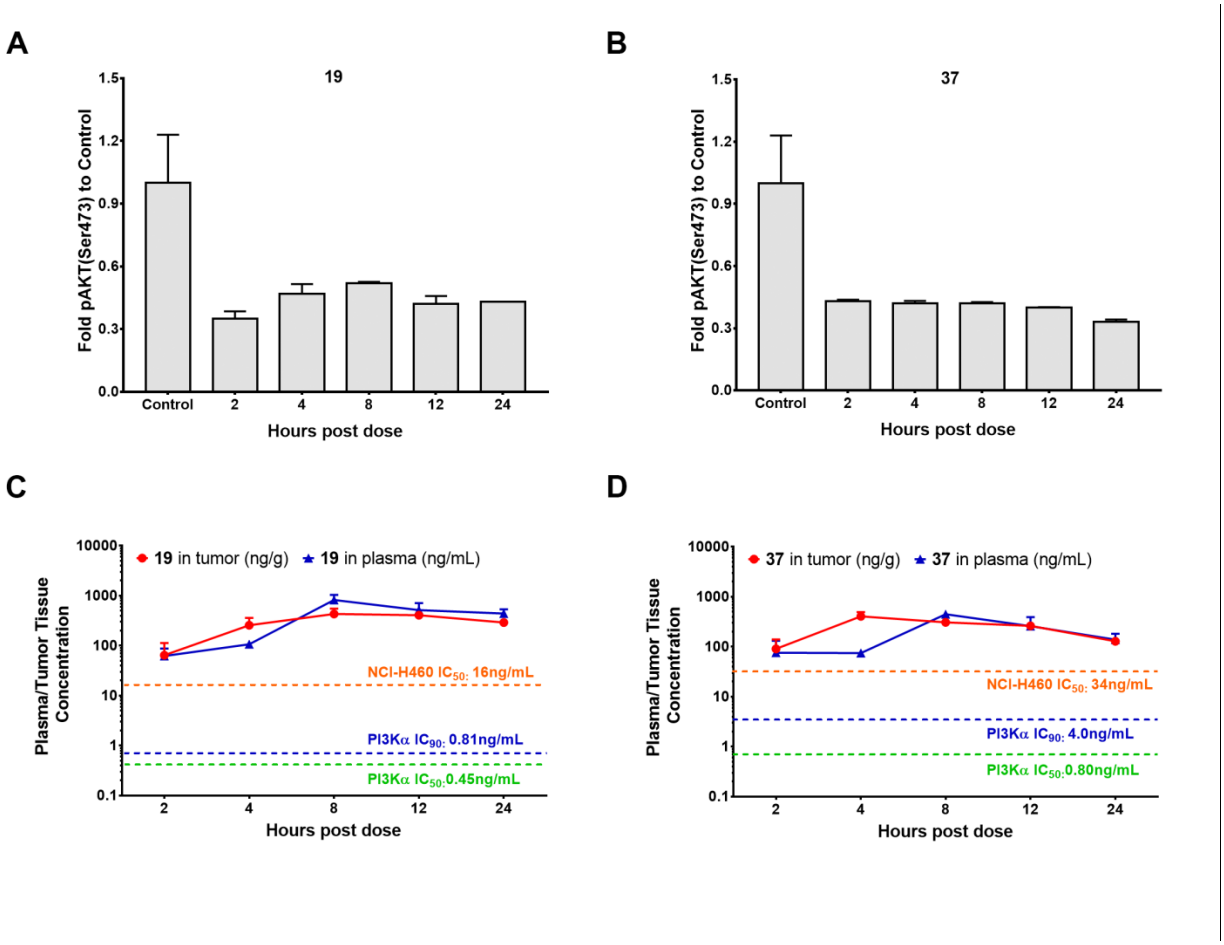

Figure 9. Pharmacodynamic response of **19** and **37** in the NCI-H460 xenograft model following a single oral dose of 10 mg/kg. pAKT(S473) levels were determined at 2, 4, 8, 12 and 24 h post-administration (A and B). Compound concentrations in plasma and tumor tissues were measured at the same time point and the dashed lines represent the PI3Kα IC_{50} value (green), the PI3Kα IC_{90} value (blue) and the NCI-H460 antiproliferative IC_{50} value (orange), respectively. Results are expressed as the mean ± SD (n = 3 for each time point).

We further evaluated the safety profiles of these compounds. In the hERG inhibition assay, all tested compounds showed low hERG channel activity with IC_{50} values of >10 μM, indicating

that they had low cardiotoxicity potential. We also studied their mutagenicity by the bacterial reverse mutation (AMES) test. Compounds **19**, **20** and **43** were non-mutagenic at the tested concentrations (0.5–500 μg/plate) with or without metabolic activation (using the five tester strains: TA97, TA98, TA100, TA102 and TA1535). For compound **37**, however, we found that its AMES test was positive at the concentration of 500 μg/plate in strains TA97, TA98, TA100, and TA1535; it was also positive in strain T1535 at a concentration of 50 μg/plate with the S9 mix. Compounds **19**, **20**, **37** and **43** were also tested in cytochrome P450 (CYP450) inhibition assays for a range of isoforms including CYP1A2, CYP2D6, CYP2C9, CYP2C19, CYP2E1 and CYP3A4, and their IC_{50} values against all these CYP450 isoforms were greater than 10 μM, confirming their low liability for drug-drug interactions. Single-dose toxicity studies were also performed for compounds **19**, **20**, **37** and **43**, and their maximum tolerated doses were determined to be >40 mg/kg.

Table 5. The safety profiles of compounds **19**, **20**, **37** and **43**

Compd.	hERG (IC_{50}, μM)[a]	AMES[b]	cytochrome P450 (IC_{50}, μM)[c]	Single-dose Toxicity (MTD, mg/kg)[d]
19	>10	Negative	>10	>40
20	>10	Negative	>10	>50
37	>10	Positive	>10	>40
43	>10	Negative	>10	>40

[a]hERG assays were performed using wide-type Chinese hamster ovary cells expressing hERG potassium channels; [b]compounds were tested at concentrations from 0.5–500 μg/plate with or without metabolic activation using the five tester strains TA97, TA98, TA100, TA102 and TA1535; [c]the cytochrome P450 isoforms included CYP1A2, CYP2D6, CYP2C9, CYP2C19, CYP2E1 and CYP3A4; [d]mice were observed for 14 d after a single-dose oral administration.

Chemistry

As shown in scheme 1, compound **10** was synthesized by Suzuki coupling of compound **51** and **52a**, which were prepared according to the reported methods.[21, 37]

Scheme 1. Synthesis of compound **10** [a]

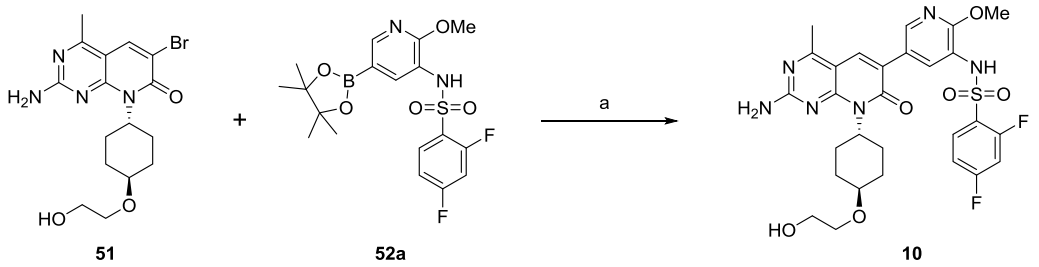

[a] Reagents and conditions: (a) $PdCl_2(dppf)$, 2M K_2CO_3, dioxane, 100 ^oC, Ar, 4h, 53%.

The preparation of compounds **11-36** are illustrated in scheme 2. The starting material **53** was brominated by NBS to afford compound **54**, which was then reacted with triphosgene to give **55**. Aminolysis of **55** by N,O-dimethylhydroxylamine hydrochloride afforded compound **56**, which was converted to compound **57**. The 2-amino-4-methylquinazoline core structure was constructed by reaction of compound **57** with cyanamide and concentrated hydrochloric acid, and the resulting **58** was then reacted with 2,5-hexanedione to yield **59**, which was further demethylated to afford the general intermediate **60**. **60** was converted to **61-76** via nucleophilic substitution reaction or Mitsunobu reaction, followed by removing the amino-protective group to give compound **77-92**. Finally, compounds **58** and **77-92** were coupled with various aryl boronic esters to afford the final products **11-36**.

Scheme 2. Synthesis of compound **11-36**.[a]

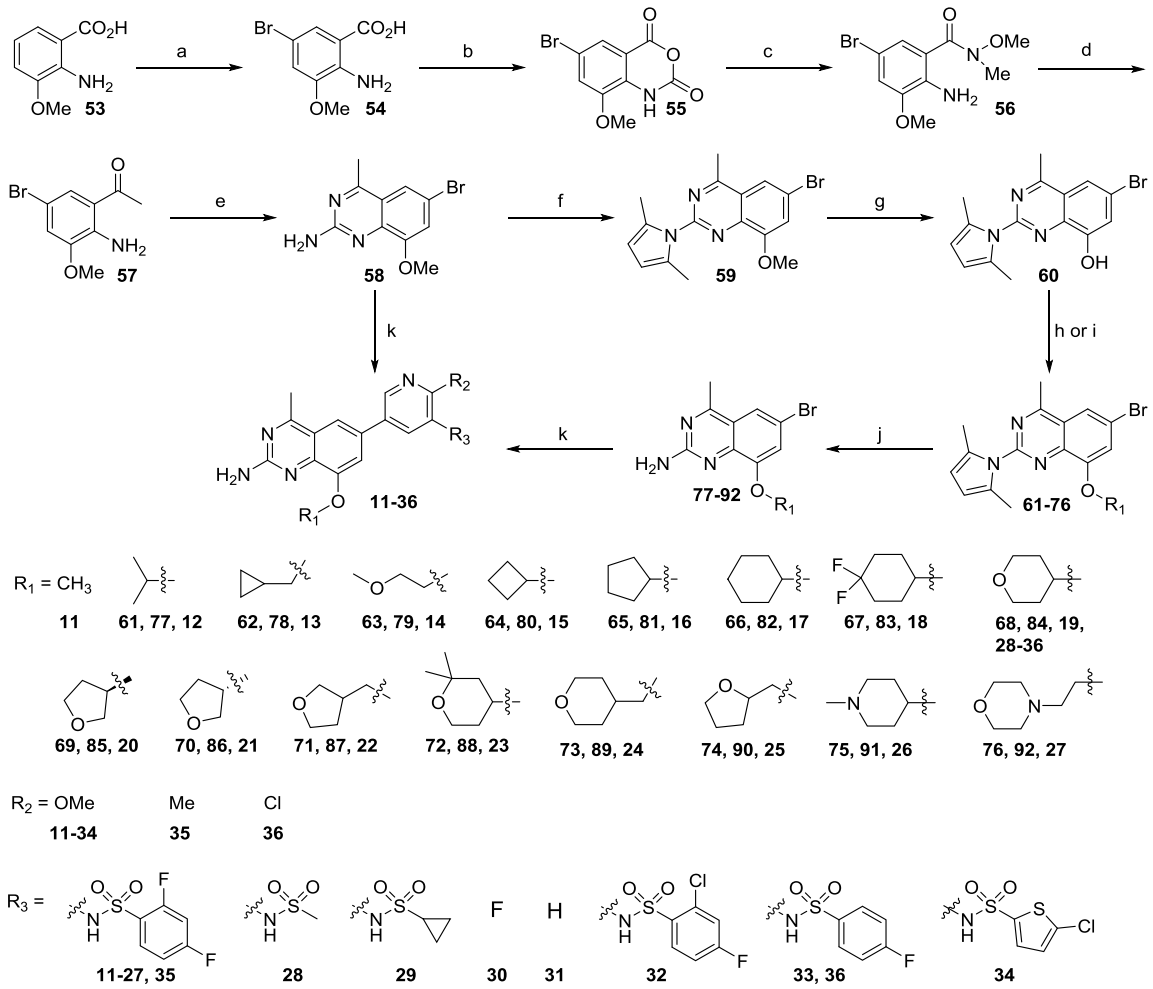

[a] Reagents and conditions: (a) NBS, DMF, rt, 2 h, 95%; (b) triphosgene, THF, reflux, 3 h, 80%; (c) *N*,*O*-dimethylhydroxylamine hydrochloride, TEA, dioxane, reflux, overnight, 91%; (d) CH_3MgBr, THF, -20 ^oC, 30 min, 26%; (e) conc. HCl, 50% cyanamide in water, 120 °C, 15 min, 98%; (f) 2,5-hexanedione, *p*-toluenesulfonic acid, NMP, toluene, 160 °C, 6 h, 87%; (g) $AlCl_3$, DCE, 80 °C, 1.5 h, 77%; (h) alkyl bromide, K_2CO_3, acetonitrile, sealed tube, reflux, overnight, 58-98%; (i) ROH, DEAD, PPh_3, THF, rt, overnight, 42-94%; (j) hydroxylamine hydrochloride, EtOH, H_2O, reflux, overnight, 27-85%; (k) aryl boronic ester, $PdCl_2$(dppf), 2M K_2CO_3, dioxane, 100 ^oC, Ar, 4h, 25-95%.

The synthetic procedure of compound **37-50** is described in scheme 3. Compound **80-82** and **84-89** were alkylated or acylated to afford compound **93-105**, which was then coupled with aryl boronic esters to afford the final products **37-50**.

Scheme 3. Synthesis of compound **37-50**.[a]

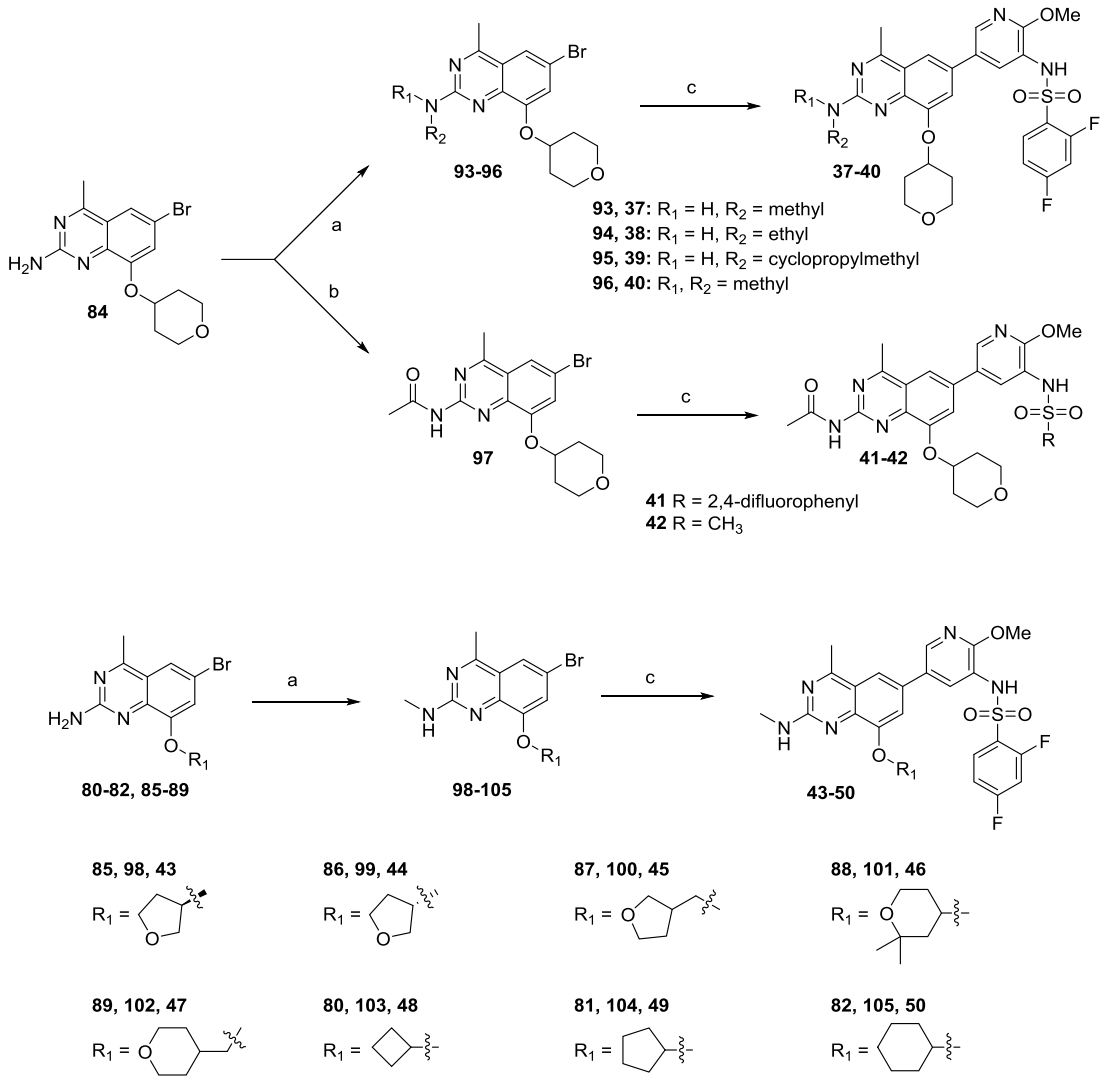

[a] Reagents and conditions: (a) alkyl halide, NaH, DMF, rt, 4 h, 15-31%; (b) acyl chloride, pyridine, DMF, rt, 4 h, 76%; (c) aryl boronic ester, $PdCl_2(dppf)$, 2M K_2CO_3, dioxane, 100 ^oC, Ar, 4h, 30-87%.

CONCLUSION

In summary, we identified a class of novel quinazoline derivatives as highly potent PI3K inhibitors through a hybridization followed by scaffold hopping strategy. Systematic SAR studies led to the discovery of the promising anticancer compounds **19**, **20**, **37** and **43** with favorable drug-like properties. These promising compounds displayed nanomolar enzymatic potencies as well as sub-micromolar anti-proliferative effects on a broad panel of human cancer cell lines. Compound **19**, an exemplar of these compounds, showed excellent kinase selectivity with an S(1) score of 0.015 against 468 kinases and mutants using DiscoverX's Kinomescan assay. The PK profiles of compounds **19**, **20**, **37** and **43** were also favorable. Compared with **19** and **20**, **37** and **43** exhibited higher brain penetration, with AUC values of 895 and 742 ng/g*h at the oral dose of 30 mg/kg, respectively. Several lung cancer and gastric cancer xenograft models were performed to demonstrate the robust in vivo efficacies of these compounds. Of particular note, the HGC-27 gastric xenograft model was the most sensitive to these compounds, showing significant tumor regression. In the orthotopic U87-MG brain xenograft model, compounds **37** and **43** (with reasonable brain penetration properties) were highly effective, with TGIs of >90%, and thus, were comparable to TMZ. Furthermore, preliminary safety assessments including hERG channel inhibition assays, AMES, CYP450 inhibition assays and single-dose toxicity studies demonstrated an acceptable safety profile. Overall, these pharmacological and safety data have compelled us to advance **19** and **43** into formal preclinical evaluations, the results of which will be reported in due course.

Experimental Procedures

Chemistry. Starting materials, solvents, and reagents were commercially available and used without further purification. ^{1}H spectra were recorded on a Varian 400 MHz NMR spectrometer or a JOEL 400 MHz NMR spectrometer, referenced to trimethylsilane (TMS). ^{13}C spectra were recorded on a Bruker 400 MHz or 600 MHz NMR spectrometer. Chemical shifts are expressed as δ units in ppm (in NMR description, s = singlet, d = doublet, t = triplet, q = quartet, m = multiplet, and br = broad peak). Melting points were determined on a Yanaco MP-J3 micro melting point apparatus and the maximum temperature was 300 °C. HRMS spectra were acquired by electrospray ionization (ESI) in positive ion mode using Thermo LCQ Deca XP Max mass spectrometer.

Purity of all compounds tested in biological assays were determined to be >95% by LCMS analysis. The following analytical method was used to determine chemical purity of final compounds: HPLC-Agilent 1100, water with 0.1% formic acid (mobile phase A), acetonitrile (mobile phase B), HALO C18, 2.7 μM, 4.6 x 50 mm, 25 ℃, 5–95% buffer B in 3.0 min, 95% in 2.0 min, 95–5% in 0.1 min, 5% in 0.9 min, 1.8 mL/min, 254 nm, equipped with Agilent G1946D, APCI.

All final compounds passed the PAINS[39] filter using False Positive Remover, Web-GCB13, 2010.[40]

General synthetic procedure for compounds 10-50

A mixture of compound **51**, **58** and **77-105** (1.0 equivalent), aryl boronic acid or ester (1.2 equivalent) and 2M aqueous K_2CO_3 solution (3.0 equivalent) in dioxane was degassed and then $PdCl_2$(dppf) (0.05-0.10 equivalent) was added. The mixture was degassed and back-filled with argon (three cycles), and then stirred at 100 °C under Ar atmosphere for 5 h. The reaction

mixture was cooled to rt, diluted with water and EtOAc, acidified with 2M HCl solution until the pH value was 5-6. The two layers were separated and the aqueous layer was extracted with EtOAc (30 mL×2). The combined organic layers were washed with water and brine, dried over Na_2SO_4, filtered and concentrated. The residue was purified by column chromatography (silica gel, DCM/MeOH = 50:1, v/v) to afford the desired products **10-50.**

***N*-(5-(2-amino-8-((*1r*,*4r*)-4-(2-hydroxyethoxy)cyclohexyl)-4-methyl-7-oxo-7,8-dihydropyrido[2,3-*d*]pyrimidin-6-yl)-2-methoxypyridin-3-yl)-2,4-difluorobenzenesulfonamide (10)**

Compound **10** was prepared from 2-amino-6-bromo-8-((*1r*,*4r*)-4-(2-hydroxyethoxy)cyclohexyl)-4-methylpyrido[2,3-*d*]pyrimidin-7(8*H*)-one (**51**) and *N*-(2-methoxy-5-(4,4,5,5-tetramethyl-1,3,2-dioxaborolan-2-yl)pyridin-3-yl)-2,4-difluorobenzenesulfonamide (yellow solid, 53% yield).^{1}H NMR (400 MHz,) δ 10.19 (s, 1H), 8.27 (d, *J* = 2.3 Hz, 1H), 7.99 (s, 1H), 7.93 (d, *J* = 2.1 Hz, 1H), 7.73 (td, *J* = 8.6, 6.3 Hz, 1H), 7.58 (ddd, *J* = 10.5, 9.3, 2.5 Hz, 1H), 7.26 – 7.11 (m, 3H), 5.44 (br s, 1H), 4.56 (t, *J* = 4.8 Hz, 1H), 3.63 (s, 3H), 3.55 – 3.35 (m, 5H), 3.07 – 2.63 (m, 2H), 2.55 (s, 3H), 2.18 – 2.06 (m, 2H), 1.64 – 1.50 (m, 2H), 1.34 – 1.20 (m, 2H). HRMS (ESI): m/z $[M + H]^+$ calcd for $C_{28}H_{31}O_6N_6F_2S$, 617.1988, found: 617.1975.

***N*-(5-(2-amino-8-methoxy-4-methylquinazolin-6-yl)-2-methoxypyridin-3-yl)-2,4-difluorobenzenesulfonamide (11)**

Compound **11** was prepared from compound **58** and *N*-(2-methoxy-5-(4,4,5,5-tetramethyl-1,3,2-dioxaborolan-2-yl)pyridin-3-yl)-2,4-difluorobenzenesulfonamide (yellow solid, 41% yield). ^{1}H NMR (400 MHz, DMSO-d_6) δ 10.28 (s, 1H), 8.46 (d, *J* = 2.4 Hz, 1H), 7.97 (d, *J* = 2.4 Hz, 1H), 7.76 (dt, *J* = 8.6, 6.4 Hz, 1H), 7.65 (d, *J* = 1.7 Hz, 1H), 7.63 – 7.55 (m, 1H), 7.31 (d, *J* = 1.7 Hz, 1H), 7.26 – 7.18 (m, 1H), 6.83 (s, 2H), 3.95 (s, 3H), 3.64 (s, 3H), 2.76 (s, 3H). ^{13}C NMR

(101 MHz, DMSO-d_6) δ 169.5, 165.1 (dd, $J_{C\text{-}F}$ = 255, 11.8 Hz), 159.7, 159.4 (dd, $J_{C\text{-}F}$ = 263, 13.6 Hz), 157.5, 153.5, 143.5, 142.6, 134.6, 131.9 (d, $J_{C\text{-}F}$ = 10.8 Hz), 129.9, 129.0, 125.3 (dd, $J_{C\text{-}F}$ = 14.5, 3.6 Hz), 119.4, 119.3, 114.5, 111.8 (dd, $J_{C\text{-}F}$ = 22.2, 3.4 Hz), 110.4, 105.8 (t, $J_{C\text{-}F}$ = 26.2 Hz), 55.6, 53.3, 21.7. HRMS (ESI): m/z $[M + H]^+$ calcd for $C_{22}H_{20}O_4N_5F_2S$, 488.1199, found: 488.1194.

***N*-(5-(2-amino-8-isopropoxy-4-methylquinazolin-6-yl)-2-methoxypyridin-3-yl)-2,4-difluorobenzenesulfonamide (12)**

Compound **12** was prepared from compound **77** and *N*-(2-methoxy-5-(4,4,5,5-tetramethyl-1,3,2-dioxaborolan-2-yl)pyridin-3-yl)-2,4-difluorobenzenesulfonamide (yellow solid, 63% yield).^{1}H NMR (400 MHz, DMSO-d_6) δ 10.30 (s, 1H), 8.44 (d, J = 2.3 Hz, 1H), 7.94 (d, J = 2.3 Hz, 1H), 7.76 (dt, J = 8.6, 6.4 Hz, 1H), 7.64 (d, J = 1.6 Hz, 1H), 7.63 – 7.56 (m, 1H), 7.33 (s, 1H), 7.22 (dt, J = 8.4, 2.0 Hz, 1H), 6.83 (s, 2H), 5.00 – 4.89 (m, 1H), 3.64 (s, 3H), 2.75 (s, 3H), 1.34 (d, J = 6.0 Hz, 6H). ^{13}C NMR (151 MHz, DMSO-d_6) δ 169.4, 165.0 (dd, $J_{C\text{-}F}$ = 254, 11.7 Hz), 159.44, 159.38 (dd, $J_{C\text{-}F}$ = 258, 13.4 Hz), 157.3, 151.5, 144.2, 142.4, 134.3, 131.8 (d, $J_{C\text{-}F}$ = 10.7 Hz), 129.8, 129.0, 125.3 (dd, $J_{C\text{-}F}$ = 14.2, 2.6 Hz), 119.7, 119.6, 114.6, 113.4, 111.8 (dd, $J_{C\text{-}F}$ = 22.0, 2.6 Hz), 105.8 (t, $J_{C\text{-}F}$ = 26.1 Hz), 69.9, 53.3, 21.8, 21.7. HRMS (ESI): m/z $[M + H]^+$ calcd for $C_{24}H_{24}O_4N_5F_2S$, 516.1512, found: 516.1488.

***N*-(5-(2-amino-8-(cyclopropylmethoxy)-4-methylquinazolin-6-yl)-2-methoxypyridin-3-yl)-2,4-difluorobenzenesulfonamide (13)**

Compound **13** was prepared from compound **78** and *N*-(2-methoxy-5-(4,4,5,5-tetramethyl-1,3,2-dioxaborolan-2-yl)pyridin-3-yl)-2,4-difluorobenzenesulfonamide (yellow solid, 35% yield).^{1}H NMR (400 MHz, DMSO-d_6) δ 10.27 (s, 1H), 8.43 (d, J = 2.2 Hz, 1H), 7.94 (d, J = 2.2 Hz, 1H), 7.75 (dt, J = 8.6, 6.4 Hz, 1H), 7.63 (d, J = 1.6 Hz, 1H), 7.62 – 7.55 (m, 1H), 7.27 (d, J =

1.6 Hz, 1H), 7.24 – 7.18 (m, 1H), 6.85 (br s, 2H), 4.00 (d, J = 7.0 Hz, 2H), 3.63 (s, 3H), 2.75 (s, 3H), 1.37 – 1.27 (m, 1H), 0.67 – 0.57 (m, 2H), 0.40 – 0.33 (m, 2H). ^{13}C NMR (101 MHz, DMSO-d_6) δ 169.4, 165.0 (dd, $J_{C\text{-}F}$ = 255, 11.8 Hz), 159.6, 159.4 (dd, $J_{C\text{-}F}$ = 259, 13.5 Hz), 157.4, 152.9, 143.5, 142.6, 134.7, 131.8 (d, $J_{C\text{-}F}$ = 10.7 Hz), 129.9, 129.0, 125.3 (dd, $J_{C\text{-}F}$ = 14.4, 3.6 Hz), 119.4, 114.4, 111.8 (dd, $J_{C\text{-}F}$ = 22.2, 3.2 Hz), 111.4, 105.8 (t, $J_{C\text{-}F}$ = 26.2 Hz), 73.0, 53.2, 21.7, 10.2, 3.5. HRMS (ESI): m/z $[M + H]^+$ calcd for $C_{25}H_{24}O_4N_5F_2S$, 528.1512, found: 528.1487.

_N_-(5-(2-amino-8-(2-methoxyethoxy)-4-methylquinazolin-6-yl)-2-methoxypyridin-3-yl)-2,4-difluorobenzenesulfonamide (14)

Compound **14** was prepared from compound **79** and *N*-(2-methoxy-5-(4,4,5,5-tetramethyl-1,3,2-dioxaborolan-2-yl)pyridin-3-yl)-2,4-difluorobenzenesulfonamide (yellow solid, 56% yield).^{1}H NMR (400 MHz, DMSO-d_6) δ 10.32 (br s, 1H), 8.43 (s, 1H), 7.95 (s, 1H), 7.76 (dt, J = 8.5, 6.6 Hz, 1H), 7.64 (d, J = 1.4 Hz, 1H), 7.63 – 7.55 (m, 1H), 7.34 (d, J = 1.4 Hz, 1H), 7.22 (dt, J = 8.4, 2.4 Hz, 1H), 6.87 (s, 2H), 4.35 – 4.28 (m, 2H), 3.79 – 3.73 (m, 2H), 3.64 (s, 3H), 3.35 (s, 3H), 2.75 (s, 3H). HRMS (ESI): m/z $[M + H]^+$ calcd for $C_{24}H_{24}O_5N_5F_2S$, 532.1461, found: 532.1445.

_N_-(5-(2-amino-8-cyclobutoxy-4-methylquinazolin-6-yl)-2-methoxypyridin-3-yl)-2,4-difluorobenzenesulfonamide (15)

Compound **15** was prepared from compound **80** and *N*-(2-methoxy-5-(4,4,5,5-tetramethyl-1,3,2-dioxaborolan-2-yl)pyridin-3-yl)-2,4-difluorobenzenesulfonamide (yellow solid, 50% yield).^{1}H NMR (400 MHz, DMSO-d_6) δ 10.30 (s, 1H), 8.42 (d, J = 2.3 Hz, 1H), 7.92 (d, J = 2.3 Hz, 1H), 7.77 (dt, J = 8.6, 6.4 Hz, 1H), 7.64 (d, J = 1.6 Hz, 1H), 7.63 – 7.55 (m, 1H), 7.23 (dt, J = 8.6, 2.4 Hz, 1H), 7.12 (d, J = 1.6 Hz, 1H), 6.84 (s, 2H), 4.94 (p, J = 7.2 Hz, 1H), 3.66 (s, 3H),

2.75 (s, 3H), 2.55 – 2.46 (m, 2H), 2.19 – 2.06 (m, 2H), 1.89 – 1.62 (m, 2H). ^{13}C NMR (101 MHz, DMSO-d_6) δ 169.5, 165.1 (dd, $J_{C\text{-}F}$ = 255, 11.8 Hz), 159.6, 159.4 (dd, $J_{C\text{-}F}$ = 259, 13.6 Hz), 157.3, 151.1, 143.4, 142.4, 134.2, 131.8 (d, $J_{C\text{-}F}$ = 10.8 Hz), 129.8, 128.9, 125.3 (dd, $J_{C\text{-}F}$ = 14.4, 3.7 Hz), 119.520, 119.497, 114.5, 111.84 (dd, $J_{C\text{-}F}$ = 21.9, 3.5 Hz), 111.79, 105.8 (t, $J_{C\text{-}F}$ = 26.2 Hz), 71.1, 53.3, 30.1, 21.7, 12.9. HRMS (ESI): m/z $[M + H]^+$ calcd for $C_{25}H_{24}O_4N_5F_2S$, 528.1512, found: 528.1494.

_N_-(5-(2-amino-8-(cyclopentyloxy)-4-methylquinazolin-6-yl)-2-methoxypyridin-3-yl)-2,4-difluorobenzenesulfonamide (16)

Compound **16** was prepared from compound **81** and *N*-(2-methoxy-5-(4,4,5,5-tetramethyl-1,3,2-dioxaborolan-2-yl)pyridin-3-yl)-2,4-difluorobenzenesulfonamide (yellow solid, 54% yield).^{1}H NMR (400 MHz, DMSO-d_6) δ 10.30 (s, 1H), 8.43 (d, J = 2.4 Hz, 1H), 7.93 (d, J = 2.4 Hz, 1H), 7.77 (dt, J = 8.4, 6.4 Hz, 1H), 7.63 (d, J = 1.8 Hz, 1H), 7.63 – 7.56 (m, 1H), 7.27 (d, J = 1.6 Hz, 1H), 7.22 (dt, J = 8.4, 2.2 Hz, 1H), 6.79 (s, 2H), 5.14 – 5.08 (m, 1H), 3.66 (s, 3H), 2.75 (s, 3H), 2.10 – 1.93 (m, 2H), 1.88 – 1.69 (m, 4H), 1.69 – 1.51 (m, 2H). ^{13}C NMR (151 MHz, DMSO-d_6) δ 169.4, 165.0 (dd, $J_{C\text{-}F}$ = 254, 11.6 Hz), 159.5, 159.4 (dd, $J_{C\text{-}F}$ = 258, 13.4 Hz), 157.3, 151.8, 144.0, 142.3, 134.2, 131.8 (d, $J_{C\text{-}F}$ = 10.7 Hz), 129.8, 128.9, 125.3 (dd, $J_{C\text{-}F}$ = 14.3, 3.0 Hz), 119.6 (×2), 114.4, 113.0, 111.8 (dd, $J_{C\text{-}F}$ = 22.2, 2.6 Hz), 105.8 (t, $J_{C\text{-}F}$ = 26.1 Hz), 79.4, 53.3, 32.2, 23.9, 21.7. HRMS (ESI): m/z $[M + H]^+$ calcd for $C_{26}H_{26}O_4N_5F_2S$, 542.1668, found: 542.1651.

_N_-(5-(2-amino-8-(cyclohexyloxy)-4-methylquinazolin-6-yl)-2-methoxypyridin-3-yl)-2,4-difluorobenzenesulfonamide (17)

Compound **17** was prepared from compound **82** and *N*-(2-methoxy-5-(4,4,5,5-tetramethyl-1,3,2-dioxaborolan-2-yl)pyridin-3-yl)-2,4-difluorobenzenesulfonamide as a yellow foamed solid

(51% yield).[1]H NMR (400 MHz, DMSO-d_6) δ 10.28 (s, 1H), 8.42 (d, J = 2.3 Hz, 1H), 7.93 (d, J = 2.3 Hz, 1H), 7.76 (dt, J = 8.4, 6.4 Hz, 1H), 7.63 (d, J = 1.6 Hz, 1H), 7.62 – 7.56 (m, 1H), 7.36 (d, J = 1.4 Hz, 1H), 7.22 (dt, J = 8.4, 2.0 Hz, 1H), 6.76 (s, 2H), 4.70 – 4.60 (m, 1H), 3.65 (s, 3H), 2.74 (s, 3H), 2.09 – 1.97 (m, 2H), 1.85 – 1.71 (m, 2H), 1.66 – 1.30 (m, 6H). ^{13}C NMR (101 MHz, DMSO-d_6) δ 169.5, 165.0 (dd, $J_{C\text{-}F}$ = 255, 11.8 Hz), 159.41 (dd, $J_{C\text{-}F}$ = 259, 13.6 Hz), 159.40, 157.3, 151.3, 144.3, 142.5, 134.4, 131.8 (d, $J_{C\text{-}F}$ = 10.7 Hz), 129.8, 129.0, 125.3 (dd, $J_{C\text{-}F}$ = 14.4, 3.6 Hz), 119.8, 119.4, 114.8, 113.9, 111.8 (dd, $J_{C\text{-}F}$ = 22.6, 3.3 Hz), 105.8 (t, $J_{C\text{-}F}$ = 26.2 Hz), 75.4, 53.3, 31.5, 25.2, 23.6, 21.7. HRMS (ESI): m/z $[M + H]^+$ calcd for $C_{27}H_{28}O_4N_5F_2S$, 556.1825, found: 556.1801.

_N_-(5-(2-amino-8-((4,4-difluorocyclohexyl)oxy)-4-methylquinazolin-6-yl)-2-methoxypyridin-3-yl)-2,4-difluorobenzenesulfonamide (18)

Compound **18** was prepared from compound **83** and *N*-(2-methoxy-5-(4,4,5,5-tetramethyl-1,3,2-dioxaborolan-2-yl)pyridin-3-yl)-2,4-difluorobenzenesulfonamide (yellow oil, 84% yield).[1]H NMR (400 MHz, DMSO-d_6) δ 10.28 (s, 1H), 8.43 (d, J = 2.2 Hz, 1H), 7.96 (d, J = 2.2 Hz, 1H), 7.76 (dt, J = 8.4, 6.6 Hz, 1H), 7.69 (d, J = 1.4 Hz, 1H), 7.63 – 7.54 (m, 1H), 7.50 (d, J = 1.4 Hz, 1H), 7.22 (dt, J = 8.4, 2.0 Hz, 1H), 6.76 (s, 2H), 4.97 – 4.88 (m, 1H), 3.64 (s, 3H), 2.76 (s, 3H), 2.28 – 2.11 (m, 2H), 2.08 – 1.81 (m, 6H). ^{13}C NMR (151 MHz, DMSO-d_6) δ 169.6, 165.0 (dd, $J_{C\text{-}F}$ = 254, 11.6 Hz), 159.44, 159.40 (dd, $J_{C\text{-}F}$ = 258, 13.4 Hz), 157.4, 151.0, 144.6, 142.6, 134.6, 131.8 (d, $J_{C\text{-}F}$ = 10.7 Hz), 129.6, 129.0, 125.3 (dd, $J_{C\text{-}F}$ = 14.3, 2.3 Hz), 123.8 (t, $J_{C\text{-}F}$ = 240 Hz), 119.8, 119.5, 115.68, 115.62, 111.8 (dd, $J_{C\text{-}F}$ = 22.0, 2.4 Hz), 105.8 (t, $J_{C\text{-}F}$ = 26.0 Hz), 72.3, 53.2, 29.9 (t, $J_{C\text{-}F}$ = 24.2 Hz), 27.0 (t, $J_{C\text{-}F}$ = 4.3 Hz), 21.7. HRMS (ESI): m/z $[M + H]^+$ calcd for $C_{27}H_{26}O_4N_5F_4S$, 592.1636, found: 592.1616.

_N_-(5-(2-amino-4-methyl-8-((tetrahydro-2_H_-pyran-4-yl)oxy)quinazolin-6-yl)-2-methoxypyridin-3-yl)-2,4-difluorobenzenesulfonamide (19)

Compound **19** was prepared from compound **84** and *N*-(2-methoxy-5-(4,4,5,5-tetramethyl-1,3,2-dioxaborolan-2-yl)pyridin-3-yl)-2,4-difluorobenzenesulfonamide (yellow solid, 45% yield). ^{1}H NMR (400 MHz, DMSO-d_6) δ 10.29 (s, 1H), 8.44 (d, J = 2.2 Hz, 1H), 7.96 (d, J = 2.2 Hz, 1H), 7.76 (dt, J = 8.4, 2.4 Hz, 1H), 7.66 (d, J = 1.2 Hz, 1H), 7.64 – 7.54 (m, 1H), 7.46 (d, J = 1.2 Hz, 1H), 7.23 (dt, J = 8.6, 2.0 Hz, 1H), 6.79 (s, 2H), 4.97 – 4.82 (m, 1H), 3.98 – 3.89 (m, 2H), 3.64 (s, 3H), 3.56 – 3.45 (m, 2H), 2.75 (s, 3H), 2.10 – 1.99 (m, 2H), 1.75 – 1.58 (m, 2H). ^{13}C NMR (101 MHz, DMSO-d_6) δ 169.6, 165.1 (dd, $J_{C\text{-}F}$ = 254, 11.8 Hz), 159.5, 159.4 (dd, $J_{C\text{-}F}$ = 259, 13.5 Hz), 157.4, 150.9, 144.4, 142.7, 134.7, 131.8 (d, $J_{C\text{-}F}$ = 10.7 Hz), 129.7, 129.0, 125.3 (dd, $J_{C\text{-}F}$ = 14.5, 3.5 Hz), 119.8, 119.4, 115.3, 114.7, 111.8 (dd, $J_{C\text{-}F}$ = 22.2, 3.4 Hz), 105.8 (t, $J_{C\text{-}F}$ = 26.3 Hz), 72.6, 64.9, 53.3, 32.0, 21.7. HRMS (ESI): m/z [M + H]$^+$ calcd for $C_{26}H_{26}O_5N_5F_2S$, 558.1617, found: 558.1595.

(_R_)-_N_-(5-(2-amino-4-methyl-8-((tetrahydrofuran-3-yl)oxy)quinazolin-6-yl)-2-methoxypyridin-3-yl)-2,4-difluorobenzenesulfonamide (20)

Compound **20** was prepared from compound **85** and *N*-(2-methoxy-5-(4,4,5,5-tetramethyl-1,3,2-dioxaborolan-2-yl)pyridin-3-yl)-2,4-difluorobenzenesulfonamide (yellow solid, 34% yield).^{1}H NMR (400 MHz, DMSO-d_6) δ 10.28 (s, 1H), 8.44 (d, J = 2.3 Hz, 1H), 7.97 (d, J = 2.3 Hz, 1H), 7.82 – 7.72 (m, 1H), 7.67 (d, J = 1.5 Hz, 1H), 7.64 – 7.53 (m, 1H), 7.32 (d, J = 1.5 Hz, 1H), 7.22 (dt, J = 8.4, 2.0 Hz, 1H), 6.83 (s, 2H), 5.43 – 5.29 (m, 1H), 4.02 – 3.85 (m, 3H), 3.83 – 3.74 (m, 1H), 3.65 (s, 3H), 2.75 (s, 3H), 2.35 – 2.22 (m, 1H), 2.08 – 2.01 (m, 1H). ^{13}C NMR (101 MHz, DMSO-d_6) δ 169.5, 165.1 (dd, $J_{C\text{-}F}$ = 255, 11.7 Hz), 159.6, 159.4 (dd, $J_{C\text{-}F}$ = 258, 13.6 Hz), 157.4, 151.3, 144.0, 142.5, 134.5, 131.8 (d, $J_{C\text{-}F}$ = 10.8 Hz), 129.7, 128.9, 125.3 (dd, $J_{C\text{-}F}$ = 14.2,

3.1 Hz), 119.6, 119.5, 115.1, 113.3, 111.8 (dd, $J_{C\text{-}F}$ = 21.6, 2.4 Hz), 105.8 (t, J = 26.2 Hz), 78.0, 72.3, 66.6, 53.3, 32.3, 21.7. HRMS (ESI): m/z $[M + H]^+$ calcd for $C_{25}H_{24}O_5N_5F_2S$, 544.1461, found: 544.1453.

(*S*)-*N*-(5-(2-amino-4-methyl-8-((tetrahydrofuran-3-yl)oxy)quinazolin-6-yl)-2-methoxypyridin-3-yl)-2,4-difluorobenzenesulfonamide (21)

Compound **21** was prepared from compound **86** and *N*-(2-methoxy-5-(4,4,5,5-tetramethyl-1,3,2-dioxaborolan-2-yl)pyridin-3-yl)-2,4-difluorobenzenesulfonamide (yellow solid, 48% yield). ^{1}H NMR (400 MHz, DMSO-d_6) δ 10.28 (s, 1H), 8.44 (d, J = 2.3 Hz, 1H), 7.97 (d, J = 2.3 Hz, 1H), 7.76 (dt, J = 8.6, 6.4 Hz, 1H), 7.67 (d, J = 1.6 Hz, 1H), 7.64 – 7.53 (m, 1H), 7.32 (d, J = 1.6 Hz, 1H), 7.22 (dt, J = 8.6, 2.3 Hz, 1H), 6.84 (s, 2H), 5.43 – 5.29 (m, 1H), 4.00 – 3.85 (m, 3H), 3.83 – 3.73 (m, 1H), 3.65 (s, 3H), 2.75 (s, 3H), 2.35 – 2.22 (m, 1H), 2.12 – 2.01 (m, 1H). ^{13}C NMR (101 MHz, DMSO-d_6) δ 169.7, 165.1 (dd, $J_{C\text{-}F}$ = 255, 11.6 Hz), 159.5, 159.4 (dd, $J_{C\text{-}F}$ = 259, 13.7 Hz), 157.4, 151.2, 143.8, 142.6, 134.7, 131.8 (d, $J_{C\text{-}F}$ = 10.6 Hz), 129.7, 128.9, 125.3 (dd, $J_{C\text{-}F}$ = 14.3, 3.7 Hz), 119.6, 119.4, 115.1, 113.3, 111.8 (dd, $J_{C\text{-}F}$ = 22.1, 3.3 Hz), 105.8 (t, J = 26.3 Hz), 78.0, 72.3, 66.6, 53.3, 32.3, 21.8. HRMS (ESI): m/z $[M + H]^+$ calcd for $C_{25}H_{24}O_5N_5F_2S$, 544.1461, found: 544.1453.

***N*-(5-(2-amino-4-methyl-8-((tetrahydrofuran-3-yl)methoxy)quinazolin-6-yl)-2-methoxypyridin-3-yl)-2,4-difluorobenzenesulfonamide (22)**

Compound **22** was prepared from compound **87** and *N*-(2-methoxy-5-(4,4,5,5-tetramethyl-1,3,2-dioxaborolan-2-yl)pyridin-3-yl)-2,4-difluorobenzenesulfonamide (yellow solid, 61% yield). ^{1}H NMR (400 MHz, DMSO-d_6) δ 10.27 (s, 1H), 8.45 (d, J = 2.2 Hz, 1H), 7.97 (d, J = 2.2 Hz, 1H), 7.75 (dt, J = 8.4, 6.4 Hz, 1H), 7.66 (d, J = 1.2 Hz, 1H), 7.63 – 7.54 (m, 1H), 7.38 (d, J = 1.2 Hz, 1H), 7.21 (dt, J = 8.4, 2.2 Hz, 1H), 6.80 (s, 2H), 4.19 – 4.03 (m, 2H), 3.85 – 3.77 (m, 2H),

3.73 – 3.60 (m, 5H), 2.85 – 2.70 (m, 4H), 2.12 – 1.99 (m, 1H), 1.79 – 1.69 (m, 1H). ^{13}C NMR (151 MHz, DMSO-d_6) δ 169.4, 165.0 (dd, $J_{C\text{-}F}$ = 254, 11.7 Hz), 159.6, 159.4 (dd, $J_{C\text{-}F}$ = 258, 13.4 Hz), 157.4, 152.8, 143.6, 142.6, 134.6, 131.8 (d, $J_{C\text{-}F}$ = 10.7 Hz), 129.8, 129.0, 125.3 (dd, $J_{C\text{-}F}$ = 14.3, 3.2 Hz), 119.50, 119.5, 114.8, 112.1, 111.7 (dd, $J_{C\text{-}F}$ = 22.2, 2.6 Hz), 105.8 (t, $J_{C\text{-}F}$ = 26.1 Hz), 70.5, 70.0, 66.8, 53.2, 38.2, 28.7, 21.7. HRMS (ESI): m/z $[M + H]^+$ calcd for $C_{26}H_{26}O_5N_5F_2S$, 558.1617, found: 558.1609.

_N_-(5-(2-amino-8-((2,2-dimethyltetrahydro-2_H_-pyran-4-yl)oxy)-4-methylquinazolin-6-yl)-2-methoxypyridin-3-yl)-2,4-difluorobenzenesulfonamide (23)

Compound **23** was prepared from compound **88** and *N*-(2-methoxy-5-(4,4,5,5-tetramethyl-1,3,2-dioxaborolan-2-yl)pyridin-3-yl)-2,4-difluorobenzenesulfonamide as a yellow foamed solid (60% yield).^{1}H NMR (400 MHz, DMSO-d_6) δ 10.29 (s, 1H), 8.44 (d, J = 2.3 Hz, 1H), 7.96 (d, J = 2.3 Hz, 1H), 7.76 (dt, J = 8.6, 6.4 Hz, 1H), 7.65 (d, J = 1.6 Hz, 1H), 7.63 – 7.54 (m, 1H), 7.44 (d, J = 1.6 Hz, 1H), 7.22 (dt, J = 8.4, 2.4 Hz, 1H), 6.78 (s, 2H), 5.08 – 4.93 (m, 1H), 3.82 – 3.66 (m, 2H), 3.65 (s, 3H), 2.75 (s, 3H), 2.13 – 1.93 (m, 2H), 1.59 – 1.41 (m, 2H), 1.25 (s, 3H), 1.22 (s, 3H). ^{13}C NMR (101 MHz, DMSO-d_6) δ 169.5, 165.0 (dd, $J_{C\text{-}F}$ = 255, 11.8 Hz), 159.5, 159.4 (dd, $J_{C\text{-}F}$ = 259, 13.5 Hz), 157.4, 150.9, 144.3, 142.6, 134.5, 131.8 (d, $J_{C\text{-}F}$ = 10.7 Hz), 129.7, 129.0, 125.3 (dd, $J_{C\text{-}F}$ = 14.5, 3.6 Hz), 119.8, 119.5, 115.1, 114.1, 111.8 (dd, $J_{C\text{-}F}$ = 22.3, 3.2 Hz), 105.8 (t, $J_{C\text{-}F}$ = 26.3 Hz), 72.3, 71.2, 59.1, 53.3, 42.0, 32.0, 30.8, 23.3, 21.7. HRMS (ESI): m/z $[M + H]^+$ calcd for $C_{28}H_{30}O_5N_5F_2S$, 586.1930, found: 586.1920.

_N_-(5-(2-amino-4-methyl-8-((tetrahydro-2_H_-pyran-4-yl)methoxy)quinazolin-6-yl)-2-methoxypyridin-3-yl)-2,4-difluorobenzenesulfonamide (24)

Compound **24** was prepared from compound **89** and *N*-(2-methoxy-5-(4,4,5,5-tetramethyl-1,3,2-dioxaborolan-2-yl)pyridin-3-yl)-2,4-difluorobenzenesulfonamide (yellow solid, 36%

yield).[1]H NMR (400 MHz, DMSO-d_6) δ 10.28 (s, 1H), 8.45 (d, J = 2.1 Hz, 1H), 7.97 (d, J = 2.2 Hz, 1H), 7.76 (dt, J = 8.6, 6.4 Hz, 1H), 7.64 (s, 1H), 7.63 – 7.55 (m, 1H), 7.34 (s, 1H), 7.22 (dt, J = 8.6, 2.4 Hz, 1H), 6.79 (s, 2H), 4.05 (d, J = 6.6 Hz, 2H), 3.90 (dd, J = 11.0, 3.0 Hz, 2H), 3.64 (s, 3H), 3.37 (t, J = 11.0 Hz, 2H), 2.75 (s, 3H), 2.20 – 2.05 (m, 1H), 1.84 – 1.74 (m, 2H), 1.38 (qd, J = 12.2, 4.2 Hz, 2H). ^{13}C NMR (101 MHz, DMSO-d_6) δ 169.4, 165.0 (dd, $J_{C\text{-}F}$ = 255, 11.8 Hz), 159.6, 159.4 (dd, $J_{C\text{-}F}$ = 259, 13.1 Hz), 157.4, 152.8, 143.6, 142.6, 134.6, 131.8 (d, $J_{C\text{-}F}$ = 10.7 Hz), 129.9, 129.0, 125.3 (d, $J_{C\text{-}F}$ = 13.5 Hz), 119.4 (×2), 114.5, 111.8 (dd, $J_{C\text{-}F}$ = 21.4, 2.0 Hz), 111.6, 105.8 (t, J = 26.2 Hz), 72.9, 66.6, 53.3, 34.4, 29.4, 21.7. HRMS (ESI): m/z $[M + H]^+$ calcd for $C_{27}H_{28}O_5N_5F_2S$, 572.1774, found: 572.1761.

_N_-(5-(2-amino-4-methyl-8-((tetrahydrofuran-2-yl)methoxy)quinazolin-6-yl)-2-methoxypyridin-3-yl)-2,4-difluorobenzenesulfonamide (25)

Compound **25** was prepared from compound **90** and *N*-(2-methoxy-5-(4,4,5,5-tetramethyl-1,3,2-dioxaborolan-2-yl)pyridin-3-yl)-2,4-difluorobenzenesulfonamide (yellow solid, 57% yield).[1]H NMR (400 MHz, DMSO-d_6) δ 10.28 (s, 1H), 8.45 (d, J = 2.3 Hz, 1H), 7.97 (d, J = 2.3 Hz, 1H), 7.76 (dt, J = 8.6, 6.4 Hz, 1H), 7.65 (d, J = 1.6 Hz, 1H), 7.63 – 7.55 (m, 1H), 7.37 (d, J = 1.6 Hz, 1H), 7.22 (dt, J = 8.4, 2.0 Hz, 1H), 6.85 (s, 2H), 4.32 – 4.22 (m, 1H), 4.20 – 4.08 (m, 2H), 3.87 – 3.79 (m, 1H), 3.71 (dt, J = 7.6, 6.4 Hz, 1H), 3.64 (s, 3H), 2.75 (s, 3H), 2.11 – 2.00 (m, 1H), 2.00 – 1.80 (m, 2H), 1.78 – 1.67 (m, 1H). ^{13}C NMR (101 MHz, DMSO-d_6) δ 169.5, 165.1 (dd, $J_{C\text{-}F}$ = 255, 11.8 Hz), 159.6, 159.4 (dd, $J_{C\text{-}F}$ = 259, 13.5 Hz), 157.4, 152.8, 143.4, 142.7, 134.7, 131.8 (d, $J_{C\text{-}F}$ = 10.9 Hz), 129.9, 129.0, 125.3 (dd, $J_{C\text{-}F}$ = 14.5, 3.6 Hz), 119.4 (×2), 114.7, 111.8 (dd, $J_{C\text{-}F}$ = 21.9, 3.0 Hz), 111.7, 105.8 (t, J = 26.2 Hz), 76.6, 71.1, 67.4, 53.3, 27.9, 25.1, 21.8. HRMS (ESI): m/z $[M + H]^+$ calcd for $C_{26}H_{26}O_5N_5F_2S$, 558.1617, found: 558.1608.

_N_-(5-(2-amino-4-methyl-8-((1-methylpiperidin-4-yl)oxy)quinazolin-6-yl)-2-methoxypyridin-3-yl)-2,4-difluorobenzenesulfonamide (26)

Compound **26** was prepared from compound **91** and *N*-(2-methoxy-5-(4,4,5,5-tetramethyl-1,3,2-dioxaborolan-2-yl)pyridin-3-yl)-2,4-difluorobenzenesulfonamide (yellow solid, 53% yield).^{1}H NMR (400 MHz, DMSO-d_6) δ 10.56 (br s, 1H), 8.40 (d, J = 2.4 Hz, 1H), 7.94 (d, J = 2.4 Hz, 1H), 7.76 (dt, J = 8.6, 6.4 Hz, 1H), 7.71 (d, J = 1.6 Hz, 1H), 7.61 – 7.51 (m, 2H), 7.22 (dt, J = 8.4, 2.1 Hz, 1H), 6.84 (s, 2H), 4.95 – 4.85 (m, 1H), 3.64 (s, 3H), 3.10 – 2.95(m, 2H), 2.76 (s, 3H), 2.69 (s, 3H), 2.25 – 2.13 (m, 2H), 2.07 – 1.95(m, 2H). ^{13}C NMR (101 MHz, DMSO-d_6) δ 169.7, 164.9 (dd, $J_{C\text{-}F}$ = 254, 11.7 Hz), 159.5, 159.4 (dd, $J_{C\text{-}F}$ = 258, 13.5 Hz), 157.5, 150.7, 144.6, 141. 8, 133.9, 131.8 (d, $J_{C\text{-}F}$ = 10.5 Hz), 129.5, 129.3, 125.8 (dd, $J_{C\text{-}F}$ = 14.6, 3.3 Hz), 120.6, 119.9, 116.1, 111.7 (dd, $J_{C\text{-}F}$ = 22.1, 3.2 Hz), 105.7 (t, $J_{C\text{-}F}$ = 26.2 Hz), 70.7, 53.2, 50.7, 42.6, 27.8, 21.7. HRMS (ESI): m/z $[M + H]^+$ calcd for $C_{27}H_{29}O_4N_6F_2S$, 571.1934, found: 571.1924.

_N_-(5-(2-amino-4-methyl-8-(2-morpholinoethoxy)quinazolin-6-yl)-2-methoxypyridin-3-yl)-2,4-difluorobenzenesulfonamide (27)

Compound **27** was prepared from compound **92** and *N*-(2-methoxy-5-(4,4,5,5-tetramethyl-1,3,2-dioxaborolan-2-yl)pyridin-3-yl)-2,4-difluorobenzenesulfonamide (yellow foamed solid, 69% yield).^{1}H NMR (400 MHz, DMSO-d_6) δ 8.44 (d, J = 2.2 Hz, 1H), 7.97 (d, J = 2.2 Hz, 1H), 7.76 (dt, J = 8.6, 6.4 Hz, 1H), 7.65 (d, J = 1.6 Hz, 1H), 7.58 (ddd, J = 10.4, 9.4, 2.4 Hz, 1H), 7.38 (d, J = 1.6 Hz, 1H), 7.26 – 7.17 (m, 1H), 6.84 (s, 2H), 4.31 (t, J = 6.0 Hz, 2H), 3.64 (s, 3H), 3.61 (t, J = 4.6 Hz, 4H), 2.81 (t, J = 6.0 Hz, 2H), 2.75 (s, 3H), 2.61 – 2.52 (m, 4H).^{13}C NMR (151 MHz, DMSO-d_6) δ 169.4, 165.0 (dd, $J_{C\text{-}F}$ = 254, 11.7 Hz), 159.6, 159.4 (dd, $J_{C\text{-}F}$ = 258, 13.4 Hz), 157.4, 152.6, 143.5, 142.4, 134.4, 131.8 (d, $J_{C\text{-}F}$ = 10.6 Hz), 129.8, 129.0, 125.3 (d, $J_{C\text{-}F}$ = 13.1 Hz),

119.7, 119.4, 114.7, 111.9, 111.7 (dd, J_{C-F} = 22.1, 2.5 Hz), 105.8 (t, J = 26.1 Hz), 66.1, 65.8, 57.0, 53.6, 53.2, 21.7. HRMS (ESI): m/z $[M + H]^+$ calcd for $C_{27}H_{29}O_5N_6F_2S$, 587.1883, found: 587.1855.

_N_-(5-(2-amino-4-methyl-8-((tetrahydro-2_H_-pyran-4-yl)oxy)quinazolin-6-yl)-2-methoxypyridin-3-yl)methanesulfonamide (28)

Compound **28** was prepared from compound **84** and *N*-(2-methoxy-5-(4,4,5,5-tetramethyl-1,3,2-dioxaborolan-2-yl)pyridin-3-yl)methanesulfonamide (yellow solid, 45% yield). ^{1}H NMR (400 MHz, DMSO-d_6) δ 9.34 (s, 1H), 8.43 (d, J = 2.3 Hz, 1H), 7.95 (d, J = 2.3 Hz, 1H), 7.70 (d, J = 1.6 Hz, 1H), 7.47 (d, J = 1.6 Hz, 1H), 6.77 (s, 2H), 4.97 – 4.81 (m, 1H), 3.98 (s, 3H), 3.96 – 3.88 (m, 2H), 3.55 – 3.44 (m, 2H), 3.08 (s, 3H), 2.75 (s, 3H), 2.10 – 2.00 (m, 2H), 1.76 – 1.57 (m, 2H). ^{13}C NMR (101 MHz, DMSO-d_6) δ 169.5, 159.5, 156.4, 150.9, 144.4, 141.3, 132.0, 129.9, 129.4, 121.0, 119.8, 115.4, 115.0, 72.7, 64.9, 53.8, 40.9, 32.0, 21.7. HRMS (ESI): m/z $[M + H]^+$ calcd for $C_{21}H_{26}O_5N_5S$, 460.1649, found: 460.1629.

_N_-(5-(2-amino-4-methyl-8-((tetrahydro-2_H_-pyran-4-yl)oxy)quinazolin-6-yl)-2-methoxypyridin-3-yl)cyclopropanesulfonamide (29)

Compound **29** was prepared from compound **84** and *N*-(2-methoxy-5-(4,4,5,5-tetramethyl-1,3,2-dioxaborolan-2-yl)pyridin-3-yl)cyclopropanesulfonamide (yellow solid, 87% yield). ^{1}H NMR (400 MHz, DMSO-d_6) δ 9.37 (s, 1H), 8.43 (d, J = 2.3 Hz, 1H), 7.97 (d, J = 2.3 Hz, 1H), 7.69 (d, J = 1.8 Hz, 1H), 7.47 (d, J = 1.8 Hz, 1H), 6.78 (s, 2H), 4.97 – 4.80 (m, 1H), 3.98 (s, 3H), 3.96 – 3.88 (m, 2H), 3.57 – 3.44 (m, 2H), 2.83 – 2.70 (m, 4H), 2.12 – 1.98 (m, 2H), 1.74 – 1.61 (m, 2H), 1.01 – 0.89 (m, 4H). ^{13}C NMR (101 MHz, DMSO-d_6) δ 169.5, 159.5, 156.7, 150.9, 144.4, 141.3, 132.2, 129.7, 129.4, 121.1, 119.8, 115.3, 114.9, 72.7, 64.90, 53.7, 32.0, 30.6, 21.7, 5.1. HRMS (ESI): m/z $[M + H]^+$ calcd for $C_{23}H_{28}O_5N_5S$, 486.1806, found: 486.1784.

6-(5-fluoro-6-methoxypyridin-3-yl)-4-methyl-8-((tetrahydro-2*H*-pyran-4-yl)oxy)quinazolin-2-amine (30)

Compound **30** was prepared from compound **84** and (5-fluoro-6-methoxypyridin-3-yl)boronic acid (yellow solid, 53% yield). ^{1}H NMR (400 MHz, DMSO-d_6) δ 8.47 (d, J = 2.0 Hz, 1H), 8.21 (dd, J = 12.0, 2.0 Hz, 1H), 7.79 (d, J = 1.6 Hz, 1H), 7.54 (d, J = 1.6 Hz, 1H), 6.78 (s, 2H), 4.98 – 4.84 (m, 1H), 4.00 (s, 3H), 3.98 – 3.88 (m, 2H), 3.59 – 3.45 (m, 2H), 2.76 (s, 3H), 2.12 – 1.99 (m, 2H), 1.74 – 1.59 (m, 2H). ^{13}C NMR (151 MHz, DMSO-d_6) δ 169.6, 159.5, 151.5 (d, $J_{C\text{-}F}$ = 11.4 Hz), 150.8, 147.6, 145.9, 144.5, 139.2 (d, $J_{C\text{-}F}$ = 5.5 Hz), 130.3, 128.4, 122.29 (d, $J_{C\text{-}F}$ = 15.9 Hz), 119.8, 115.5, 114.5, 72.6, 64.9, 53.6, 32.0, 21.7. HRMS (ESI): m/z [M + H]$^+$ calcd for $C_{20}H_{22}O_3N_4F$, 385.1670, found: 385.1653.

6-(6-methoxypyridin-3-yl)-4-methyl-8-((tetrahydro-2*H*-pyran-4-yl)oxy)quinazolin-2-amine (31)

Compound **31** was prepared from compound **84** and (6-methoxypyridin-3-yl)boronic acid as a yellow solid (95% yield). ^{1}H NMR (400 MHz, DMSO-d_6) δ 8.61 (d, J = 2.6 Hz, 1H), 8.14 (dd, J = 8.6, 2.6 Hz, 1H), 7.73 (d, J = 1.8 Hz, 1H), 7.51 (d, J = 1.8 Hz, 1H), 6.93 (dd, J = 8.6 Hz, 1H), 6.75 (s, 2H), 4.96 – 4.84 (m, 1H), 3.97 – 3.86 (m, 5H), 3.56 – 3.45 (m, 2H), 2.75 (s, 3H), 2.12 – 2.00 (m, 2H), 1.73 – 1.59 (m, 2H). ^{13}C NMR (151 MHz, DMSO-d_6) δ 169.4, 162.8, 159.4, 150.8, 144.9, 144.2, 137.7, 129.8, 129.2, 119.8, 115.0, 114.7, 110.4, 72.6, 64.9, 53.2, 32.0, 21.7. HRMS (ESI): m/z [M + H]$^+$ calcd for $C_{20}H_{23}O_3N_4$, 367.1765, found: 367.1749.

***N*-(5-(2-amino-4-methyl-8-((tetrahydro-2*H*-pyran-4-yl)oxy)quinazolin-6-yl)-2-methoxypyridin-3-yl)-2-chloro-4-fluorobenzenesulfonamide (32)**

Compound **32** was prepared from compound **84** and *N*-(2-methoxy-5-(4,4,5,5-tetramethyl-1,3,2-dioxaborolan-2-yl)pyridin-3-yl)-2-chloro-4-fluorobenzenesulfonamide (yellow solid, 81%

yield). ^{1}H NMR (400 MHz, DMSO-d_6) δ 10.17 (s, 1H), 8.42 (d, J = 2.3 Hz, 1H), 7.94 (dd, J = 8.8, 6.0 Hz, 1H), 7.90 (d, J = 2.4 Hz, 1H), 7.76 (dd, J = 8.8, 2.4 Hz, 1H), 7.62 (d, J = 1.6 Hz, 1H), 7.43 (d, J = 1.4 Hz, 1H), 7.40 – 7.33 (m, 1H), 6.79 (s, 2H), 4.94 – 4.81 (m, 1H), 3.98 – 3.89 (m, 2H), 3.66 (s, 3H), 3.57 – 3.45 (m, 2H), 2.75 (s, 3H), 2.10 – 1.99 (m, 2H), 1.74 – 1.58 (m, 2H). ^{13}C NMR (101 MHz, DMSO-d_6) δ 169.6, 163.9 (d, $J_{C\text{-}F}$ = 256 Hz), 159.5, 157.1, 150.9, 144.4, 142.4, 134.7 (d, $J_{C\text{-}F}$ = 3.4 Hz), 133.7, 133.3 (d, $J_{C\text{-}F}$ = 11.5 Hz), 133.0 (d, $J_{C\text{-}F}$ = 10.1 Hz), 129.7, 129.1, 119.8, 119.7, 119.2 (d, $J_{C\text{-}F}$ = 26.1 Hz), 115.3, 114.7, 114.5 (d, $J_{C\text{-}F}$ = 21.8 Hz), 72.7, 64.9, 53.3, 32.0, 21.7. HRMS (ESI): m/z $[M + H]^+$ calcd for $C_{26}H_{26}O_5N_5ClFS$, 574.1322, found: 574.1296.

_N_-(5-(2-amino-4-methyl-8-((tetrahydro-2_H_-pyran-4-yl)oxy)quinazolin-6-yl)-2-methoxypyridin-3-yl)-4-fluorobenzenesulfonamide (33)

Compound **33** was prepared from compound **84** and *N*-(2-methoxy-5-(4,4,5,5-tetramethyl-1,3,2-dioxaborolan-2-yl)pyridin-3-yl)-4-fluorobenzenesulfonamide as a yellow solid (93% yield). ^{1}H NMR (400 MHz, DMSO-d_6) δ 10.04 (s, 1H), 8.39 (d, J = 2.4 Hz, 1H), 7.88 (d, J = 2.4 Hz, 1H), 7.86 – 7.79 (m, 2H), 7.61 (d, J = 1.8 Hz, 1H), 7.47 – 7.39 (m, 3H), 6.79 (s, 2H), 4.95 – 4.82 (m, 1H), 3.98 – 3.89 (m, 2H), 3.65 (s, 3H), 3.56 – 3.42 (m, 2H), 2.75 (s, 3H), 2.11 – 1.98 (m, 2H), 1.74 – 1.59 (m, 2H). ^{13}C NMR (101 MHz, DMSO-d_6) δ 169.5, 164.3 (d, $J_{C\text{-}F}$ = 252 Hz), 159.5, 156.6, 150.9, 144.4, 141.9, 136.8 (d, $J_{C\text{-}F}$ = 2.9 Hz), 132.6, 129.8 (d, $J_{C\text{-}F}$ = 9.7 Hz), 129.6, 129.1, 120.1, 119.8, 116.2 (d, $J_{C\text{-}F}$ = 22.9 Hz), 115.2, 114.7, 72.7, 64.9, 53.3, 32.0, 21.7. HRMS (ESI): m/z $[M + H]^+$ calcd for $C_{26}H_{27}O_5N_5FS$, 540.1711, found: 540.1687.

_N_-(5-(2-amino-4-methyl-8-((tetrahydro-2_H_-pyran-4-yl)oxy)quinazolin-6-yl)-2-methoxypyridin-3-yl)-5-chlorothiophene-2-sulfonamide (34)

Compound **34** was prepared from compound **84** and *N*-(2-methoxy-5-(4,4,5,5-tetramethyl-1,3,2-dioxaborolan-2-yl)pyridin-3-yl)-5-chlorothiophene-2-sulfonamide as a yellow solid (45% yield). ^{1}H NMR (400 MHz, DMSO-d_6) δ 10.34 (s, 1H), 8.46 (d, J = 2.4 Hz, 1H), 7.95 (d, J = 2.4 Hz, 1H), 7.67 (d, J = 1.6 Hz, 1H), 7.47 (d, J = 1.6 Hz, 1H), 7.39 (d, J = 4.0 Hz, 1H), 7.24 (d, J = 4.0 Hz, 1H), 6.80 (s, 2H), 4.95 – 4.84 (m, 1H), 4.00 – 3.86 (m, 2H), 3.74 (s, 3H), 3.58 – 3.45 (m, 2H), 2.76 (s, 3H), 2.11 – 2.00 (m, 2H), 1.77 – 1.60 (m, 2H). ^{13}C NMR (101 MHz, DMSO-d_6) δ 169.7, 159.4, 157.1, 150.8, 144.1, 142.4, 139.3, 135.1, 133.4, 132.1, 129.7, 129.2, 127.8, 119.8, 119.7, 115.3, 114.7, 72.7, 64.9, 53.5, 32.0, 21.8. HRMS (ESI): m/z $[M + H]^+$ calcd for $C_{24}H_{25}O_5N_5ClS_2$, 562.0980, found: 562.0956.

_N_-(5-(2-amino-4-methyl-8-((tetrahydro-2_H_-pyran-4-yl)oxy)quinazolin-6-yl)-2-methylpyridin-3-yl)-2,4-difluorobenzenesulfonamide (35)

A mixture of compound **84** (75 mg, 0.22 mmol), KOAc (65 mg, 0.66 mmol) and bis(pinacolato)diboron (64 mg, 0.25 mmol) in dioxane (8 mL) was degassed, and then $PdCl_2$(dppf) (16 mg, 0.022 mmol) was added. The resulting reaction mixture was degassed and back-filled with argon (three cycles), and then stirred at 100 °C under Ar atmosphere for 4 h. After cooling to rt, *N*-(5-bromo-2-methylpyridin-3-yl)-2,4-difluorobenzenesulfonamide (91 mg, 0.25 mmol) and 2M aqueous K_2CO_3 solution (0.44 mL, 0.88 mmol) were added to the reaction mixture. The resulting mixture was degassed, and then $PdCl_2$(dppf) (16 mg, 0.022 mmol) was added. The mixture was degassed and back-filled with argon (three cycles), and then stirred at 100 °C under Ar atmosphere for 5 h. The reaction mixture was cooled to rt, diluted with water (30 mL) and EtOAc (30 mL), acidified with 2M HCl solution until the pH value was 5-6. The two layers were separated and the aqueous layer was extracted with EtOAc (30 mL×2). The combined organic layers were washed with water (50 mL) and brine (50 mL), dried over Na_2SO_4,

filtered and concentrated. The residue was purified by preparative TLC (silica gel, DCM/MeOH/ammonium hydroxide = 15:1:0.1, v/v) to afford the product **35** as a yellow solid (35 mg, 29% yield). ^{1}H NMR (400 MHz, DMSO-d_6) δ 10.45 (s, 1H), 8.73 (s, 1H), 7.80 (dt, J = 8.4, 6.4 Hz, 1H), 7.72 – 7.54 (m, 3H), 7.40 (s, 1H), 7.27 (dt, J = 8.4, 2.0 Hz, 1H), 6.84 (s, 2H), 4.91 – 4.80 (m, 1H), 3.98 – 3.88 (m, 2H), 3.58 – 3.43 (m, 2H), 2.73 (s, 3H), 2.33 (s, 3H), 2.08 – 1.98 (m, 2H), 1.77 – 1.58 (m, 2H). ^{13}C NMR (101 MHz, DMSO-d_6) δ 169.6, 165.2 (dd, $J_{C\text{-}F}$ = 255, 11.8 Hz), 159.6, 159.1 (dd, $J_{C\text{-}F}$ = 258, 13.5 Hz), 153.2, 150.9, 144.8 (br s), 144.7, 133.8, 132.0 (d, $J_{C\text{-}F}$ = 10.9 Hz), 131.9, 131.1 (br s), 128.9, 125.1 (dd, $J_{C\text{-}F}$ = 14.0, 2.1 Hz), 119.7, 115.8, 114.8, 112.4 (dd, $J_{C\text{-}F}$ = 22.2, 3.1 Hz), 106.2 (t, $J_{C\text{-}F}$ = 26.2 Hz), 72.7, 64.8, 31.9, 21.7, 20.2. HRMS (ESI): m/z $[M + H]^+$ calcd for $C_{26}H_{26}O_4N_5F_2S$, 542.1668, found: 542.1649.

***N*-(5-(2-amino-4-methyl-8-((tetrahydro-2*H*-pyran-4-yl)oxy)quinazolin-6-yl)-2-chloropyridin-3-yl)-4-fluorobenzenesulfonamide (36)**

A mixture of compound **84** (75 mg, 0.22 mmol), KOAc (65 mg, 0.66 mmol) and bis(pinacolato)diboron (64 mg, 0.25 mmol) in dioxane (8 mL) was degassed, and then $PdCl_2$(dppf) (16 mg, 0.022 mmol) was added. The resulting reaction mixture was degassed and back-filled with argon (three cycles), and then stirred at 100 °C under Ar atmosphere for 4 h. After cooling to rt, *N*-(5-bromo-2-chloropyridyn-3-yl)-4-fluorobenzenesulfonamide (91 mg, 0.25 mmol) and 2M aqueous K_2CO_3 solution (0.44 mL, 0.88 mmol) were added to the reaction mixture. The resulting mixture was degassed, and then $PdCl_2$(dppf) (16 mg, 0.022 mmol) was added. The mixture was degassed and back-filled with argon (three cycles), and then stirred at 100 °C under Ar atmosphere for 5 h. The reaction mixture was cooled to rt, diluted with water (30 mL) and EtOAc (30 mL), acidified with 2M HCl solution until the pH value was 5-6. The two layers were separated and the aqueous layer was extracted with EtOAc (30 mL×2). The

combined organic layers were washed with water (50 mL) and brine (50 mL), dried over Na_2SO_4, filtered and concentrated. The residue was purified by preparative TLC (silica gel, DCM/MeOH/ammonium hydroxide = 15:1:0.1, v/v) to afford the product **36** as a yellow solid (30 mg, 25% yield). ^{1}H NMR (400 MHz, DMSO-d_6) δ 10.53 (s, 1H), 8.67 (d, J = 1.7 Hz, 1H), 7.99 (d, J = 2.3 Hz, 1H), 7.87 – 7.77 (m, 2H), 7.71 (d, J = 1.7 Hz, 1H), 7.51 – 7.40 (m, 3H), 6.90 (s, 2H), 4.95 – 4.82 (m, 1H), 3.98 – 3.88 (m, 2H), 3.57 – 3.44 (m, 2H), 2.76 (s, 3H), 2.12 – 1.95 (m, 2H), 1.75 – 1.59 (m, 2H). HRMS (ESI): m/z $[M + H]^+$ calcd for $C_{25}H_{24}O_4N_5ClFS$, 544.1216, found: 544.1199.

2,4-difluoro-*N*-(2-methoxy-5-(4-methyl-2-(methylamino)-8-((tetrahydro-2*H*-pyran-4-yl)oxy)quinazolin-6-yl)pyridin-3-yl)benzenesulfonamide (37)

Compound **37** was prepared from compound **93** and *N*-(2-methoxy-5-(4,4,5,5-tetramethyl-1,3,2-dioxaborolan-2-yl)pyridin-3-yl)-2,4-difluorobenzenesulfonamide (yellow solid, 70% yield). ^{1}H NMR (400 MHz, DMSO-d_6) δ 10.28 (s, 1H), 8.42 (d, J = 2.0 Hz, 1H), 7.93 (d, J = 2.0 Hz, 1H), 7.83 – 7.66 (m, 2H), 7.63 – 7.53 (m, 1H), 7.50 (s, 1H), 7.28 (q, J = 4.0 Hz, 1H), 7.21 (dt, J = 8.4, 2.0 Hz, 1H), 4.97 – 4.88 (m 1H), 4.01 – 3.88 (m, 2H), 3.64 (s, 3H), 3.53 – 3.44 (m, 2H), 2.91 (d, J = 4.4 Hz, 3H), 2.76 (s, 3H), 2.08 – 1.90 (m, 2H), 1.81 – 1.63 (m, 2H). ^{13}C NMR (101 MHz, DMSO-d_6) δ 169.3, 165.0 (dd, $J_{C\text{-}F}$ = 255, 11.3 Hz), 159.4 (dd, $J_{C\text{-}F}$ = 259, 13.5 Hz), 158.7, 157.4, 151.1, 144.8, 142.5, 134.6, 131.8 (d, $J_{C\text{-}F}$ = 10.9 Hz), 129.5, 128.9, 125.3 (dd, $J_{C\text{-}F}$ = 14.8, 3.4 Hz), 120.1, 119.4, 118.9, 116.6, 111.8 (dd, $J_{C\text{-}F}$ = 22.0, 2.7 Hz), 105.8 (t, J = 26.3 Hz), 73.7, 64.4, 53.3, 32.0, 27.9, 21.8. HRMS (ESI): m/z $[M + H]^+$ calcd for $C_{27}H_{28}O_5N_5F_2S$, 572.1774, found: 572.1763.

***N*-(5-(2-(ethylamino)-4-methyl-8-((tetrahydro-2*H*-pyran-4-yl)oxy)quinazolin-6-yl)-2-methoxypyridin-3-yl)-2,4-difluorobenzenesulfonamide (38)**

Compound **38** was prepared from compound **94** and *N*-(2-methoxy-5-(4,4,5,5-tetramethyl-1,3,2-dioxaborolan-2-yl)pyridin-3-yl)-2,4-difluorobenzenesulfonamide (yellow solid, 64% yield). ^{1}H NMR (400 MHz, DMSO-d_6) δ 10.28 (s, 1H), 8.42 (d, J = 2.1 Hz, 1H), 7.93 (d, J = 2.3 Hz, 1H), 7.80 – 7.69 (m, 2H), 7.59 (ddd, J = 10.4, 9.6, 2.4 Hz, 1H), 7.49 (d, J = 1.2 Hz, 1H), 7.35 (t, J = 5.0 Hz, 1H), 7.26 – 7.16 (m, 1H), 4.95 – 4.87 (m, 1H), 3.98 – 3.89 (m, 2H), 3.64 (s, 3H), 3.52 – 3.36 (m, 4H), 2.75 (s, 3H), 2.05 – 1.92 (m, 2H), 1.80 – 1.63 (m, 2H), 1.19 (t, J = 7.1 Hz, 3H). ^{13}C NMR (101 MHz, DMSO-d_6) δ 169.3, 165.0 (dd, $J_{C\text{-}F}$ = 255, 11.8 Hz), 159.4 (dd, $J_{C\text{-}F}$ = 259, 13.5 Hz), 158.0, 157.4, 151.1, 144.8, 142.4, 134.4, 131.8 (d, $J_{C\text{-}F}$ = 10.7 Hz), 129.4, 128.8, 125.3 (dd, $J_{C\text{-}F}$ = 14.5, 3.6 Hz), 120.1, 119.5, 119.2, 116.6, 111.7 (dd, $J_{C\text{-}F}$ = 22.2, 3.3 Hz), 105.8 (t, J = 26.2 Hz), 73.8, 64.4, 53.2, 35.5, 31.9, 21.7, 14.5. HRMS (ESI): m/z $[M + H]^+$ calcd for $C_{28}H_{30}O_5N_5F_2S$, 586.1930, found: 586.1903.

_N_-(5-(2-((cyclopropylmethyl)amino)-4-methyl-8-((tetrahydro-2_H_-pyran-4-yl)oxy)quinazolin-6-yl)-2-methoxypyridin-3-yl)-2,4-difluorobenzenesulfonamide (39)

Compound **39** was prepared from compound **95** and *N*-(2-methoxy-5-(4,4,5,5-tetramethyl-1,3,2-dioxaborolan-2-yl)pyridin-3-yl)-2,4-difluorobenzenesulfonamide as a yellow solid (55% yield). ^{1}H NMR (400 MHz, DMSO-d_6) δ 10.28 (s, 1H), 8.43 (d, J = 2.4 Hz, 1H), 7.94 (d, J = 2.4 Hz, 1H), 7.80 – 7.70 (m, 2H), 7.63 – 7.55 (m, 1H), 7.48 (d, J = 1.2 Hz, 1H), 7.45 (br s, 1H), 7.22 (dt, J = 8.4, 2.0 Hz, 1H), 4.96 – 4.86 (m, 1H), 4.00 – 3.89 (m, 2H), 3.64 (s, 3H), 3.54 – 3.42 (m, 2H), 3.28 (t, J = 6.4 Hz, 2H), 2.76 (s, 3H), 2.06 – 1.94 (m, 2H), 1.80 – 1.63 (m, 2H), 1.21 – 1.05 (m, 1H), 0.50 – 0.38 (m, 2H), 0.29 (q, J = 4.8 Hz, 2H). ^{13}C NMR (101 MHz, DMSO-d_6) δ 169.4, 165.0 (dd, $J_{C\text{-}F}$ = 255, 11.7 Hz), 159.4 (dd, $J_{C\text{-}F}$ = 258, 13.8 Hz), 158.2, 157.4, 151.1, 144.7, 142.6, 134.6, 131.8 (d, $J_{C\text{-}F}$ = 11.3 Hz), 129.5, 128.8, 125.3 (dd, $J_{C\text{-}F}$ = 14.4, 3.5 Hz), 120.1, 119.4, 118.9, 116.7, 111.8 (dd, $J_{C\text{-}F}$ = 22.2, 3.0 Hz), 105.8 (t, J = 26.2 Hz), 73.7, 64.4, 53.3, 45.1,

31.9, 21.8, 11.0, 3.3. HRMS (ESI): m/z $[M + H]^+$ calcd for $C_{30}H_{32}O_5N_5F_2S$, 612.2087, found: 612.2067.

_N_-(5-(2-(dimethylamino)-4-methyl-8-((tetrahydro-2_H_-pyran-4-yl)oxy)quinazolin-6-yl)-2-methoxypyridin-3-yl)-2,4-difluorobenzenesulfonamide (40)

Compound **40** was prepared from compound **96** and *N*-(2-methoxy-5-(4,4,5,5-tetramethyl-1,3,2-dioxaborolan-2-yl)pyridin-3-yl)-2,4-difluorobenzenesulfonamide (yellow solid, 72% yield). ^{1}H NMR (400 MHz, DMSO-d_6) δ 10.28 (s, 1H), 8.44 (d, J = 2.3 Hz, 1H), 7.95 (d, J = 2.3 Hz, 1H), 7.80 – 7.70 (m, 2H), 7.63 – 7.55 (m, 1H), 7.52 (d, J = 2.0 Hz, 1H), 7.22 (td, J = 8.8, 2.4 Hz, 1H), 4.98 – 4.89 (m, 1H), 4.02 – 3.87 (m, 2H), 3.64 (s, 3H), 3.53 – 3.44 (m, 2H), 3.25 (s, 6H), 2.81 (s, 3H), 2.06 – 1.91 (m, 2H), 1.78 – 1.66 (m, 2H). ^{13}C NMR (101 MHz, DMSO-d_6) δ 169.2, 165.1 (dd, $J_{C\text{-}F}$ = 255, 11.8 Hz), 159.4 (dd, $J_{C\text{-}F}$ = 259, 13.5 Hz), 157.9, 157.4, 151.1, 144.9, 142.6, 134.6, 131.8 (d, $J_{C\text{-}F}$ = 10.9 Hz), 129.4, 129.0, 125.2 (dd, $J_{C\text{-}F}$ = 14.4, 3.8 Hz), 119.4, 119.2, 118.5, 116.5, 111.8 (dd, $J_{C\text{-}F}$ = 22.2, 3.2 Hz), 105.8 (t, J = 26.3 Hz), 73.5, 64.3, 53.3, 36.6, 31.9, 21.8. HRMS (ESI): m/z $[M + H]^+$ calcd for $C_{28}H_{30}O_5N_5F_2S$, 586.1930, found: 586.1920.

_N_-(6-(5-((2,4-difluorophenyl)sulfonamido)-6-methoxypyridin-3-yl)-4-methyl-8-((tetrahydro-2_H_-pyran-4-yl)oxy)quinazolin-2-yl)acetamide (41)

Compound **41** was prepared from compound **97** and *N*-(2-methoxy-5-(4,4,5,5-tetramethyl-1,3,2-dioxaborolan-2-yl)pyridin-3-yl)-2,4-difluorobenzenesulfonamide (yellow solid, 87% yield). ^{1}H NMR (400 MHz, DMSO-d_6) δ 10.55 (s, 1H), 10.32 (s, 1H), 8.52 (d, J = 2.0 Hz, 1H), 8.06 (d, J = 2.0 Hz, 1H), 7.91 (d, J = 1.0 Hz, 1H), 7.76 (dt, J = 8.6, 6.8 Hz, 1H), 7.69 (d, J = 1.0 Hz, 1H), 7.64 – 7.55 (m, 1H), 7.22 (dt, J = 8.8, 2.4 Hz, 1H), 5.16 – 5.07 (m, 1H), 3.96 – 3.89 (m, 2H), 3.65 (s, 3H), 3.58 – 3.45 (m, 2H), 2.91 (s, 3H), 2.36 (s, 3H), 2.09 – 1.99 (m, 2H), 1.79 – 1.63 (m, 2H). ^{13}C NMR (151 MHz, DMSO-d_6) δ 170.6, 169.8, 165.0 (dd, $J_{C\text{-}F}$ = 254, 11.6 Hz), 159.4 (dd,

$J_{C\text{-}F}$ = 258, 13.4 Hz), 157.9, 152.9, 152.1, 143.2, 142.6, 135.1, 133.3, 131.8 (d, $J_{C\text{-}F}$ = 10.7 Hz), 129.1, 125.3 (dd, $J_{C\text{-}F}$ = 14.3, 3.2 Hz), 122.3, 119.5, 116.6, 115.3, 111.8 (dd, $J_{C\text{-}F}$ = 22.0, 2.7 Hz), 105.8 (t, J = 26.1 Hz), 73.1, 64.4, 53.3, 31.7, 24.9, 21.9. HRMS (ESI): m/z $[M + H]^+$ calcd for $C_{28}H_{28}O_6N_5F_2S$, 600.1723, found: 600.1700.

_N_-(6-(6-methoxy-5-(methylsulfonamido)pyridin-3-yl)-4-methyl-8-((tetrahydro-2_H_-pyran-4-yl)oxy)quinazolin-2-yl)acetamide (42)

Compound **42** was prepared from compound **97** and *N*-(2-methoxy-5-(4,4,5,5-tetramethyl-1,3,2-dioxaborolan-2-yl)pyridin-3-yl)methanesulfonamide (yellow solid, 56% yield).^{1}H NMR (400 MHz, DMSO-d_6) δ 10.55 (s, 1H), 9.39 (s, 1H), 8.51 (d, J = 2.3 Hz, 1H), 8.04 (d, J = 2.3 Hz, 1H), 7.93 (d, J = 1.7 Hz, 1H), 7.70 (d, J = 1.7 Hz, 1H), 5.16 – 5.08 (m, 1H), 3.99 (s, 3H), 3.97 – 3.87 (m, 2H), 3.55 – 3.47 (m, 2H), 3.10 (s, 3H), 2.91 (s, 3H), 2.36 (s, 3H), 2.11 – 1.98 (m, 2H), 1.78 – 1.64 (m, 2H). ^{13}C NMR (101 MHz, DMSO-d_6) δ 170.5, 169.8, 156.8, 152.9, 152.0, 142.6, 141.7, 133.7, 132.2, 129.2, 122.3, 122.1, 116.9, 115.4, 73.2, 64.4, 53.8, 40.9, 31.7, 24.9, 21.9. HRMS (ESI): m/z $[M + H]^+$ calcd for $C_{23}H_{28}O_6N_5S$, 502.1755, found: 502.1734.

(_R_)-2,4-difluoro-_N_-(2-methoxy-5-(4-methyl-2-(methylamino)-8-((tetrahydrofuran-3-yl)oxy)quinazolin-6-yl)pyridin-3-yl)benzenesulfonamide (43)

Compound **43** was prepared from compound **98** and *N*-(2-methoxy-5-(4,4,5,5-tetramethyl-1,3,2-dioxaborolan-2-yl)pyridin-3-yl)-2,4-difluorobenzenesulfonamide (yellow solid, 63% yield). ^{1}H NMR (400 MHz, DMSO-d_6) δ 10.28 (s, 1H), 8.44 (d, J = 2.2 Hz, 1H), 7.96 (d, J = 2.2 Hz, 1H), 7.80 – 7.70 (m, 2H), 7.63 – 7.54 (m, 1H), 7.38 (s, 1H), 7.29 (q, J = 4.8 Hz, 1H), 7.25 – 7.17 (m, 1H), 5.43 – 5.36 (m, 1H), 4.00 – 3.89 (m, 3H), 3.83 – 3.76 (m, 1H), 3.64 (s, 3H), 2.91 (d, J = 4.8 Hz, 3H), 2.76 (s, 3H), 2.28 – 2.15 (m, 1H), 2.15 – 2.02 (m, 1H). ^{13}C NMR (101 MHz, DMSO-d_6) δ 169.2, 165.1 (dd, $J_{C\text{-}F}$ = 255, 11.7 Hz), 159.4 (dd, $J_{C\text{-}F}$ = 259, 13.4 Hz), 158.7, 157.4,

151.4, 144.1, 142.6, 134.7, 131.8 (d, $J_{C\text{-}F}$ = 10.8 Hz), 129.5, 128.8, 125.2 (dd, $J_{C\text{-}F}$ = 14.5, 3.6 Hz), 119.9, 119.4, 116.7, 116.1, 111.8 (dd, $J_{C\text{-}F}$ = 22.1, 3.3 Hz), 105.8 (t, J = 26.1 Hz), 79.3 (br s), 72.4, 66.5, 53.3, 32.6, 27.9, 21.9. HRMS (ESI): m/z $[M + H]^+$ calcd for $C_{26}H_{26}O_5N_5F_2S$, 558.1617, found: 558.1609.

(*S*)-2,4-difluoro-*N*-(2-methoxy-5-(4-methyl-2-(methylamino)-8-((tetrahydrofuran-3-yl)oxy)quinazolin-6-yl)pyridin-3-yl)benzenesulfonamide (44)

Compound **44** was prepared from compound **99** and *N*-(2-methoxy-5-(4,4,5,5-tetramethyl-1,3,2-dioxaborolan-2-yl)pyridin-3-yl)-2,4-difluorobenzenesulfonamide (yellow solid, 30% yield). ^{1}H NMR (400 MHz, DMSO-d_6) δ 10.28 (s, 1H), 8.44 (d, J = 2.4 Hz, 1H), 7.97 (d, J = 2.4 Hz, 1H), 7.80 – 7.70 (m, 2H), 7.59 (ddd, J = 10.4, 9.2, 2.4 Hz, 1H), 7.38 (s, 1H), 7.29 (q, J = 4.8 Hz, 1H), 7.22 (dt, J = 8.4, 2.4 Hz, 1H), 5.43 – 5.36 (m, 1H), 4.03 – 3.87 (m, 3H), 3.79 (dt, J = 8.2, 4.6 Hz, 1H), 3.64 (s, 3H), 2.91 (d, J = 4.8 Hz, 3H), 2.76 (s, 3H), 2.28 – 2.16 (m, 1H), 2.15 – 2.04 (m, 1H). ^{13}C NMR (101 MHz, DMSO-d_6) δ 169.2, 165.0 (dd, $J_{C\text{-}F}$ = 255, 11.6 Hz), 159.4 (dd, $J_{C\text{-}F}$ = 258, 13.2 Hz), 158.8, 157.4, 151.4, 144.2, 142.6, 134.7, 131.8 (d, $J_{C\text{-}F}$ = 10.5 Hz), 129.5, 128.8, 125.3 (dd, $J_{C\text{-}F}$ = 14.6, 3.0 Hz), 119.9, 119.4, 116.6, 116.1, 111.8 (dd, $J_{C\text{-}F}$ = 22.1, 3.5 Hz), 105.8 (t, J = 26.2 Hz), 79.3 (br s), 72.4, 66.5, 53.3, 32.6, 27.9, 21.8. HRMS (ESI): m/z $[M + H]^+$ calcd for $C_{26}H_{26}O_5N_5F_2S$, 558.1617, found: 558.1594.

2,4-difluoro-*N*-(2-methoxy-5-(4-methyl-2-(methylamino)-8-((tetrahydrofuran-3-yl)methoxy)quinazolin-6-yl)pyridin-3-yl)benzenesulfonamide (45)

Compound **45** was prepared from compound **100** and *N*-(2-methoxy-5-(4,4,5,5-tetramethyl-1,3,2-dioxaborolan-2-yl)pyridin-3-yl)-2,4-difluorobenzenesulfonamide as a yellow solid (79% yield). ^{1}H NMR (400 MHz, DMSO-d_6) δ 10.27 (s, 1H), 8.44 (d, J = 2.1 Hz, 1H), 7.96 (d, J = 2.2 Hz, 1H), 7.75 (dt, J = 8.6, 6.4 Hz, 1H), 7.68 (d, J = 1.6 Hz, 1H), 7.63 – 7.53 (m, 1H), 7.41 (s,

1H), 7.28 – 7.16 (m, 2H), 4.26 – 4.16 (m, 1H), 4.11 (dd, J = 9.2, 8.0 Hz, 1H), 3.89 – 3.79 (m, 2H), 3.70 (dt, J = 8.0, 6.4 Hz, 2H), 3.63 (s, 3H), 2.90 (d, J = 4.8 Hz, 3H), 2.82 – 2.70 (m, 4H), 2.12 – 2.00 (m, 1H), 1.85 – 1.72 (m, 1H). ^{13}C NMR (151 MHz, DMSO-d_6) δ 169.0, 165.0 (dd, $J_{C\text{-}F}$ = 254, 11.6 Hz), 159.4 (dd, $J_{C\text{-}F}$ = 258, 13.5 Hz), 158.8, 157.4, 152.9, 143.7, 142.6, 134.6, 131.8 (d, $J_{C\text{-}F}$ = 10.9 Hz), 129.7, 128.9, 125.2 (d, $J_{C\text{-}F}$ = 13.0 Hz), 119.6, 119.4, 115.3, 114.0 (br s), 111.7 (dd, $J_{C\text{-}F}$ = 22.1, 2.5 Hz), 105.8 (t, J = 26.1 Hz), 79.3 (br s), 71.0, 69.9, 66.9, 53.2, 38.4, 28.6, 27.8, 21.8. HRMS (ESI): m/z [M + H]$^+$ calcd for $C_{27}H_{28}O_5N_5F_2S$, 572.1774, found: 572.1752.

_N_-(5-(8-((2,2-dimethyltetrahydro-2_H_-pyran-4-yl)oxy)-4-methyl-2-(methylamino)quinazolin-6-yl)-2-methoxypyridin-3-yl)-2,4-difluorobenzenesulfonamide (46)

Compound **46** was prepared from compound **101** and *N*-(2-methoxy-5-(4,4,5,5-tetramethyl-1,3,2-dioxaborolan-2-yl)pyridin-3-yl)-2,4-difluorobenzenesulfonamide (yellow solid, 81% yield). ^{1}H NMR (400 MHz, DMSO-d_6) δ 10.28 (s, 1H), 8.43 (d, J = 2.4 Hz, 1H), 7.94 (d, J = 2.4 Hz, 1H), 7.79 – 7.71 (m, 2H), 7.59 (ddd, J = 10.4, 9.2, 2.4 Hz, 1H), 7.46 (d, J = 1.8 Hz, 1H), 7.27 (q, J = 4.8 Hz, 1H), 7.25 – 7.18 (m, 1H), 5.16 – 4.97 (m, 1H), 3.85 – 3.76 (m, 1H), 3.64 (s, 3H), 3.62 – 3.53 (m, 1H), 2.90 (d, J = 4.8 Hz, 3H), 2.76 (s, 3H), 2.04 – 1.91 (m, 2H), 1.66 – 1.50 (m, 2H), 1.29 (s, 3H), 1.18 (s, 3H). ^{13}C NMR (101 MHz, DMSO-d_6) δ 169.2, 165.0 (dd, $J_{C\text{-}F}$ = 255, 11.7 Hz), 159.4 (dd, $J_{C\text{-}F}$ = 259, 13.4 Hz), 158.7, 157.4, 151.1, 144.6, 142.5, 134.5, 131.8 (d, $J_{C\text{-}F}$ = 10.9 Hz), 129.5, 128.9, 125.3 (dd, $J_{C\text{-}F}$ = 14.4, 3.5 Hz), 120.0, 119.5, 118.1 (br s), 116.3 (br s), 111.8 (dd, $J_{C\text{-}F}$ = 22.2, 3.4 Hz), 105.8 (t, J = 26.2 Hz), 72.4, 71.9, 58.5, 53.3, 41.9, 31.6, 29.7, 27.8, 25.0, 21.8. HRMS (ESI): m/z [M + H]$^+$ calcd for $C_{29}H_{32}O_5N_5F_2S$, 600.2087, found: 600.2067.

_N_-(2-methoxy-5-(4-methyl-2-(methylamino)-8-((tetrahydro-2_H_-pyran-4-yl)methoxy)quinazolin-6-yl)pyridin-3-yl)-2,4-difluoro-benzenesulfonamide (47)

Compound **47** was prepared from compound **102** and *N*-(2-methoxy-5-(4,4,5,5-tetramethyl-1,3,2-dioxaborolan-2-yl)pyridin-3-yl)-2,4-difluorobenzenesulfonamide (yellow solid, 80% yield). ^{1}H NMR (400 MHz, DMSO-d_6) δ 10.27 (s, 1H), 8.44 (d, J = 2.0 Hz, 1H), 7.95 (d, J = 2.0 Hz, 1H), 7.76 (dt, J = 8.6, 6.3 Hz, 1H), 7.65 (d, J = 1.6 Hz, 1H), 7.63 – 7.54 (m, 1H), 7.37 (s, 1H), 7.28 – 7.17 (m, 2H), 4.08 (d, J = 6.4 Hz, 2H), 3.95 – 3.87 (m, 2H), 3.64 (s, 3H), 3.37 (dt, J = 11.6, 2.0 Hz, 2H), 2.90 (d, J = 4.8 Hz, 3H), 2.75 (s, 3H), 2.19 – 2.05 (m, 1H), 1.85 – 1.74 (m, 2H), 1.49 – 1.35 (m, 2H). ^{13}C NMR (101 MHz, DMSO-d_6) δ 168.9, 165.0 (dd, $J_{C\text{-}F}$ = 255, 11.8 Hz), 159.4 (dd, $J_{C\text{-}F}$ = 259, 13.3 Hz), 158.8, 157.4, 153.0, 143.7, 142.4, 134.4, 131.8 (d, $J_{C\text{-}F}$ = 10.8 Hz), 129.8, 128.9, 125.3 (dd, $J_{C\text{-}F}$ = 14.5, 3.5 Hz), 119.5, 114.9, 113.1 (br s), 111.7 (dd, $J_{C\text{-}F}$ = 22.2, 3.2 Hz), 105.7 (t, J = 26.3 Hz), 79.3 (br s), 73.3, 66.6, 53.2, 34.6, 29.3, 27.8, 21.8. HRMS (ESI): m/z $[M + H]^+$ calcd for $C_{28}H_{30}O_5N_5F_2S$, 586.1930, found: 586.1909.

_N_-(5-(8-cyclobutoxy-4-methyl-2-(methylamino)quinazolin-6-yl)-2-methoxypyridin-3-yl)-2,4-difluorobenzenesulfonamide (48)

Compound **48** was prepared from compound **103** and *N*-(2-methoxy-5-(4,4,5,5-tetramethyl-1,3,2-dioxaborolan-2-yl)pyridin-3-yl)-2,4-difluorobenzenesulfonamide (yellow solid, 80% yield). ^{1}H NMR (400 MHz, DMSO-d_6) δ 10.29 (s, 1H), 8.41 (d, J = 2.4 Hz, 1H), 7.91 (d, J = 2.4 Hz, 1H), 7.77 (dt, J = 8.6, 6.4 Hz, 1H), 7.59 (ddd, J = 10.4, 9.2, 2.4 Hz, 1H), 7.31 – 7.17 (m, 2H), 7.14 (d, J = 1.2 Hz, 1H), 5.05 – 4.88 (m, 1H), 3.66 (s, 3H), 2.91 (d, J = 4.8 Hz, 3H), 2.75 (s, 3H), 2.55 – 2.45 (m, 2H), 2.22 – 2.09 (m, 2H), 1.90 – 1.78 (m, 1H), 1.76 – 1.61 (m, 1H). ^{13}C NMR (101 MHz, DMSO-d_6) δ 169.0, 165.1 (dd, $J_{C\text{-}F}$ = 255, 11.7 Hz), 159.4 (dd, $J_{C\text{-}F}$ = 259, 13.4 Hz), 158.9, 157.3, 151.2, 143.5, 142.3, 134.1, 131.8 (d, $J_{C\text{-}F}$ = 10.7 Hz), 129.7, 128.8, 125.3 (dd, $J_{C\text{-}F}$

= 14.4, 3.6 Hz), 119.6, 114.8, 112.7 (br s), 111.8 (dd, $J_{C\text{-}F}$ = 22.2, 3.3 Hz), 105.8 (t, J = 26.2 Hz), 71.4, 53.3, 30.2, 27.9, 21.8, 12.8. HRMS (ESI): m/z $[M + H]^+$ calcd for $C_{26}H_{26}O_4N_5F_2S$, 542.1668, found: 542.1649.

_N_-(5-(8-(cyclopentyloxy)-4-methyl-2-(methylamino)quinazolin-6-yl)-2-methoxypyridin-3-yl)-2,4-difluorobenzenesulfonamide (49)

Compound **49** was prepared from compound **104** and *N*-(2-methoxy-5-(4,4,5,5-tetramethyl-1,3,2-dioxaborolan-2-yl)pyridin-3-yl)-2,4-difluorobenzenesulfonamide (yellow solid, 58% yield). ^{1}H NMR (400 MHz, DMSO-d_6) δ 10.28 (s, 1H), 8.43 (d, J = 2.4 Hz, 1H), 7.92 (d, J = 2.4 Hz, 1H), 7.76 (dt, J = 8.6, 6.4 Hz, 1H), 7.67 (d, J = 1.6 Hz, 1H), 7.64 – 7.55 (m, 1H), 7.32 (s, 1H), 7.27 – 7.17 (m, 2H), 5.20 – 5.13 (m, 1H), 3.65 (s, 3H), 2.90 (d, J = 4.8 Hz, 3H), 2.75 (s, 3H), 1.99 – 1.87 (m, 2H), 1.87 – 1.75 (m, 4H), 1.69 – 1.55 (m, 2H). ^{13}C NMR (101 MHz, DMSO-d_6) δ 169.0, 165.1 (dd, $J_{C\text{-}F}$ = 255, 11.7 Hz), 159.4 (dd, $J_{C\text{-}F}$ = 259, 13.5 Hz), 158.7, 157.3, 151.9, 144.4, 142.4, 134.3, 131.8 (d, $J_{C\text{-}F}$ = 10.8 Hz), 129.7, 128.8, 125.3 (dd, $J_{C\text{-}F}$ = 14.5, 3.6 Hz), 119.8, 119.5, 115.8 (br s), 115.2 (br s), 111.8 (dd, $J_{C\text{-}F}$ = 22.2, 3.1 Hz), 105.8 (t, J = 26.2 Hz), 80.4, 53.3, 32.3, 27.8, 23.7, 21.8. HRMS (ESI): m/z $[M + H]^+$ calcd for $C_{27}H_{28}O_4N_5F_2S$, 556.1825, found: 556.1801.

_N_-(5-(8-(cyclohexyloxy)-4-methyl-2-(methylamino)quinazolin-6-yl)-2-methoxypyridin-3-yl)-2,4-difluorobenzenesulfonamide (50)

Compound **50** was prepared from compound **105** and *N*-(2-methoxy-5-(4,4,5,5-tetramethyl-1,3,2-dioxaborolan-2-yl)pyridin-3-yl)-2,4-difluorobenzenesulfonamide (yellow solid 70% yield). ^{1}H NMR (400 MHz, DMSO-d_6) δ 10.28 (s, 1H), 8.42 (d, J = 2.4 Hz, 1H), 7.92 (d, J = 2.4 Hz, 1H), 7.76 (dt, J = 8.6, 6.4 Hz, 1H), 7.70 (d, J = 1.2 Hz, 1H), 7.59 (ddd, J = 10.4, 9.2, 2.4 Hz, 1H), 7.41 (d, J = 1.2 Hz, 1H), 7.28 – 7.18 (m, 2H), 4.76 – 4.66 (m, 1H), 3.65 (s, 3H), 2.91 (d, J = 4.8

Hz, 3H), 2.75 (s, 3H), 2.04 – 1.91 (m, 2H), 1.88 – 1.73 (m, 2H), 1.67 – 1.47 (m, 3H), 1.39 – 1.27 (m, 3H). ^{13}C NMR (101 MHz, DMSO-d_6) δ 169.2, 165.1 (dd, $J_{C\text{-}F}$ = 255, 11.8 Hz), 159.4 (dd, $J_{C\text{-}F}$ = 259, 13.5 Hz), 158.6, 157.3, 151.6, 144.8, 142.4, 134.4, 131.8 (d, $J_{C\text{-}F}$ = 10.9 Hz), 129.6, 128.9, 125.3 (dd, $J_{C\text{-}F}$ = 14.4, 3.6 Hz), 120.0, 119.5, 118.4 (br s), 116.1 (br s), 111.8 (dd, $J_{C\text{-}F}$ = 22.3, 3.3 Hz), 105.8 (t, J = 26.2 Hz), 76.7, 53.3, 31.5, 27.8, 25.3, 23.1, 21.8. HRMS (ESI): m/z $[M + H]^+$ calcd for $C_{28}H_{30}O_4N_5F_2S$, 570.1981, found: 570.1956.

2-amino-5-bromo-3-methoxybenzoic acid (54)

To a solution of 2-amino-3-methoxybenzoic acid **53** (25.08 g, 150 mmol) in DMF (200 mL) was added NBS (28.04 g， 157.5 mmol) in 5 portions over 20 minutes. The resulting reaction mixture was stirred at rt for 2 hours. The mixture was diluted with water (2 L), extracted with EtOAc (500 mL×4). The combined organic layers were washed with water (500 mL×3) and brine (500 mL), dried over anhydrous Na_2SO_4, filtered and concentrated to afford the product as a black solid (35 g, 95% yield), which was used directly in the next step without further purification. ^{1}H NMR (400 MHz, DMSO-d_6) δ 7.42 (d, J = 2.2 Hz, 1H), 7.07 (d, J = 2.2 Hz, 1H), 3.84 (s, 3H).

6-bromo-8-methoxy-2*H*-benzo[*d*][1,3]oxazine-2,4(1*H*)-dione (55)

A mixture of compound **54** (35 g, 142.2 mmol) and triphosgene (32 g, 107.8 mmol) in THF (350 mL) was refluxed for 3 hours. After cooling to rt, the resulting solid was collected by suction filtration, washed with PE/EtOAc solution (1:1, v/v, 200 mL), and dried to afford the product **55** as a yellow solid (30.78 g, 80% yield). ^{1}H NMR (400 MHz, DMSO-d_6) δ 11.43 (s, 1H), 7.56 (d, J = 2.0 Hz, 1H), 7.55 (d, J = 2.0 Hz, 1H), 3.92 (s, 3H).

2-amino-5-bromo-*N*,3-dimethoxy-*N*-methylbenzamide (56)

A mixture of compound **55** (30.78 g, 113.12 mmol), *N*,*O*-dimethylhydroxylamine hydrochloride (16.55 g, 169.68 mmol) and TEA (26.7 mL, 192.3 mmol) in dioxane (300 mL) was refluxed overnight. The volatiles were removed under reduced pressure, and the residue was diluted with water (500 mL), extracted with EtOAc (200 mL×3). The combined organic layers were washed with water (200 mL×2) and brine (200 mL), dried with anhydrous (Na_2SO_4), filtered and concentrated. The residue was purified by column chromatography (silica gel, PE/EtOAc=4:1, v/v) to afford the product **56** as a yellow oil (29.73 g, 91% yield). ^{1}H NMR (400 MHz, DMSO-d_6) δ 7.01 (d, J = 2.0 Hz, 1H), 6.97 (d, J = 2.0 Hz, 1H), 5.10 (br s, 2H), 3.82 (s, 3H), 3.53 (s, 3H), 3.22 (s, 3H).

1-(2-amino-5-bromo-3-methoxyphenyl)ethan-1-one (57)

To a solution of compound **56** (29.73 g, 103 mmol) in anhydrous THF (300 mL) at -20 °C under argon atmosphere was added MeMgBr (1M in THF, 206 mL, 206 mmol) dropwise over 30 minutes. The resulting reaction mixture was stirred at -20 °C for 30 minutes, and then quenched with saturated aqueous NH_4Cl solution. The mixture was diluted with water (1 L) and extracted with EtOAc (300 mL×3). The combined organic layers were washed with water (300 mL×2) and brine (300 mL), dried over anhydrous Na_2SO_4, filtered and concentrated. The residue was purified by column chromatography (silica gel, PE/EtOAc= 15:1, v/v) to afford the product **57** as a yellow oil (6.5 g, 26% yield). ^{1}H NMR (400 MHz, DMSO-d_6) δ 7.50 (d, J = 2.0 Hz, 1H), 7.08 (d, J = 2.0 Hz, 1H), 7.04 (s, 2H), 3.84 (s, 3H), 2.51 (s, 3H).

6-bromo-8-methoxy-4-methylquinazolin-2-amine (58)

A mixture of compound **57** (7.41 g, 30.36 mmol) and concentrated hydrochloric acid (10 mL) in 50% cyanamide in water (74 mL) was stirred at 120 °C for 15 minutes. The reaction mixture was cooled to rt and diluted with water (300 mL). The resulting solid was collected by suction

filtration, washed with water (100 mL) and ethanol (30 mL), dried to affor the product **58** as a light yellow solid (8.00 g, 98%yield). ^{1}H NMR (400 MHz, DMSO-d_6) δ 7.67 (d, J = 2.0 Hz, 1H), 7.20 (d, J = 2.0 Hz, 1H), 6.90 (br s, 2H), 3.88 (s, 3H), 2.67 (s, 3H).

6-bromo-2-(2,5-dimethyl-1*H*-pyrrol-1-yl)-8-methoxy-4-methylquinazoline (59)

A mixture of compound **58 (**8.00 g, 29.84 mmol), 2,5-hexanedione (13.61 g, 119.36 mmol) and p-toluenesulfonic acid monohydrate (0.568 g, 2.98 mmol) in NMP (80 mL) and toluene (80 mL) was refluxed at 160 °C for 6 h. The reaction mixture was cooled to rt, concentrated under reduced pressure, diluted with water (400 mL) and extracted with EtOAc (100 mL×3). The combined organic layers were washed with water (100 mL×3) and brine (100 mL), dried over anhydrous Na_2SO_4, filtered and concentrated. The residue was purified by column chromatography (silica gel, PE/EtOAc= 30:1, v/v) to afford the product **59** as a yellow solid (8.95 g, 87% yield). ^{1}H NMR (400 MHz, DMSO-d_6) δ 8.04 (d, J = 1.8 Hz, 1H), 7.57 (d, J = 1.8 Hz, 1H), 5.84 (s, 2H), 4.01 (s, 3H), 2.92 (s, 3H), 2.30 (s, 6H).

6-bromo-2-(2,5-dimethyl-1*H*-pyrrol-1-yl)-4-methylquinazolin-8-ol (60)

To a solution of compound **59** (3.27 g, 9.56 mmol) in DCE (300 mL) was added $AlCl_3$ (3.83 g, 28.68 mmol). The resulting reaction mixture was stirred at 80 °C for 1.5 h. The reaction mixture was cooled to rt, diluted with water (300 mL) and extracted with DCM (300 mL×2). The combined organic layers were washed with water (200 mL) and brine (100 mL), dried over anhydrous Na_2SO_4, filtered and concentrated. The residue was purified with column chromatography (silica gel, PE/EtOAc = 50:1, v/v) to afford the product **60** as a yellow solid (2.41 g, 77% yield). ^{1}H NMR (400 MHz, DMSO-d_6) δ 10.64 (s, 1H), 7.93 (d, J = 2.0 Hz, 1H), 7.44 (d, J = 2.0 Hz, 1H), 5.84 (s, 2H), 2.91 (s, 3H), 2.29 (s, 6H).

6-bromo-2-(2,5-dimethyl-1*H*-pyrrol-1-yl)-8-isopropoxy-4-methylquinazoline (61)

A mixture of compound **60** (0.762 g, 2.3 mmol), isopropyl bromide (2.829 g, 23 mmol) and K_2CO_3, (3.177 g, 23 mmol) in acetonitrile (20 mL) in a sealed tube was stirred at 60 °C overnight. The reaction mixture was cooled to rt and filtered. Silica gel (3 g) was added to the filtrate and the resulting mixture was evaporated to dry under reduced pressure. The residue was purified by column chromatography (silica gel, PE/EtOAc = 40:1, v/v) to afford the product **61** as a yellow oil (0.500 g, 58% yield). ^{1}H NMR (400 MHz, DMSO-d_6) δ 8.02 (d, J = 1.8 Hz, 1H), 7.59 (d, J = 1.8 Hz, 1H), 5.85 (s, 2H), 4.98 – 4.88 (m, 1H), 2.92 (s, 3H), 2.34 (s, 6H), 1.36 (d, J = 6.0 Hz, 6H).

6-bromo-8-(cyclopropylmethoxy)-2-(2,5-dimethyl-1*H*-pyrrol-1-yl)-4-methylquinazoline (**62**)

In a similar manner to **61**, compound **62** was prepared from **60** and (bromomethyl)cyclopropane (white solid 61% yield). ^{1}H NMR (400 MHz, DMSO-d_6) δ 7.64 (d, J = 1.8 Hz, 1H), 7.14 (d, J = 1.8 Hz, 1H), 6.91 (s, 2H), 3.90 (d, J = 7.2 Hz, 2H), 2.65 (s, 3H), 1.33 – 1.23 (m, 1H), 0.65 – 0.55 (m, 2H), 0.35 (q, J = 4.8 Hz, 2H).

6-bromo-2-(2,5-dimethyl-1*H*-pyrrol-1-yl)-8-(2-methoxyethoxy)-4-methylquinazoline (63)

In a similar manner to **61**, compound **63** was prepared from **60** and 2-Methoxyethyl chloride (yellow oil, 61% yield). ^{1}H NMR (400 MHz, DMSO-d_6) δ 7.80 (d, J = 1.9 Hz, 1H), 7.31 (d, J = 1.9 Hz, 1H), 5.90 (s, 2H), 4.33 (t J = 4.8 Hz, 2H), 3.90 (t, J = 4.8 Hz, 3H), 3.48 (s, 3H), 2.91 (s, 3H), 2.43 (s, 6H).

6-bromo-8-cyclobutoxy-2-(2,5-dimethyl-1*H*-pyrrol-1-yl)-4-methylquinazoline (64)

In a similar manner to **61**, compound **64** was prepared from **60** and cyclobutyl bromide (yellow oil, 78% yield). ^{1}H NMR (400 MHz, DMSO-d_6) δ 8.02 (d, J = 1.9 Hz, 1H), 7.35 (d, J = 1.9 Hz, 1H), 5.85 (s, 2H), 4.98 (p, J = 7.0 Hz, 1H), 2.91 (s, 3H), 2.60 – 2.51 (m, 2H), 2.33 (s, 6H), 2.19 – 2.05 (m, 2H), 1.92 – 1.77 (m, 1H), 1.77 – 1.64 (m, 1H).

6-bromo-8-(cyclopentyloxy)-2-(2,5-dimethyl-1*H*-pyrrol-1-yl)-4-methylquinazoline (65)

In a similar manner to **61**, compound **65** was prepared from **60** and cyclopentyl bromide (yellow oil, 98% yield). ^{1}H NMR (500 MHz, DMSO-d_6) δ 8.00 (d, J = 1.5 Hz, 1H), 7.53 (d, J = 1.5 Hz, 1H), 5.85 (s, 2H), 5.18 – 5.09 (m, 1H), 2.91 (s, 3H), 2.34 (s, 6H), 2.03 – 1.92 (m, 2H), 1.89 – 1.80 (m, 2H), 1.80 – 1.70 (m, 2H), 1.69 – 1.58 (m, 2H).

6-bromo-8-(cyclohexyloxy)-2-(2,5-dimethyl-1*H*-pyrrol-1-yl)-4-methylquinazoline (66)

In a similar manner to **61**, compound **66** was prepared from **60** and cyclohexyl bromide (yellow oil, 82% yield). ^{1}H NMR (500 MHz, DMSO-d_6) δ 8.00 (d, J = 2.0 Hz, 1H), 7.61 (d, J = 2.0 Hz, 1H), 5.85 (s, 2H), 4.79 – 4.72 (m, 1H), 2.91 (s, 3H), 2.35 (s, 6H), 1.95 – 1.86 (m, 2H), 1.79 – 1.70 (m, 2H), 1.69 – 1.57 (m, 2H), 1.56 – 1.31 (m, 4H).

6-bromo-8-((4,4-difluorocyclohexyl)oxy)-2-(2,5-dimethyl-1*H*-pyrrol-1-yl)-4-methylquinazoline (67)

To a mixture of compound **60** (408 mg, 1.23 mmol), triphenylphosphine (387 mg, 1.48 mmol) and 4,4-difluorocyclohexan-1-ol (180 mg, 1.33 mmol) in anhydrous THF (10 mL) was added DEAD (257 mg, 1.47 mmol) at rt under Ar atmosphere. The resulting reaction mixture was stirred at rt overnight. Silica gel (2 g) was added and the mixture was evaporated to dry under reduced pressure. The residue was purified by column chromatography (silica gel, PE/EtOAc=30:1, v/v) to afford the product **67** as a yellow oil (230 mg, 42% yield). ^{1}H NMR (400 MHz, $CDCl_3$) δ 7.82 (d, J = 1.8 Hz, 1H), 7.31 (d, J = 1.8 Hz, 1H), 5.92 (s, 2H), 4.85 – 4.77 (m, 1H), 2.91 (s, 3H), 2.45 (s, 6H), 2.28 – 2.14 (m, 4H), 2.07 – 1.92 (m, 4H).

6-bromo-2-(2,5-dimethyl-1*H*-pyrrol-1-yl)-4-methyl-8-((tetrahydro-2*H*-pyran-4-yl)oxy)quinazoline (68)

In a similar manner to **67**, compound **68** was prepared from **60** and tetrahydro-2*H*-pyran-4-ol (yellow oil, 50% yield). ^{1}H NMR (400 MHz, DMSO-d_6) δ 8.04 (d, J = 1.9 Hz, 1H), 7.70 (d, J = 1.8 Hz, 1H), 5.86 (s, 2H), 5.01 – 4.91 (m, 1H), 3.94 – 3.80 (m, 2H), 3.56 (ddd, J = 11.2, 8.0, 3.2 Hz, 2H), 2.92 (s, 3H), 2.36 (s, 3H), 2.09 – 1.94 (m, 2H), 1.77 – 1.65 (m, 2H).

(*R*)-6-bromo-2-(2,5-dimethyl-1*H*-pyrrol-1-yl)-4-methyl-8-((tetrahydrofuran-3-yl)oxy)quinazoline (69)

In a similar manner to **67**, compound **69** was prepared from **60** and (*S*)-3-hydroxytetrahydrofuran (yellow oil, 94% yield). ^{1}H NMR (400 MHz, $CDCl_3$) δ 7.82 (d, J = 1.6 Hz, 1H), 7.22 (d, J = 1.6 Hz, 1H), 5.91 (s, 2H), 5.22 – 5.14 (m, 1H), 4.18 – 3.94 (m, 4H), 2.91 (s, 3H), 2.45 (s, 6H), 2.33 – 2.26 (m, 2H).

(*S*)-6-bromo-2-(2,5-dimethyl-1*H*-pyrrol-1-yl)-4-methyl-8-((tetrahydrofuran-3-yl)oxy)quinazoline (70)

In a similar manner to **67**, compound **70** was prepared from **60** and (*R*)-3-hydroxytetrahydrofuran as a yellow oil (93% yield). ^{1}H NMR (400 MHz, DMSO-d_6) δ 8.05 (d, J = 1.8 Hz, 1H), 7.58 (d, J = 1.8 Hz, 1H), 5.85 (s, 2H), 5.38 – 5.31 (m, 1H), 4.06 – 3.75 (m, 4H), 2.92 (s, 3H), 2.34 (s, 6H), 2.32 – 2.24 (m, 1H), 2.13 – 2.02 (m, 1H).

6-bromo-2-(2,5-dimethyl-1*H*-pyrrol-1-yl)-4-methyl-8-((tetrahydrofuran-3-yl)methoxy)quinazoline (71)

In a similar manner to **67**, compound **71** was prepared from **60** and (tetrahydrofuran-3-yl)methanol (yellow oil 72% yield). ^{1}H NMR (400 MHz, DMSO-d_6) δ 8.03 (d, J = 1.6 Hz, 1H), 7.58 (d, J = 1.6 Hz, 1H), 5.85 (s, 2H), 4.23 – 4.08 (m, 2H), 3.88 – 3.75 (m, 2H), 3.69 (dd, J = 14.8, 7.6 Hz, 1H), 3.62 (dd, J = 8.6, 5.6 Hz, 1H), 2.92 (s, 3H), 2.84 – 2.71 (m, 1H), 2.35 (s, 6H), 2.12 – 2.00 (m, 1H), 1.81 – 1.70 (m, 1H).

6-bromo-2-(2,5-dimethyl-1*H*-pyrrol-1-yl)-8-((2,2-dimethyltetrahydro-2*H*-pyran-4-yl)oxy)-4-methylquinazoline (72)

In a similar manner to **67**, compound **72** was prepared from **60** and 2,2-dimethyloxan-4-ol (yellow oil, 47% yield). ^{1}H NMR (400 MHz, $CDCl_3$) δ 7.81 (d, *J* = 1.9 Hz, 1H), 7.29 (d, *J* = 1.9 Hz, 1H), 4.85 – 4.76 (m, 1H), 4.03 – 3.95 (m, 1H), 3.80 – 3.70 (m, 1H), 2.91 (s, 3H), 2.44 (s, 6H), 2.17 – 2.08 (m, 1H), 2.08 – 1.99 (m, 1H), 1.92 – 1.75 (m, 2H), 1.34 (s, 3H), 1.28 (s, 3H).

6-bromo-2-(2,5-dimethyl-1*H*-pyrrol-1-yl)-4-methyl-8-((tetrahydro-2*H*-pyran-4-yl)methoxy)quinazoline (73)

In a similar manner to **67**, compound **73** was prepared from **60** and tetrahydropyran-4-methanol (yellow oil, 71% yield). ^{1}H NMR (400 MHz, DMSO-d_6) δ 8.02 (d, *J* = 1.9 Hz, 1H), 7.55 (d, *J* = 1.9 Hz, 1H), 5.85 (s, 2H), 4.07 (d, *J* = 6.2 Hz, 2H), 3.94 – 3.86 (m, 2H), 3.36 (dt, *J* = 11.6, 2.0 Hz, 2H), 2.91 (s, 3H), 2.35 (s, 6H), 2.19 – 2.03 (m, 1H), 1.78 – 1.69 (m, 2H), 1.52 – 1.37 (m, 2H).

6-bromo-2-(2,5-dimethyl-1*H*-pyrrol-1-yl)-4-methyl-8-((tetrahydrofuran-2-yl)methoxy)quinazoline (74)

In a similar manner to **67**, compound **74** was prepared from **60** and tetrahydrofurfuryl alcohol (yellow oil, 89% yield). ^{1}H NMR (400 MHz, DMSO-d_6) δ 8.03 (d, *J* = 1.8 Hz, 1H), 7.58 (d, *J* = 1.8 Hz, 1H), 5.85 (s, 2H), 4.32 – 4.14 (m, 3H), 3.86 – 3.77 (m, 1H), 3.74 – 3.66 (m, 1H), 2.92 (s, 3H), 2.34 (s, 6H), 2.10 – 1.91 (m, 2H), 1.90 – 1.77 (m, 2H).

6-bromo-2-(2,5-dimethyl-1*H*-pyrrol-1-yl)-4-methyl-8-((1-methylpiperidin-4-yl)oxy)quinazoline (75)

In a similar manner to **67**, compound **75** was prepared from **60** and *N*-methyl-4-piperidinol as a yellow oil (56% yield). ^{1}H NMR (400 MHz, $CDCl_3$) δ 8.02 (d, *J* = 2.0 Hz, 1H), 7.64 (d, *J* = 2.0

Hz, 1H), 5.86 (s, 2H), 4.88 – 4.73 (m, 1H), 2.91 (s, 3H), 2.64 – 2.54 (m, 2H), 2.37 (s, 6H), 2.35 – 2.25 (m, 2H), 2.18 (s, 3H), 2.04 – 1.89 (m, 2H), 1.87 – 1.71 (m, 2H).

4-(2-((6-bromo-2-(2,5-dimethyl-1*H*-pyrrol-1-yl)-4-methylquinazolin-8-yl)oxy)ethyl)morpholine (76)

In a similar manner to **67**, compound **76** was prepared from **60** and 2-(morpholin-4-yl)ethanol as a crude product containing $P(O)Ph_3$, which was used directly in the next step. ^{1}H NMR (400 MHz, $CDCl_3$) δ 8.02 (d, J = 2.0 Hz, 1H), 7.64 (d, J = 2.0 Hz, 1H), 5.85 (s, 2H), 4.33 (t, J = 5.1 Hz, 2H), 4.04 (q, J = 7.0 Hz, 4H), 3.64 – 3.46 (m, 4H), 2.92 (s, 3H), 2.81 (t, J = 5.1 Hz, 2H), 2.53 (s, 6H).

6-bromo-8-isopropoxy-4-methylquinazolin-2-amine (77)

A mixture of compound **61** (494 mg, 1.32 mmol) and hydroxylamine hydrocloride (459 mg, 6.6 mmol) in EtOH (10 mL) and water (1 mL) was refluxed overnight. The reaction mixture was evaporated to dry under reduced pressure, diluted with water (50 mL), neutralized with saturated aqueous $NaHCO_3$ solution, and extracted with DCM (30 mL×3). The combined organic layers were washed with water (50 mL) and brine (50 mL), dried over anhydrous Na_2SO_4, filtered and concentrated. The residue was purified by column chromatography (silica gel, DCM/MeOH = 70:1, v/v) to afford the product **77** as a yellow solid (270 mg, 69% yield). ^{1}H NMR (400 MHz, DMSO-d_6) δ 7.64 (d, J = 2.0 Hz, 1H), 7.22 (d, J = 2.0 Hz, 1H), 6.84 (s, 2H), 4.86 – 4.75 (m, 1H), 2.65 (s, 3H), 1.31 (d, J = 6.0 Hz, 6H).

6-bromo-8-(cyclopropylmethoxy)-4-methylquinazolin-2-amine (78)

In a similar manner to **77**, compound **78** was prepared from **62** (white solid, 40% yield). ^{1}H NMR (400 MHz, DMSO-d_6) δ 7.64 (d, J = 1.8 Hz, 1H), 7.14 (d, J = 1.8 Hz, 1H), 6.91 (s, 2H),

3.90 (d, J = 7.2 Hz, 2H), 2.65 (s, 3H), 1.33 – 1.23 (m, 1H), 0.65 – 0.55 (m, 2H), 0.35 (q, J = 4.8 Hz, 2H).

6-bromo-8-(2-methoxyethoxy)-4-methylquinazolin-2-amine (79)

In a similar manner to **77**, compound **79** was prepared from **63** as a yellow solid (80% yield). ^{1}H NMR (400 MHz, DMSO-d_6) δ 7.67 (d, J = 1.8 Hz, 1H), 7.23 (d, J = 1.8 Hz, 1H), 6.90 (s, 2H), 4.21 (t, J = 4.4 Hz, 2H), 3.90 (t, J = 4.4 Hz, 3H), 3.32 (s, 3H), 2.66 (s, 3H).

6-bromo-8-cyclobutoxy-4-methylquinazolin-2-amine (80)

In a similar manner to **77**, compound **80** was prepared from **64** (yellow solid, 33% yield). ^{1}H NMR (400 MHz, DMSO-d_6) δ 7.65 (d, J = 2.0 Hz, 1H), 7.00 (d, J = 2.0 Hz, 1H), 6.89 (s, 2H), 4.81 (p, J = 7.0 Hz, 1H), 2.65 (s, 3H), 2.49 – 2.42 (m, 2H), 2.16 – 2.00 (m, 2H), 1.89 – 1.57 (m, 2H).

6-bromo-8-(cyclopentyloxy)-4-methylquinazolin-2-amine (81)

In a similar manner to **77**, compound **81** was prepared from **65** (yellow solid, 41% yield). ^{1}H NMR (400 MHz, DMSO-d_6) δ 7.64 (d, J = 2.0 Hz, 1H), 7.16 (d, J = 2.0 Hz, 1H), 6.83 (s, 2H), 5.00 – 4.94 (m, 1H), 2.65 (s, 3H), 2.04 – 1.91 (m, 2H), 1.80 – 1.68 (m, 4H), 1.66 – 1.53 (m, 2H).

6-bromo-8-(cyclohexyloxy)-4-methylquinazolin-2-amine (82)

In a similar manner to **77**, compound **82** was prepared from **66** (yellow solid, 44% yield). ^{1}H NMR (400 MHz, DMSO-d_6) δ 7.64 (d, J = 2.0 Hz, 1H), 7.25 (d, J = 2.0 Hz, 1H), 6.83 (s, 2H), 4.58 – 4.45 (m, 1H), 2.65 (s, 3H), 2.04 – 1.95 (m, 2H), 1.82 – 1.67 (m, 2H), 1.65 – 1.27 (m, 6H).

6-bromo-8-((4,4-difluorocyclohexyl)oxy)-4-methylquinazolin-2-amine (83)

In a similar manner to **77**, compound **83** was prepared from **67** (yellow solid, 64% yield). ^{1}H NMR (400 MHz, $CDCl_3$) δ 7.65 (d, J = 1.6 Hz, 1H), 7.20 (d, J = 1.6 Hz, 1H), 5.28 (br s, 2H), 4.71 – 4.62 (m, 1H), 2.74 (s, 3H), 2.41 – 2.23 (m, 2H), 2.23 – 2.10 (m, 2H), 2.07 – 1.86 (m, 4H).

6-bromo-4-methyl-8-((tetrahydro-2*H*-pyran-4-yl)oxy)quinazolin-2-amine (84)

In a similar manner to **77**, compound **84** was prepared from **68** (yellow solid, 39% yield). ^{1}H NMR (400 MHz, DMSO-d_6) δ 7.68 (d, J = 2.0 Hz, 1H), 7.36 (d, J = 2.0 Hz, 1H), 6.85 (s, 2H), 4.82 – 4.73 (m, 1H), 3.94 – 3.87 (m, 2H), 3.53 – 3.45 (m, 2H), 2.65 (s, 3H), 2.05 – 1.96 (m, 2H), 1.68 – 1.58 (m, 2H). MS (ESI+) m/z 337.8, 339.8 $[M + H]^+$.

(*R*)-6-bromo-4-methyl-8-((tetrahydrofuran-3-yl)oxy)quinazolin-2-amine (85)

In a similar manner to **77**, compound **85** was prepared from **69** (yellow solid, 79% yield). ^{1}H NMR (400 MHz, DMSO-d_6) δ 7.69 (d, J = 2.0 Hz, 1H), 7.21 (d, J = 2.0 Hz, 1H), 6.89 (s, 2H), 5.25 – 5.18 (m, 1H), 3.97 – 3.83 (m, 3H), 3.80 – 3.72 (m, 1H), 2.66 (s, 3H), 2.33 – 2.21 (m, 1H), 2.05 – 1.93 (m, 1H).

(*S*)-6-bromo-4-methyl-8-((tetrahydrofuran-3-yl)oxy)quinazolin-2-amine (86)

In a similar manner to **77**, compound **86** was prepared from **70** as a yellow solid (70% yield). ^{1}H NMR (400 MHz, DMSO-d_6) δ 7.69 (d, J = 2.0 Hz, 1H), 7.21 (d, J = 2.0 Hz, 1H), 6.90 (s, 2H), 5.25 – 5.18 (m, 1H), 3.97 – 3.82 (m, 3H), 3.80 – 3.72 (m, 1H), 2.66 (s, 3H), 2.33 – 2.21 (m, 1H), 2.05 – 1.95 (m, 1H).

6-bromo-4-methyl-8-((tetrahydrofuran-3-yl)methoxy)quinazolin-2-amine (87)

In a similar manner to **77**, compound **87** was prepared from **71** yellow solid, 49% yield). ^{1}H NMR (400 MHz, DMSO-d_6) δ 7.67 (d, J = 2.0 Hz, 1H), 7.26 (d, J = 2.0 Hz, 1H), 6.86 (s, 2H), 4.08 – 3.95 (m, 2H), 3.84 – 3.74 (m, 2H), 3.67 (dt, J = 8.0, 6.6 Hz, 1H), 3.59 (dd, J = 8.6, 5.0 Hz, 1H), 2.78 – 2.68 (m, 1H), 2.66 (s, 3H), 2.09 – 1.98 (m, 1H), 1.75 – 1.65 (m, 1H).

6-bromo-8-((2,2-dimethyltetrahydro-2*H*-pyran-4-yl)oxy)-4-methylquinazolin-2-amine (88)

In a similar manner to **77**, compound **88** was prepared from **72** (yellow solid, 48% yield). ^{1}H NMR (500 MHz, DMSO-d_6) δ 7.67 (d, J = 1.5 Hz, 1H), 7.36 (d, J = 1.5 Hz, 1H), 6.83 (s, 2H),

4.95 – 4.84 (m, 1H), 3.80 – 3.61 (m, 2H), 2.66 (s, 3H), 2.06 – 1.94 (m, 2H), 1.54 – 1.39 (m, 2H), 1.24 (s, 3H), 1.21 (s, 3H).

6-bromo-4-methyl-8-((tetrahydro-2*H*-pyran-4-yl)methoxy)quinazolin-2-amine (89)

In a similar manner to **77**, compound **89** was prepared from **73** (yellow solid, 85% yield). ^{1}H NMR (400 MHz, DMSO-d_6) δ 7.65 (d, J = 2.0 Hz, 1H), 7.22 (d, J = 2.0 Hz, 1H), 6.83 (s, 2H), 3.95 (d, J = 6.7 Hz, 2H), 3.92 – 3.84 (m, 2H), 3.40 – 3.32 (m, 2H), 2.65 (s, 3H), 2.14 – 1.99 (m, 1H), 1.78 – 1.69 (m, 2H), 1.43 – 1.28 (m, 2H).

6-bromo-4-methyl-8-((tetrahydrofuran-2-yl)methoxy)quinazolin-2-amine (90)

In a similar manner to **77**, compound **90** was prepared from **74** (yellow solid, 27% yield). ^{1}H NMR (400 MHz, DMSO-d_6) δ 7.66 (d, J = 2.0 Hz, 1H), 7.24 (d, J = 2.0 Hz, 1H), 6.91 (s, 2H), 4.28 – 4.18 (m, 1H), 4.11 – 3.98 (m, 2H), 3.87 – 3.75 (m, 1H), 3.6673 – 3.66 (m, 1H), 2.66 (s, 3H), 2.08 – 1.97 (m, 1H), 1.97 – 1.77 (m, 2H), 1.74 – 1.62 (m, 1H).

6-bromo-4-methyl-8-((1-methylpiperidin-4-yl)oxy)quinazolin-2-amine (91)

In a similar manner to **77**, compound **91** was prepared from **75** (yellow solid, 64% yield). ^{1}H NMR (400 MHz, DMSO-d_6) δ 7.66 (d, J = 2.0 Hz, 1H), 7.28 (d, J = 2.0 Hz, 1H), 6.83 (s, 2H), 4.64 – 4.47 (m, 1H), 2.78 – 2.69 (m, 2H), 2.65 (s, 3H), 2.19 (s, 3H), 2.18 – 2.10 (m, 2H), 2.04 – 1.93 (m, 2H), 1.73 – 1.60 (m, 2H).

6-bromo-4-methyl-8-(2-morpholinoethoxy)quinazolin-2-amine (92)

In a similar manner to **77**, compound **92** was prepared from **76** (yellow solid, 40% yield for 2 steps from compound **76**). ^{1}H NMR (500 MHz, DMSO-d_6) δ 7.67 (s, 1H), 7.28 (s, 1H), 6.90 (s, 2H), 4.21 (t, J = 5.9 Hz, 2H), 3.67 – 3.50 (m, 4H), 2.74 (t, J = 5.8 Hz, 2H), 2.66 (s, 3H), 2.51 (br s, 4H).

6-bromo-*N*,4-dimethyl-8-((tetrahydro-2*H*-pyran-4-yl)oxy)quinazolin-2-amine (93)

To a solution of compound **84 (**517 mg, 1.53 mmol) in anhydrous DMF (50 mL) at 0 °C was added NaH (60% dispersion in mineral oil, 153 mg, 3.82 mmol) and the resulting reaction mixture was stirred at 0 °C for 30 min. CH_3I (217 mg, 1.53 mmol) was added, and the resulting reaction mixture was stirred at rt for 3 hours. The mixture was diluted with water (250 mL), neutralized with 2M HCl solution, extracted with EtOAc (50 mL×3). The combined organic layers were washed with water (50 mL×2) and brine (50 mL), dried over Na_2SO_4, filtered and concentrated. The residue was purified by column chromatography (silica gel, DCM/EtOAc = 30:1 then 4:1, v/v) to afford compound **93** as a yellow solid (113 mg, 21%). ^{1}H NMR (400 MHz, DMSO-d_6) δ 7.74 (d, J = 1.8 Hz, 1H), 7.39 (d, J = 1.8 Hz, 1H), 7.34 (q, J = 4.8 Hz, 1H), 4.94 – 4.76 (m, 1H), 3.99 – 3.82 (m, 2H), 3.53 – 3.43 (m, 2H), 2.88 (d, J = 4.8 Hz, 3H), 2.66 (s, 3H), 2.06 – 1.88 (m, 2H), 1.77 – 1.57 (m, 2H).

6-bromo-*N*-ethyl-4-methyl-8-((tetrahydro-2*H*-pyran-4-yl)oxy)quinazolin-2-amine (94)

In a similar manner to **93**, compound **94** was prepared from **84** and CH_3CH_2I (yellow solid, 20% yield). ^{1}H NMR (400 MHz, DMSO-d_6) δ 7.73 (d, J = 1.6 Hz, 1H), 7.41 (br s, 1H), 7.38 (d, J = 1.6 Hz, 1H), 4.90 – 4.78 (m, 1H), 3.98 – 3.82 (m, 2H), 3.52 – 3.43 (m, 2H), 3.43 – 3.33 (m, 2H), 2.66 (s, 3H), 2.02 – 1.90 (m, 2H), 1.73 – 1.61 (m, 2H), 1.17 (t, J = 7.2 Hz, 3H).

6-bromo-*N*-(cyclopropylmethyl)-4-methyl-8-((tetrahydro-2*H*-pyran-4-yl)oxy)quinazolin-2-amine (95)

In a similar manner to **93**, compound **95** was prepared from **84** and (bromomethyl)cyclopropane (yellow solid, 18% yield). ^{1}H NMR (400 MHz, DMSO-d_6) δ 7.73 (s, 1H), 7.51 (br s, 1H), 7.37 (d, J = 1.7 Hz, 1H), 4.88 – 4.78 (m, 1H), 3.95 – 3.83 (m, 2H), 3.55 – 3.39 (m, 2H), 3.24 (t, J = 6.3 Hz, 2H), 2.66 (s, 3H), 2.03 – 1.91 (m, 2H), 1.74 – 1.59 (m, 2H), 1.15 – 1.06 (m, 1H), 0.45 – 0.35 (m, 2H), 0.27 (q, J = 4.4 Hz, 2H).

6-bromo-*N*,*N*,4-trimethyl-8-((tetrahydro-2*H*-pyran-4-yl)oxy)quinazolin-2-amine (96)

In a similar manner to **93**, compound **96** was prepared from **84** and CH_3I (yellow solid, 20% yield). ^{1}H NMR (400 MHz, DMSO-d_6) δ 7.76 (d, J = 1.9 Hz, 1H), 7.39 (d, J = 1.9 Hz, 1H), 4.90 – 4.82 (m, 1H), 3.96 – 3.83 (m, 2H), 3.53 – 3.44 (m, 2H), 3.22 (s, 6H), 2.71 (s, 3H), 1.99 – 1.92 (m, 2H), 1.74 – 1.63 (m, 2H).

***N*-(6-bromo-4-methyl-8-((tetrahydro-2*H*-pyran-4-yl)oxy)quinazolin-2-yl)acetamide (97)**

To a mixture of compound **84** (338 mg, 1 mmol)and pyridine (396 mg, 5 mmol) in anhydrous DMF (10 mL) was added acetyl chloride (234 mg, 3 mmol) at rt. The reaction mixture was stirred at rt for 4 h. The mixture was diluted with water (50 mL), acidified with 2M HCl solution until the pH value was 5, and then extracted with EtOAc (30 mL×3). The combined organic layers were washed with water (30 mL×2) and brine (30 mL), dried over Na_2SO_4, filtered and concentrated. The residue was purified by column chromatography (silica gel, DCM/MeOH = 70:1, v/v) to afford the product **97** as a yellow solid (290 mg, 76%). ^{1}H NMR (400 MHz, DMSO-d_6) δ 10.57 (s, 1H), 7.94 (d, J = 2.0 Hz, 1H), 7.61 (d, J = 2.0 Hz, 1H), 5.07 – 4.94 (m, 1H), 3.93 – 3.85 (m, 2H), 3.55 – 3.47 (m, 2H), 2.81 (s, 3H), 2.34 (s, 3H), 2.09 – 1.93 (m, 2H), 1.74 – 1.58 (m, 2H).

(*R*)-6-bromo-*N*,4-dimethyl-8-((tetrahydrofuran-3-yl)oxy)quinazolin-2-amine (98)

In a similar manner to **93**, compound **98** was prepared from **85** and CH_3I as a yellow solid (29% yield). ^{1}H NMR (400 MHz, DMSO-d_6) δ 7.72 (d, J = 2.0 Hz, 1H), 7.34 (q, J = 4.8 Hz, 1H), 7.25 (s, 1H), 5.32 – 5.22 (m, 1H), 3.96 – 3.86 (m, 3H), 3.81 – 3.73 (m, 1H), 2.87 (d, J = 4.8 Hz, 3H), 2.66 (s, 3H), 2.28 – 2.15 (m, 1H), 2.11 – 1.98 (m, 1H).

(*S*)-6-bromo-*N*,4-dimethyl-8-((tetrahydrofuran-3-yl)oxy)quinazolin-2-amine (99)

In a similar manner to **93**, compound **99** was prepared from **86** and CH_3I (yellow solid, 31% yield). ^{1}H NMR (400 MHz, DMSO-d_6) δ 7.72 (d, J = 2.0 Hz, 1H), 7.34 (q, J = 4.8 Hz, 1H), 7.25 (s, 1H), 5.32 – 5.22 (m, 1H), 3.96 – 3.86 (m, 3H), 3.77 (dt, J = 8.2, 4.6 Hz, 1H), 2.87 (d, J = 4.8 Hz, 3H), 2.66 (s, 3H), 2.27 – 2.17 (m, 1H), 2.09 – 1.99 (m, 1H).

6-bromo-*N*,4-dimethyl-8-((tetrahydrofuran-3-yl)methoxy)quinazolin-2-amine (100)

In a similar manner to **93**, compound **100** was prepared from **87** and CH_3I (yellow solid, 17% yield). ^{1}H NMR (400 MHz, DMSO-d_6) δ 7.68 (d, J = 2.0 Hz, 1H), 7.30 (d, J = 4.8 Hz, 1H), 7.28 (d, J = 1.7 Hz, 1H), 4.18 – 4.07 (m, 1H), 4.07 – 3.96 (m, 1H), 3.87 – 3.76 (m, 2H), 3.74 – 3.58 (m, 2H), 2.87 (d, J = 4.8 Hz, 3H), 2.78 – 2.68 (m, 1H), 2.66 (s, 3H), 2.10 – 1.96 (m, 1H), 1.82 – 1.68 (m, 1H).

6-bromo-8-((2,2-dimethyltetrahydro-2*H*-pyran-4-yl)oxy)-*N*,4-dimethylquinazolin-2-amine (101)

In a similar manner to **93**, compound **101** was prepared from **88** and CH_3I (yellow solid, 21% yield). ^{1}H NMR (400 MHz, DMSO-d_6) δ 7.72 (d, J = 2.0 Hz, 1H), 7.35 (d, J = 2.0 Hz, 1H), 7.32 (q, J = 4.8 Hz, 1H), 5.04 – 4.92 (m, 1H), 3.78 (dt, J = 12.0, 4.4 Hz, 1H), 3.58 (t, J = 10.0 Hz, 1H), 2.87 (d, J = 4.8 Hz, 3H), 2.66 (s, 3H), 2.01 – 1.83 (m, 2H), 1.67 – 1.43 (m, 2H), 1.29 (s, 3H), 1.17 (s, 3H).

6-bromo-*N*,4-dimethyl-8-((tetrahydro-2*H*-pyran-4-yl)methoxy)quinazolin-2-amine (102)

In a similar manner to **93**, compound **102** was prepared from **89** and CH_3I (yellow solid, 20% yield). ^{1}H NMR (400 MHz, DMSO-d_6) δ 7.66 (d, J = 2.0 Hz, 1H), 7.28 (q, J = 4.8 Hz, 1H), 7.24 (d, J = 1.4 Hz, 1H), 3.98 (d, J = 6.8 Hz, 2H), 3.94 – 3.84 (m, 2H), 3.35 (dt, J = 11.6, 2.0 Hz, 2H), 2.87 (d, J = 4.8 Hz, 3H), 2.66 (s, 3H), 2.16 – 2.02 (m, 1H), 1.80 – 1.71 (m, 2H), 1.39 (qd, J = 12.4, 4.4 Hz, 2H).

6-bromo-8-cyclobutoxy-*N*,4-dimethylquinazolin-2-amine (103)

In a similar manner to **93**, compound **103** was prepared from **80** and CH_3I (yellow solid, 20% yield). ^{1}H NMR (400 MHz, DMSO-d_6) δ 7.65 (d, J = 2.0 Hz, 1H), 7.30 (br s, 1H), 7.01 (d, J = 1.6 Hz, 1H), 4.84 (p, J = 7.2 Hz, 1H), 2.88 (d, J = 4.8 Hz, 3H), 2.65 (s, 3H), 2.49 – 2.42 (m, 2H), 2.19 – 2.03 (m, 2H), 1.89 – 1.75 (m, 1H), 1.74 – 1.58 (m, 1H).

6-bromo-8-(cyclopentyloxy)-*N*,4-dimethylquinazolin-2-amine (104)

In a similar manner to **93**, compound **104** was prepared from **81** and CH_3I (yellow solid, 15% yield). ^{1}H NMR (400 MHz, DMSO-d_6) δ 7.66 (d, J = 2.0 Hz, 1H), 7.27 (q, J = 4.8 Hz, 1H), 7.20 (s, 1H), 5.11 – 4.98 (m, 1H), 2.87 (d, J = 4.8 Hz, 3H), 2.66 (s, 3H), 1.98 – 1.85 (m, 2H), 1.84 – 1.68 (m, 4H), 1.68 – 1.53 (m, 2H).

6-bromo-8-(cyclohexyloxy)-*N*,4-dimethylquinazolin-2-amine (105)

In a similar manner to **93**, compound **105** was prepared from **82** and CH_3I (yellow solid, 15% yield). ^{1}H NMR (400 MHz, DMSO-d_6) δ 7.70 (d, J = 2.0 Hz, 1H), 7.34 – 7.25 (m, 2H), 4.69 – 4.54 (m, 1H), 2.87 (d, J = 4.8 Hz, 3H), 2.66 (s, 3H), 1.98 – 1.86 (m, 2H), 1.82 – 1.71 (m, 2H), 1.61 – 1.45 (m, 3H), 1.41 – 1.27 (m, 3H).

Biology and DMPK. All animal experiments were carried out in accordance with the guidelines of the Committee on Animals of the Institute of Materia Medica, Chinese Academy of Medical Science & Peking Union Medical College.

Kinase Inhibitory Activity Assay

The kinase inhibitory activity assay was performed by Shanghai ChemPartner Co., Ltd. (China). The PI3Kα inhibition assay was conducted with the Kinase-Glo assay while the PI3Kβ, γ and δ assay with ADP-Glo assay, both purchased from Promega. Briefly, the compound, PI3K enzymes, the PIP2 substrate and ATP were dissolved in the kinase buffer, which was then added

to a multi-well plate. The plate was then incubated at room temperature, followed by the addition of Kinase-Glo or ADP-Glo reagents and a briefly shaking. The kinase detection buffer was then added to the plate, which was then put into FlexStation for data collection.

The inhibitory activity assay for mTOR was performed with Lance Ultra Assay. Briefly, the compound, mTOR protein, ULight-4E-BP1 peptide substrate and ATP were diluted in the kinase buffer, which was then added to a multi-well plate and incubated at room temperature for 30 min. The quench buffer and Eu-antiphospho-4E-BP1 antibody were added, followed by incubation for 1 h. The plate was then put into PerkinElmer EnVision Reader for data collection.

The inhibitory activity against AKT was conducted with Mobility shift assay. Briefly, the compound, AKT protein and ATP were dissolved in the kinase buffer along with FAM-labeled peptide. The kinase reaction was stopped with stop buffer after incubated at room temperature. The data was collected with Caliper. For all kinase inhibitory activity assays, the curves were fitted with Graphpad Prism 5.0.

Cell Cytotoxicity Assays

T98G and PC3 cell lines were purchased from ATCC (Manassas, VA, USA). NCI-H460, MDA-MB-231, HGC-27, DU-145, U87MG, U251, SH-SY-5Y, NCI-H209, MGC-803 cell lines were from National Infrastructure of Cell Line Resource, China. T98G, PC3, NCI-460, MDA-MB-231, SH-SY-5Y and MGC-803 were cultured in DMEM medium (Gibico, USA) with 10% (v/v) Fetal Bovine Serum (Gibico, USA) and 100 units/mL penicillin/streptomycin. HGC-27, DU-145, NCI-H209 were cultured in RPMI 1640 with 10%FBS and 100 units/mL penicillin/streptomycin. U87MG and U251 were cultured in RPMI 1640 with 10%FBS,100 units/mL penicillin/streptomycin and non-essential amino acid (Gibico). U87MG/Luc was

purchased from Keyuandi (Shanghai, China) and cultured in DMEM medium with 10% FBS and 100 units/mL penicillin/streptomycin.

Cell cytotoxicity was performed with MTT (Sigma-Aldrich, USA). Cells were implanted in 96-well plates at a density of 1.5×10^3 cell/mL and the cells were treated with different compounds in various concentrations for 96 hours. MTT solution was added to each well at the final concentration of 0.5mg/mL. After incubation for 4 hours at 37 °C, the absorbance were measured by microplate reader (Biotek Instruments, Inc. USA) at 570 nm. IC_{50} values was calculated with Graphpad Prism 5 Software.

Plasma Protein Binding Assay

The assay was performed by Suzhou Truwaybio Technology Ltd. (China). The extent of plasma protein binding was determined in vitro, in human and ICR mouse by HTDialysis. Test compounds were dissolved in DMSO at 10 mM and spike the test compound to plasma for a final concentration of 2 μM. Load 150 μL plasma to one side of the dialysis equipment againest 150 μL blank buffer to the other side, and shake the dialysis equipment for 6 hours at 37 °C. Following dialysis, buffer and plasma samples were transfered to a 96-well plate. Plasma proteins were precipitate with acetonitrile containing an internal standard. The amount of the parent analyte in the plasma and buffer samples was quantified by LC-MS/MS and percent unbound fraction (%Fu) was calculated.

Pharmacokinetic Studies

Test compounds were subjected to pharmacokinetic studies on male ICR mice. For oral administration, five animals were in each group and three animals were in each group for intravenous administration. The test compounds were orally administered as 0.1%PEG400/0.5%CMC suspension (10 mg/kg) or intravenous injected as 10%DMSO saline (2

mg/kg). Blood samples were collected at 0.083, 0.25, 0.5, 1, 2, 4, 6, 8, 12 and 24 h time points following oral dosing and at 0.033, 0.083, 0.25, 0.5, 1, 2, 4, 6, 8, 12 and 24 h following intravenous dosing. Plasma samples were obtained by centrifugation, and brain tissues were homogenized in a threefold volume (w/v) of saline. Plasma and brain samples were extracted with acetonitrile containing propranolol as an internal standard using a 3:1 extractant-to-plasma ratio. The concentrations of test compounds were determined by high pressure liquid chromatography/tandem mass spectrometry (LC/MS/MS). Chromatographic separation performed on a Zobax SB-C18 column (100 mm×2.1 mm, 3.5 μm) with an isocratic mobile phase of acetonitrile/water (70:30, v/v) containing 0.1% formic acid at 0.2 mL/min flow rate. Compound detection on the mass spectrometer was performed in electrospray positive ionization mode. The selected reaction monitoring transitions were m/z 558.3→474.4 (**19**), m/z 544.4→474.5 (**20**), m/z 572.3→488.3 (**37**) and m/z 558.4→380.5 (**43**). Relevant pharmacokinetic parameters were calculated using WinNonlin software version 6.3 based on non-compartmental analysis (Pharsight Corporation, Mountain View, USA).

Orthotopic Brain Xenograft Mouse Model

For orthotopic mouse tumor model, female BALB/c athymic nude mice (Vital River Laboratories, Beijing, China) with body weight at 18-20 g were housed in standard SPF facilities. All procedures were approved by the (Peking Union Medical College) PUMC Pharmaceutical Institutional Animal Care and Use Committee. The procedure followed previous study.[41] Mice were anesthetized with 50 mg/kg pentobarbital sodium intraperitoneally, and placed in a stereotaxic restrain, and a small surgical incision was made in the skin covering the skull 2 mm to the right of the bregma. Cell suspensions (5 μL) containing approximately 1×10^6 U87MG/Luc cells were slowly (approximately 30s) injected intracranially 2.0 mm below the skull surface

using a 26-gauge needle. The needle was slowly retracted after 3 minutes. The incision was immediately sutured with surgical line, and 50,000 units of penicillin were injected into the mice to prevent infection. The animals were then warmed with heating mats and monitored until they regained consciousness. After 4 days, mice bearing intracranial tumors were randomized to receive vehicle, TMZ and test compounds dissolved in 0.1%PEG400/0.5%CMC suspension solution. Mice were orally administrated with TMZ (30 mg/kg) daily for 5 days or test compounds once daily. Animal magnetic resonance imaging (MRI) scanner (Pharma Scan 70/16 US, Bruker, Germany) was used to observe the intracranial tumor development. The parameters for MRI were as follows: a T2_TurboRARE, with TR/TE = 5000/40, 6 averages, 20 × 20 field-of-view, and 0.5 mm slice thickness. The tumor volume (TV) based on MRI was calculated as TV = L ×W× T, where L is the maximum length of tumor, W is the maximum width perpendicular to L and T is the thickness of the tumor slice (0.5 mm). Tumor volume inhibition (TGI) at the end of treatment was measured as (1- $TV_{treatment}/TV_{vehicle}$) ×100%. Statistical analyses were performed by GraphPad Prism5 software and the significance levels were evaluated using one-way ANOVA model.

Subcutaneous Tumor Xenograft Mouse Models

For subcutaneous mouse model, female athymic BALB/c nude mice (8-10 week old) were subcutaneously implanted with 1×10^7 cells of NCI-H460 or NCI-H1975 or NCI-H209 or HGC-27 or MGC-803 in 0.1 mL matrigel solution in the right flank of nude nice. After two weeks, tumor issue was harvested sterilely and tumor cells were extracted from tissue homogenate. Then, the mice were implanted with 5×10^6 tumor cells each. Seven days later when the average tumor volumes reached to 100-300 mm^3, the mice were randomized and received treatment (Day 0) Mice was administrated with positive control or test compounds once daily. Tumor volume and

body weight were monitored twice a week. Tumor volume (TV) was calculated as TV = 1/2 ×L× W^2, where L is the maximum length of tumor, W is the maximum width of tumor. The relative tumor volume (RTV) was calculated as V_t/V_0 for both treatment groups and vehicle group, while V_0 is the tumor volume at day 0, V_t is the tumor volume measured each time point. The mice were euthanized at the end of treatment. Tumor volume inhibition (TGI) at the end of treatment was measured as (1- $RTV_{treatment}/RTV_{vehicle}$) ×100%. Statistical analyses were performed by GraphPad Prism5 software and the significance levels were evaluated using one-way ANOVA model.

Pharmacokinetic-Pharmacodynamic Studies

Female athymic BALB/c nude mice (8–10 week old) were implanted with NCI-H460 tumor cells. When the tumor volumes reached to 500-600 mm^3, mice were administered orally (via gavage) at a single dose of 10 mg/kg. At different time points as indicated, animals were anaesthetized and sacrificed. Blood and tumor samples were collected. Blood samples were centrifuged to obtain the plasma for PK analysis. Tumor tissues were homogenized for PK analysis. For Akt (Ser 473) phosphorylation analysis, it follows the protocol of phospho-AKT (S473) ELISA Kit (Abcam, ab176657). The data was analyzed by GraphPad Prism 7.

ASSOCIATED CONTENT

Supporting Information.

The Supporting Information is available free of charge on the ACS Publications website.

Figure S1: magnetic resonance imaging (MRI) results for orthotopic mouse tumor model; procedures for molecular docking studies, hERG inhibition assay, AMES test, cytochrome P450

inhibition assay and single dose toxicity studies; kinase selectivity profile of key compounds in panel of 468 kinase targets, Table S1: Matrix of compound screen for of **19**, and Table S2: S-score of **19**; experimental procedures and data for the synthesis of intermediates (PDF).

Molecular formula strings (CSV)

AUTHOR INFORMATION

Corresponding Author

* X.C.: phone, +86-10-63165207; email, chxg@imm.ac.cn

* H.X.: phone, +86-10-83161089; email, xuheng@imm.ac.cn

ORCID

Heng Xu: 0000-0002-1720-5286

Author Contributions

∇ S. L. and C.W. contributed equally to this work.

Notes

The authors declare no competing financial interest.

ACKNOWLEDGMENT

Financial support from the National Key R&D Program of China (2017YFA0205400), the CAMS Innovation Fund for Medical Sciences (2017-I2M-3-011 and 2017-I2M-1-010) and National Postdoctoral Program for Innovative Talents (BX201700037) is gratefully acknowledged. We thank Dr. Xiaobing Deng for his help on molecular modeling.

ABBREVIATIONS

PI3K, phosphatidylinositol 3-kinase; PIP2, phosphatidylinositol 4,5-diphosphate; PIP3, phosphatidylinositol 3,4,5-triphosphate; RTK, receptor tyrosine kinase; GPCR, G-protein coupled receptors; PTEN, phosphatase and tensin homologue; PH, pleckstrin homology; AKT, known as protein kinase B or PKB; mTOR, mammalian target of rapamycin; mTORC1, mTOR complex 1; mTORC2, mTOR complex 2; PFS, progression-freesurvival; HNSCC, head and neck squamous cell carcinoma; NSCLC, non-small cell lung carcinoma; GBM, glioblastoma multiforme; Clearance, CL; PSA, polar surface area; TGI, tumor growth inhibition; CisPt, Cis-platin; TMZ, temozolomide; MRI, magnetic resonance imaging; hERG, human ether-a-go-go-related gene; CYP450, cytochromeP450; NBS, *N*-Bromobutanimide; DMF, *N*,*N*-Dimethylformamide; $PdCl_2$(dppf), [1,1'-Bis(diphenylphosphino)ferrocene]dichloropalladium(II); rt, room temperature; THF, tetrahydrofuran; TEA, trimethylamine; NMP, *N*-methyl-2-pyrrolidone; DCE, 1,2-dichloroethane; DEAD, Ethyl azodicarboxylate; EtOH, ethanol; DMSO, dimethyl sulfoxide.

REFERENCES

1. Vivanco, I.; Sawyers, C. L. The phosphatidylinositol 3-kinase-AKT pathway in human cancer. *Nat. Rev. Cancer* **2002**, *2*, 489−501.

2. Engelman, J. A.; Luo, J.; Cantley, L. C. The evolution of phosphatidylinositol 3-kinases as regulators of growth and metabolism. *Nat. Rev. Genet.* **2006**, *7*, 606−619.

3. Liu, P.; Cheng, H.; Roberts, T. M.; Zhao, J. J. Targeting the phosphoinositide 3-kinase pathway in cancer. *Nat. Rev. Drug Discov.* **2009**, *8*, 627−644.

4. Fruman, D. A.; Meyers, R. E.; Cantley, L. C. Phosphoinositide kinases. *Annu. Rev. Biochem.* **1998**, *67*, 481–507.

5. Katso, R.; Okkenhaug, K.; Ahmadi, K.; White, S.; Timms, J.; Waterfield, M. D. Cellular function of phosphoinositide 3‐kinases: implications for development, homeostasis, and cancer. *Annu. Rev. Cell Dev. Biol.* **2001**, *17*, 615–675.

6. Song, M. S.; Salmena, L.; Pandolfi, P. P. The functions and regulation of the PTEN tumour suppressor. *Nat. Rev. Mol. Cell Biol.* **2012**, *13*, 283–296.

7. Cantley, L. C. The phosphoinositide 3-kinase pathway. *Science* **2002**, *296*, 1655−1657.

8. Alessi, D. R.; Deak, M.; Casamayor, A.; Caudwell, F. B.; Morrice, N.; Norman, D. G.; Gaffney, P.; Reese, C. B.; MacDougall, C. N.; Harbison, D.; Ashworth, A.; Bownes, M. 3‐Phosphoinositide‐dependent protein kinase‐1 (PDK1): structural and functional homology with the Drosophila DSTPK61 kinase. *Curr. Biol.* **1997**, *7*, 776–789.

9. Stephens, L.; Anderson, K.; Stokoe, D.; Erdjument-Bromage, H.; Painter, G. F.; Holmes, A. B.; Gaffney, P. R. J.; Reese, C. B.; McCormick, F.; Tempst, P.; Coadwell, J.; Hawkins, P. T. Protein kinase B kinases that mediate phosphatidylinositol 3,4,5‐trisphosphate‐dependent activation of protein kinase B. *Science* **1998**, *279*, 710–714.

10. Sarbassov, D. D.; Ali, S. M.; Sabatini, D. M. Growing roles for the mTOR pathway. *Curr. Opin. Cell Biol.* **2005**, *17*, 596-603.

11. Wullschleger, S.; Loewith, R.; Hall, M. N. TOR signaling in growth and metabolism. *Cell* **2006**, *124*, 471–484.

12. Engelman, J. A. Targeting PI3K signalling in cancer: opportunities, challenges and limitations. *Nat. Rev. Cancer* **2009**, *9*, 550–562.

13. Yuan, T. L; Cantley, L. C. PI3K pathway alterations in cancer: variations on a theme. *Oncogene* **2008**, *27*, 5497–5510.

14. Millis, S. Z.; Ikeda, S.; Reddy, S.; Gatalica, Z.; Kurzrock, R. Landscape of phosphatidylinositol-3-kinase pathway alterations across 19 784 diverse solid tumors. *JAMA Oncol.* **2016**, *2*, 1565–1573.

15. Shuttleworth, S. J.; Silva, F. A.; Cecil, A. R. L.; Tomassi, C. D.; Hill, T. J.; Raynaud, F. I.; Clarke, P. A.; Workman, P. Progress in the preclinical discovery and clinical development of class I and dual class I/IV phosphoinositide 3-kinase (PI3K) inhibitors. *Curr. Med. Chem.* **2011**, *18*, 2686–2714.

16. Brana, I.; Siu, L. L. Clinical development of phosphatidylinositol 3-kinase inhibitors for cancer treatment. *BMC Med.* **2012**, *10*, 161.

17. Lomon So, L.; Fruman D. A. PI3K signaling in B and T lymphocytes: new developments and therapeutic advances. *Biochem. J.* **2012**, *442*, 465–481.

18. Yap, T. A.; Bjerke, L.; Clarke, P. A.; Workman, P. Drugging PI3K in cancer: refining targets and therapeutic strategies. *Curr. Opin. Pharmaco.* **2015**, *23*, 98–107.

19. Thorpe, L. M.; Yuzugullu, H.; Zhao, J. J. PI3K in cancer: divergent roles of isoforms, modes of activation and therapeutic targeting. *Nat. Rev. Cancer* **2015**, *15*, 7-24.

20. Cheng, H.; Bagrodia, S.; Bailey, S.; Edwards, M.; Hoffman, J.; Hu, Q.; Kania, R.; Knighton, D. R.; Marx, M. A.; Ninkovic, S.; Sun, S.; Zhang, E. Discovery of the highly potent

PI3K/mTOR dual inhibitor PF-04691502 through structure based drug design. *Med. Chem. Commun.* **2010**, *1*, 139-144.

21. Knight, S. D.; Adams, N. D.; Burgess, J. L.; Chaudhari, A. M.; Darcy, M. G.; Donatelli, C. A.; Luengo, J. I.; Newlander, K. A.; Parrish, C. A.; Ridgers, L.; Sarpong, M. A.; Schmidt, S. J.; Van Aller, G. S.; Carson, J. D.; Diamond, M. A.; Elkins, P. A.; Gardiner, C. M.; Garver, E.; Gilbert, S. A.; Gontarek, R. R.; Jackson, J. R.; Kershner, K. L.; Luo, L.; Raha, K.; Sherk, C. S.; Sung, C.; Sutton, D.; Tummino, P. J.; Wegrzyn, R. J.; Auger, K. R.; Dhanak, D. Discovery of GSK2126458, a highly potent inhibitor of PI3K and the mammalian target of rapamycin. *ACS Med. Chem. Lett.* **2010**, *1*, 39–43.

22. Heffron, T. P.; Ndubaku, C. O.; Salphati, L.; Alicke, B.; Cheong, J.; Drobnick, J.; Edgar, K.; Gould, S. E.; Lee, L. B.; Lesnick, J. D.; Lewis, C.; Nonomiya, J.; Pang, J.; Plise, E. G.; Sideris, S.; Wallin, J.; Wang, L.; Zhang, X.; Olivero, A. G. Discovery of clinical development candidate GDC-0084, a brain penetrant inhibitor of PI3K and mTOR. *ACS Med. Chem. Lett.* **2016**, *7*, 351−356.

23. Beaufils, F.; Cmiljanovic, N.; Cmiljanovic, V.; Bohnacker, T.; Melone, A.; Marone, R.; Jackson, E.; Zhang, X.; Sele, A.; Borsari, C.; Mestan, J.; Hebeisen, P.; Hillmann, P.; Giese, B.; Zvelebil, M.; Fabbro, D.; Williams, R. L.; Rageot, D.; Wymann, M. P. 5‑(4,6-Dimorpholino-1,3,5-triazin-2-yl)-4-(trifluoromethyl)pyridin-2-amine (PQR309), a potent, brain-penetrant, orally bioavailable, pan-class I PI3K/mTOR inhibitor as clinical candidate in oncology. *J. Med. Chem.* **2017**, *60*, 7524–7538.

24. Burger, M. T.; Pecchi, S.; Wagman, A.; Ni, Z. J.; Knapp, M.; Hendrickson, T.; Atallah, G.; Pfister, K.; Zhang, Y.; Bartulis, S.; Frazier, K.; Ng, S.; Smith, A.; Verhagen, J.; Haznedar, J.;

Huh, K.; Iwanowicz, E.; Xin, X.; Menezes, D.; Merritt, H.; Lee, I.; Wiesmann, M.; Kaufman, S.; Crawford, K.; Chin, M.; Bussiere, D.; Shoemaker, K.; Zaror, I.; Maira, S. M.; Voliva, C. F. Identification of NVP-BKM120 as a potent, selective, orally bioavailable class I PI3 kinase inhibitor for treating cancer. *ACS Med. Chem. Lett.* **2011**, *2*, 774–779.

25. Scott, W. J.; Hentemann, M. F.; Rowley, R. B.; Bull, C. O.; Jenkins, S.; Bullion, A. M.; Johnson, J.; Redman, A.; Robbins, A. H.; Esler, W.; Fracasso, R. P.; Garrison, T.; Hamilton, M.; Michels, M.; Wood, J. E.; Wilkie, D. P.; Xiao, H.; Levy, J.; Stasik, E.; Liu, N.; Schaefer, M.; Brands, M.; Lefranc,J. Discovery and SAR of novel 2,3-dihydroimidazo[1,2-c]quinazoline PI3K inhibitors: identification of Copanlisib (BAY 80-6946). *Chem. Med. Chem.* **2016**, *11*, 1517–1530.

26. Furet, P.; Guagnano, V.; Fairhurst, R. A.; Imbach-Weese, P.; Bruce, I.; Knapp, M.; Fritsch, C.; Blasco, F.; Blanz, J.; Aichholz, R.; Hamon, J.; Fabbro, D.; Caravatti, G. Discovery of NVP-BYL719 a potent and selective phosphatidylinositol-3 kinase alpha inhibitor selected for clinical evaluation. *Bioorg. Med. Chem. Lett.* **2013**, *23*, 3741–3748.

27. Mateo, J.; Ganji, G.; Lemech, C.; Burris, H. A.; Han, S.-W.; Swales, K.; Decordova, S.; DeYoung, M. P.; Smith, D. A.; Kalyana-Sundaram, S.; Wu, J.; Motwani, M.; Kumar, R.; Tolson, J. M.; Rha, S. Y.; Chung, H. C.; Eder, J. P.; Sharma, S.; Bang, Y.-J.; Infante, J. R.; Yan, L.; de Bono, J. S.; Arkenau, H.-T. A first-time-in-human study of GSK2636771, a phosphoinositide 3 kinase beta-selective inhibitor, in patients with advanced solid tumors. *Clin. Cancer Res.* **2017**, *23*, 5981-5992.

28. Lannutti, B. J.; Meadows, S. A.; Herman, S. E.; Kashishian, A.; Steiner, B.; Johnson, A. J.; Byrd, J. C.; Tyner, J. W.; Loriaux, M. M.; Deininger, M.; Druker, B. J.; Puri, K. D.; Ulrich, R. G.; Giese, N. A. CAL-101, a p110δ selective phosphatidylinositol-3-kinase inhibitor for

the treatment of B-cell malignancies, inhibits PI3K signaling and cellular viability. *Blood* **2011**, *117*, 591-594.

29. https://www.accessdata.fda.gov/drugsatfda_docs/appletter/2014/205858orig1s000ltr.pdf (accessed May 22, 2018).

30. https://www.accessdata.fda.gov/drugsatfda_docs/appletter/2017/209936orig1s000ltr.pdf (accessed May 22, 2018).

31. Baselga, J.; Im, S.-A.; Iwata, H.; Cortés, J.; De Laurentiis, M.; Jiang, Z.; Arteaga, C. L.; Jonat, W.; Clemons, M.; Ito, Y.; Awada, A.; Chia, S.; Jagiełło-Gruszfeld, A.; Pistilli, B.; Tseng, L.-M.; Hurvitz, S.; Masuda, N.; Takahashi, M.; Vuylsteke, P.; Hachemi, S.; Dharan, B.; Di Tomaso, E.; Urban, P.; Massacesi, C.; Campone, M. Buparlisib plus fulvestrant versus placebo plus fulvestrant in postmenopausal, hormone receptor-positive, HER2-negative, advanced breast cancer (BELLE-2): a randomised, double-blind, placebo-controlled, phase 3 trial. *Lance Oncol.* **2017**, *18*, 904-916

32. Rodon, J.; Dienstmann, R.; Serra, V.; Tabernero, J. Development of PI3K inhibitors: lessons learned from early clinical trials. *Nat. Rev. Clin. Oncol.* **2013**, *10*, 143–153.

33. The Cancer Genome Atlas Network. Comprehensive genomiccharacterization defines human glioblastoma genes and core pathways. *Nature* **2008**, *455*, 1061−1068.

34. Lipinski, C. A.; Lombardo, F.; Dominy, B. W.; Feeny, P. J. Experimental and computational approaches to estimate solubility and permeability in drug discovery and development settings. *Adv. Drug Deliv. Rev.* **1997**, *23*, 3-25.

35. Veber, D. F.; Johnson, S. R.; Cheng, H.-Y.; Smith, B. R.; Ward, K. W.; Kopple, K. D. Molecular properties that influence the oral bioavailability of drug candidates. *J. Med. Chem.* **2002**, *45*, 2615-2623.

36. Waring, M. J. Lipophilicity in drug discovery. *Expert Opin. Drug Discov.* **2010**, *5*, 235−248.

37. Lin, S.; Wang, C.; Ji, J.; Wu, D.; Lv, Y.; Sheng, L.; Han, F.; Dong, Y.; Zhang, K.; Yang, Y.; Li, Y.; Chen, X.; Xu, H. Discovery of new thienopyrimidine derivatives as potent and orally efficacious phosphoinositide 3-kinase inhibitors. *Bioorg. & Med. Chem.* **2018**, *26*, 637–646.

38. Heffron, T. P.; Salphati, L.; Alicke, B.; Cheong, J.; Dotson, J.; Edgar, K.; Goldsmith, R.; Gould, S. E.; Lee, L. B.; Lesnick, J. D.; Lewis, C.; Ndubaku, C.; Nonomiya, J.; Olivero, A. G.; Pang, J.; Plise, E. G.; Sideris, S.; Trapp, S.; Wallin, J.; Wang, L.; Zhang, X. The design and identification of brain penetrant inhibitors of phosphoinositide 3‑kinase α. *J. Med. Chem.* **2012**, *55*, 8007−8020.

39. Baell, J. B.; Holloway, G. A. New substructure filters for removal of pan assay interference compounds (PAINS) from screening libraries and for their exclusion in bioassays. *J. Med. Chem.* **2010**, *53*, 2719−2740.

40. http://Cbligand.org/PAINS/Search_struct.php (accessed March 12, 2018).

41. Chen, J.; Lv, H.; Hu, J.; Ji, M.; Xue, Ni.; Li, C.; Ma, S.; Zhou, Q.; Lin, B.; Li, Y.; Yu, S.; Chen, X. CAT3, a novel agent for medulloblastoma and glioblastoma treatment, inhibits tumor growth by disrupting the Hedgehog signaling pathway. *Cancer Lett.* **2016**, *381*, 391-403.

Table of Contents graphic

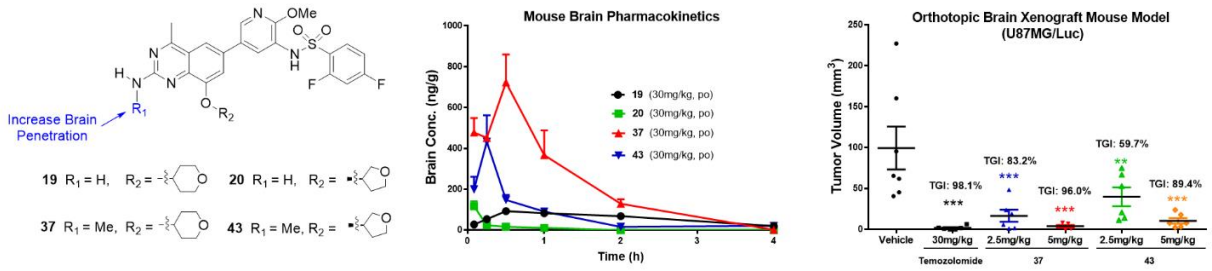

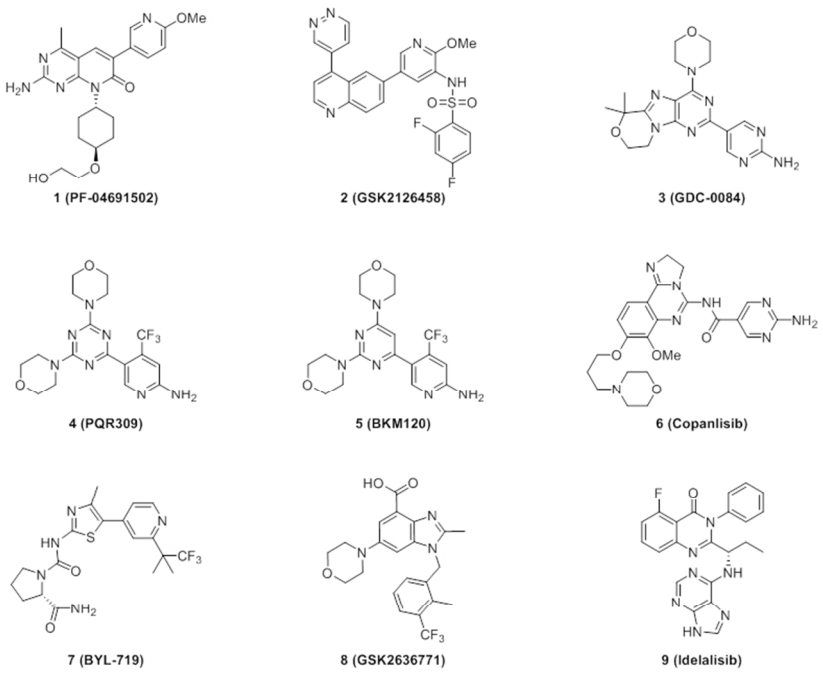

Figure 1. Selected examples of PI3K inhibitors: the dual PI3K/mTOR inhibitors 1-4, pan-PI3K inhibitors 5-6, a PI3K alpha-selective inhibitor 7, a PI3K beta-selective inhibitor 8, a PI3K delta-selective inhibitor 9.

254x190mm (96 x 96 DPI)

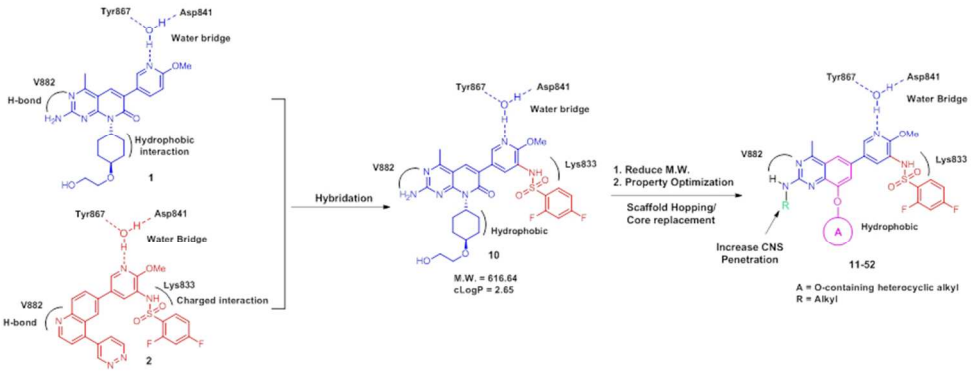

Figure 2. Design strategy of quinazoline-based PI3K inhibitors.

254x190mm (96 x 96 DPI)

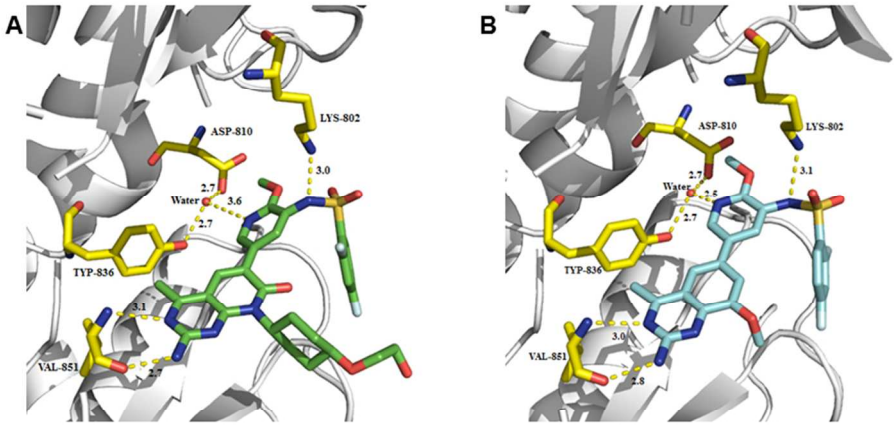

Figure 3. Predicted binding mode for 10 (A) and 11 (B) with PI3Kα (PDB ID: 4JPS). Hydrogen bonds are shown as yellow dashed lines to the hinge region (Val851), Lys802, and the conserved water molecule bridge (Tyr 836 and Asp810). Images generated by PyMol.

254x190mm (96 x 96 DPI)

A

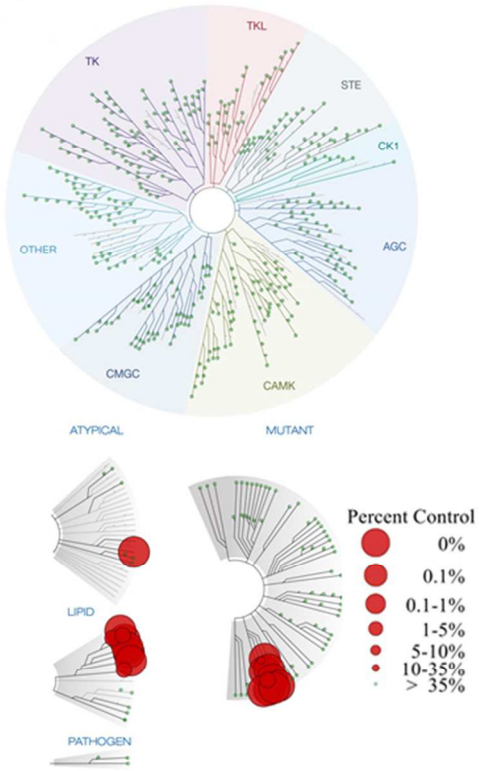

B

Compound **19**
468 target tested
18 interactions mapped
S(1) score = 0.015

Target		% Control
Class I PI3K	PI3KCA	0
	PIK3CA(C420R)	0
	PIK3CA(E542K)	0
	PIK3CA(E545A)	0
	PIK3CA(E545K)	0
	PIK3CA(H1047L)	0
	PIK3CA(H1047Y)	1.4
	PIK3CA(I800L)	0
	PIK3CA(M1043I)	12
	PIK3CA(Q546K)	0
	PIK3CB	1.6
	PIK3CD	2.4
	PIK3CG	0
Class II PI3K	PIK3C2B	0
	PIK3C2G	0
Class III PI3K	VPS34	0
PIK4CB	PIK4CB	2
mTOR	mTOR	0

Figure 4. Kinase selectivity profiling of compound 19 at a concentration of 1 μM (KinomescanTM, DiscoveRx). A) TREEspotTM interaction maps for 19 among 468 kinase targets. B) 9 non-mutant kinases were hit with <35% control binding remaining. Results for primary screen binding interactions are reported as % control, where lower numbers indicate stronger hits in the matrix. S-score is a quantitative measure of compound selectivity and it is calculated by dividing the number of kinases that compounds bind to by the total number of distinct kinases tested, excluding mutant variants.

268x223mm (72 x 72 DPI)

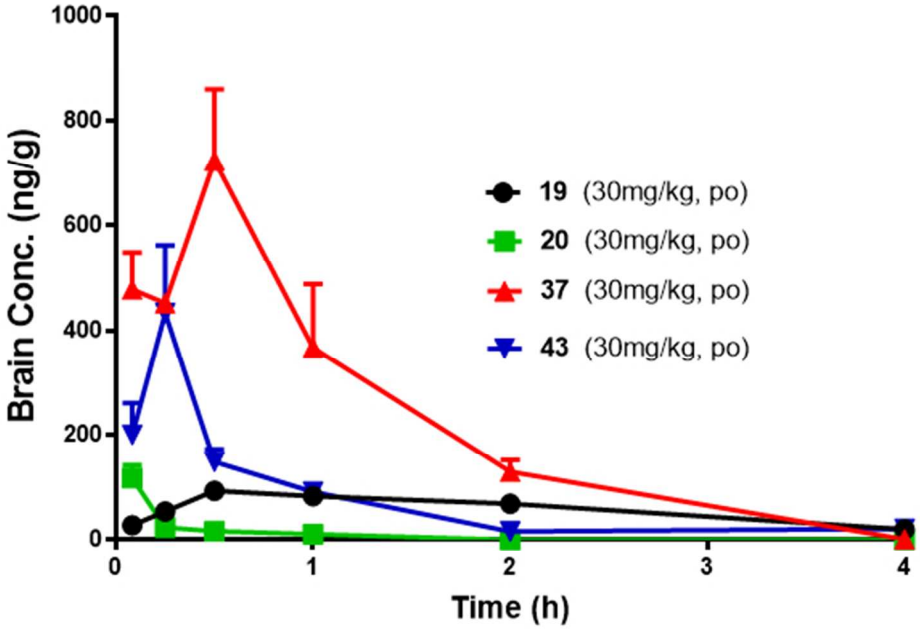

Figure 5. Brain concentration versus time curves for compounds 19, 20, 37 and 43. Results are expressed as the mean brain concentration and standard deviation (SD) (n = 3 for each time point).

52x35mm (300 x 300 DPI)

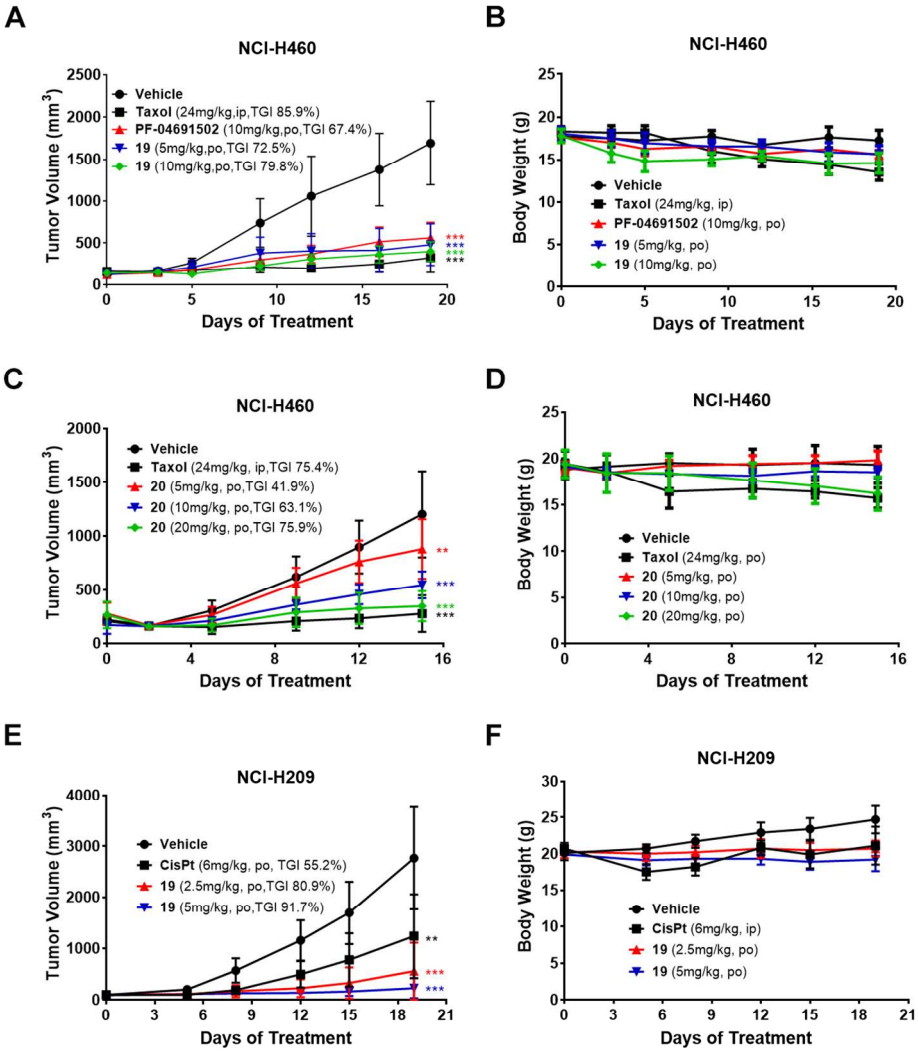

Figure 6. In vivo antitumor efficacy of compounds 19 and 20 in lung cancer xenograft models. Non-small cell lung cancer NCI-H460 cells and small cell lung cancer NCI-H209 cells were subcutaneously implanted into nude mice. A) Tumor volume changes following treatment with 19 in the NCI-H460 xenograft model; B) body weight changes after treatment with 19 in the NCI-H460 xenograft model; C) tumor volume changes following treatment with 20 in the NCI-H460 xenograft model; D) body weight changes after treatment with 20 in the NCI-H460 xenograft model; E) tumor volume changes after treatment with 19 in the NCI-H209 xenograft model; F) body weight changes after treatment with 19 in the NCI-H209 xenograft model. Results are expressed as the mean ± SD (n = 5–7 for each group); **p <0.01 and ***p <0.001 vs vehicle.

119x140mm (300 x 300 DPI)

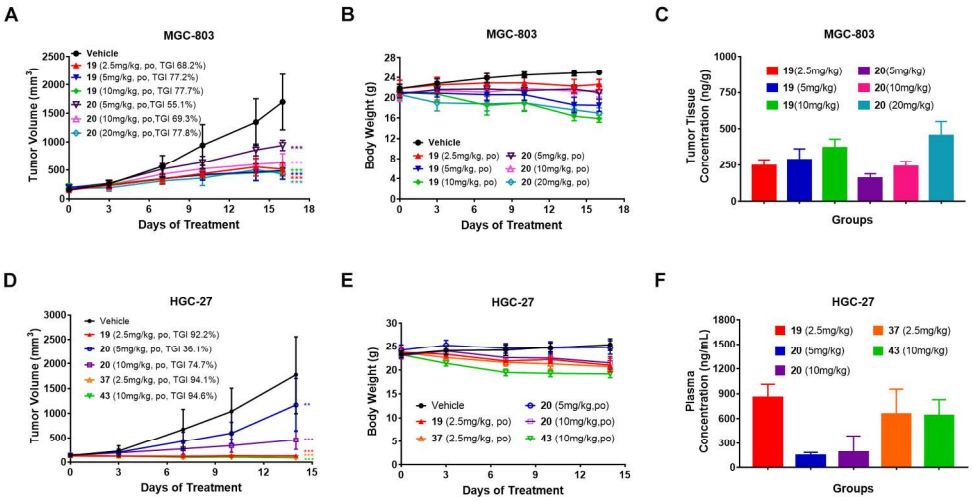

Figure 7. In vivo antitumor efficacy of compounds 19, 20, 37 and 43 in gastric cancer xenograft models. Gastric cancer MGC-803 and HGC-27 cells were subcutaneously implanted into nude mice. A) Tumor volume changes after treatment with 19 and 20 in the MGC-803 xenograft model; B) body weight changes after treatment with 19 and 20 in the MGC-803 xenograft model; C) concentrations of 19 and 20 in tumor tissue at 24h after the final dose in the MGC-803 xenograft model; D) tumor volume changes after treatment with 19, 20, 37 and 43 in the HGC-27 xenograft model; E) body weight changes after treatment with 19, 20, 37 and 43 in the HGC-27 xenograft model; F) concentrations of 19, 20, 37 and 43 in plasma at 2h after the final dose in the HGC-27 xenograft model. Results are expressed as the mean ± SD (n = 6 for each group); **p <0.01 and ***p <0.001 vs vehicle.

180x99mm (300 x 300 DPI)

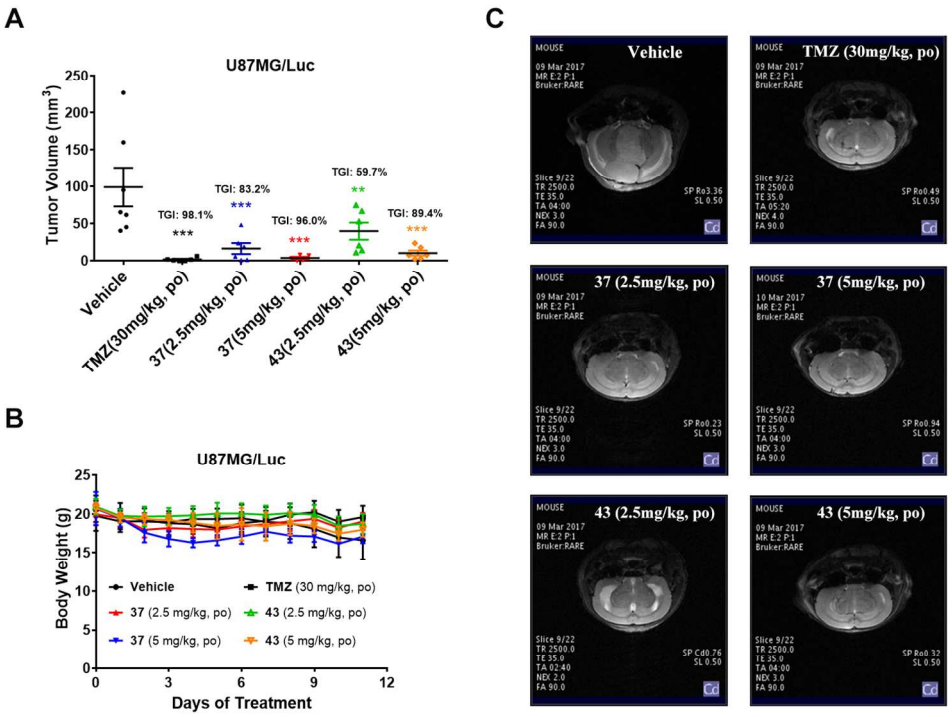

Figure 8. In vivo antitumor efficacy of 37 and 43 in the U87MG/Luc glioblastoma orthotopic xenograft model. A) Tumor volume in the mouse brain at the end of treatment; B) body weight changes; C) representative NMR images of U87MG/Luc tumors in the mouse brain at the end of treatment. Results are expressed as the mean ± SD (n = 5–7 for each group). **p <0.01 and ***p <0.001 vs vehicle. Temozolomide (TMZ) was used as the positive control.

130x99mm (300 x 300 DPI)

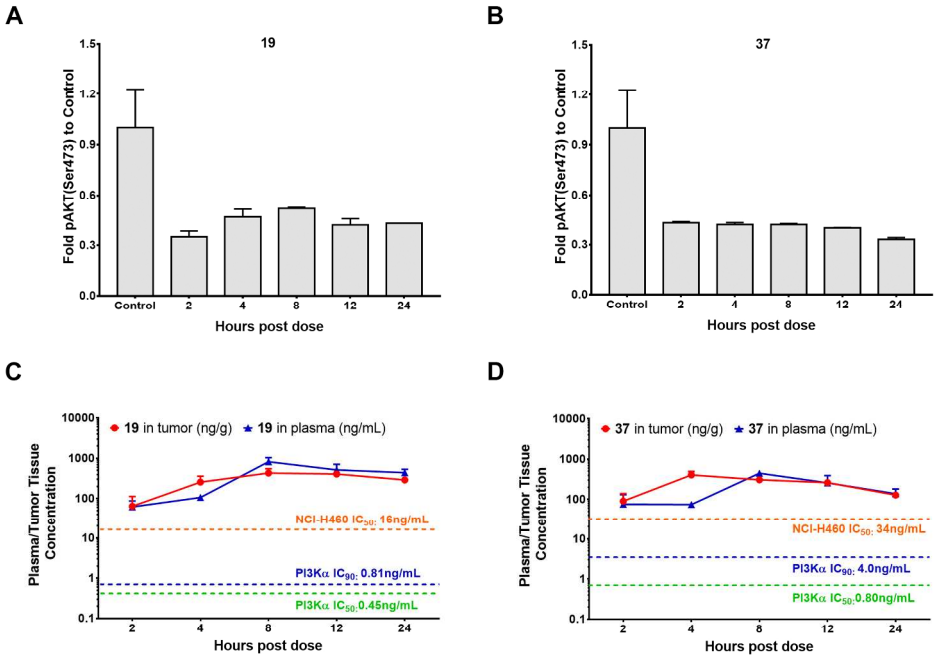

Figure 9. Pharmacodynamic response of 19 and 37 in the NCI-H460 xenograft model following a single oral dose of 10 mg/kg. pAKT(S473) levels were determined at 2, 4, 8, 12 and 24 h post-administration (A and B). Compound concentrations in plasma and tumor tissues were measured at the same time point and the dashed lines represent the PI3Kα IC50 value (green), the PI3Kα IC90 value (blue) and the NCI-H460 antiproliferative IC50 value (orange), respectively. Results are expressed as the mean ± SD (n = 3 for each time point).

199x150mm (300 x 300 DPI)

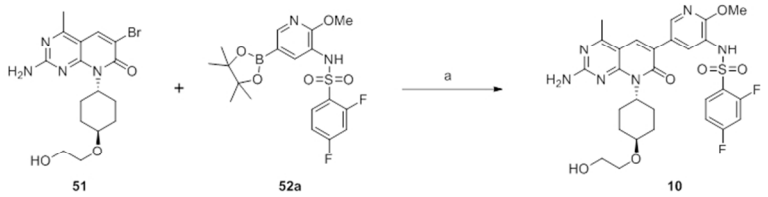

Scheme 1. Synthesis of compound 10

254x190mm (96 x 96 DPI)

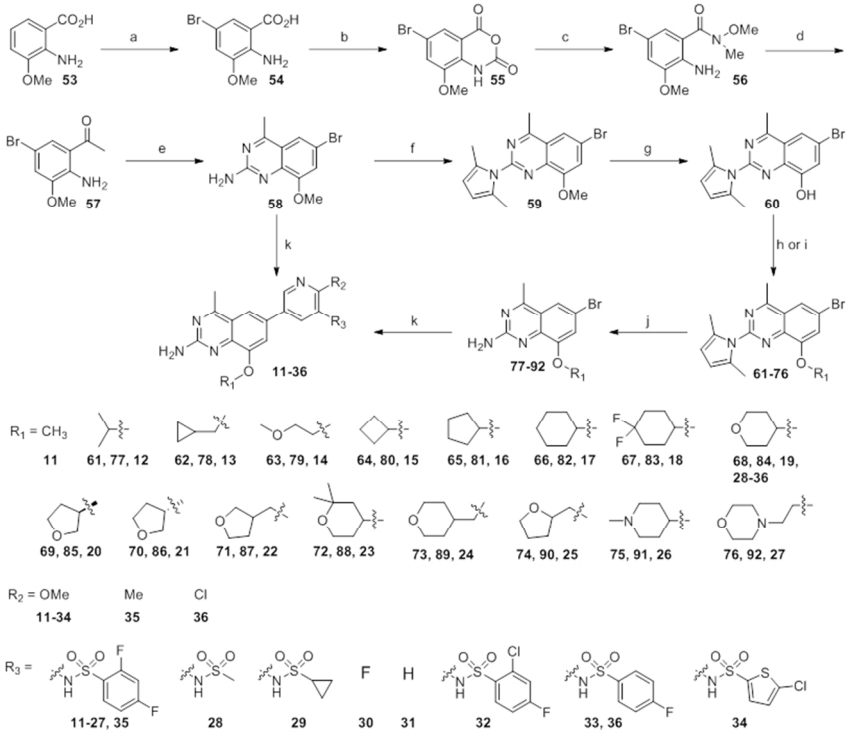

Scheme 2. Synthesis of compound 11-36

254x190mm (96 x 96 DPI)

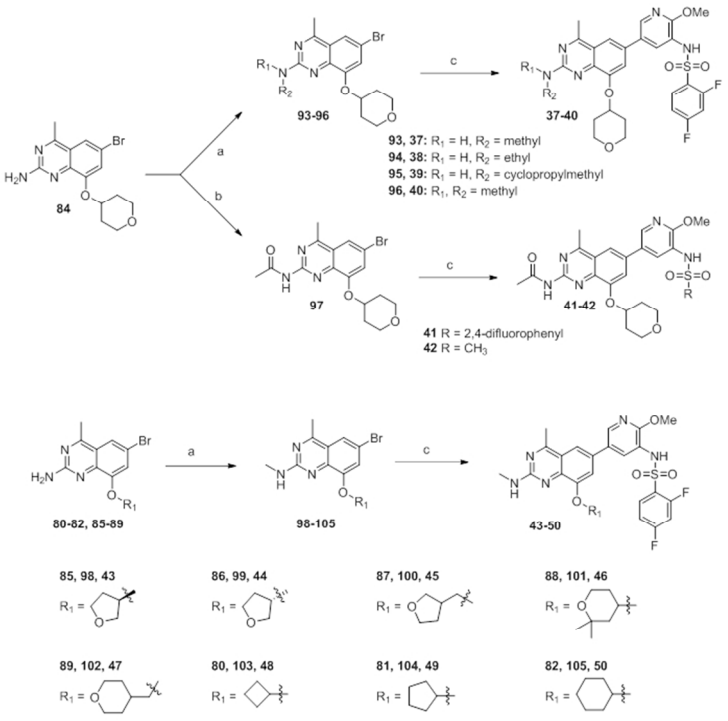

Scheme 3. Synthesis of compound 37-50

254x190mm (96 x 96 DPI)

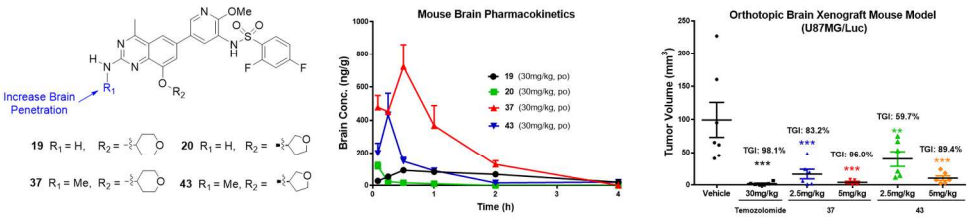

169x50mm (300 x 300 DPI)